Development and Application of the North-Central District Groundwater Flow Model

Northwest Florida Water Management District

Technical File Report 25-XX

Northwest Florida Water Management District
81 Water Management Drive
Havana, Florida 32333
(850) 539-5999
www.nwfwater.com

August 2025

NORTHWEST FLORIDA WATER MANAGEMENT DISTRICT

GOVERNING BOARD

George Roberts
Chair, Panama City

Jerry Pate
Vice Chair, Pensacola

Nick Patronis
Secretary, Panama City

John Alter
Malone

Gus Andrews
DeFuniak Springs

Ted Everett
Chipley

Kellie Ralston
Tallahassee

Anna Upton
Tallahassee

Lyle Seigler
Executive Director

DISTRICT OFFICES

Havana (Headquarters)
DeFuniak Springs
Youngstown
Milton

For additional information, write or call:

Northwest Florida Water Management District
81 Water Management Drive
Havana, Florida 32333-4712
(850) 539-5999
www.nwfwater.com

Acknowledgments

The North Central District Model was developed with the assistance of a team of professionals within the Division of Resource Management and external consultants. Primary District authors and external contractors who contributed to this effort are listed below.

Primary Authors:

J.W. Grubbs, James Sutton, and Ken Friedman

External Consultants:

Tetra Tech, Inc.

The Balmoral Group

Editorial and Supporting Contributions:

Kathleen Coates, Director, Division of Resource Management

Paul Thurman, Bureau Chief, Water Resource Evaluation

Contents

Acknowledgments 3

List of Figures 6

List of Tables 9

List of Acronyms and Abbreviations 10

Executive Summary 12

1. Introduction 15

2. Study Area Hydrology and Hydrogeology 16

2-1. Physiography and Hydrostratigraphy 18

2-2. Springs 27

2-3. Groundwater Levels 31

2-4. Surface Water Features 38

3. Conceptual Model 40

3.1 Model Domain 40

3-2. Hydraulic Properties 43

3-3. System Stresses 44

4. Numerical Model Construction 61

4-1. Model Code and Governing Equation 61

4-2. Model Domain and Discretization 62

4-3. Hydraulic Properties 70

4-4. Boundary Conditions 71

5. Model Calibration 78

5-1. Implementation of the NCDM Calibration 78

5-2. Calibration Results 104

6. Simulation of Pumping Impacts on Groundwater Flow to Jackson Blue Spring and Merritts Mill Pond 151

6-1. Development of Well Package Input Files 151

6-2. Historical and Projected Condition Simulation Results 156

7. Model Limitations 158

8. Summary 160

References 162

List of Figures

Figure 2-1. Geographic extent of the NCDM 17
Figure 2-2. Physiographic Districts in the NCDM 19
Figure 2-3. Thickness of the Surficial Aquifer System (SAS) in the NCDM domain. 22
Figure -2-4. Thickness of the Upper Confining Unit (UCU) in the NCDM domain. 23
Figure 2-5. Thickness of the Upper Floridan Aquifer (FAS) in the NCDM domain. 24
Figure 2-6. Thickness of the Lisbon-Avon Park Composite Unit in the NCDM domain. 25
Figure 2-7. Thickness of the Lower Floridan Aquifer (LFA) in the NCDM domain. 26
Figure 2-8. Merritts Mill Pond and Springs 28
Figure 2-9. Spring locations within the NCDM domain 30
Figure 2-10. Potentiometric surface map of groundwater levels in the Upper Floridan aquifer during May and June of 2010 32
Figure 2-11. Locations of Upper Floridan aquifer monitoring wells with daily historical data in the region near Jackson Blue Spring 34
Figure 2-12. Time-series plot of historical groundwater levels from well 005266 NWFWMD-PITTMAN VISA/S661 35
Figure 2-13. Time-series plot of historical groundwater levels from well 004795 INTERNATIONAL PAPER @ CYPRESS 36
Figure 2-14. Time-series plot of historical groundwater levels from well 005226 NWFWMD-BAXTER SAND PIT VISA 36
Figure 2-15. Time-series plot of historical groundwater levels from well 005408 NWFWMD-2 EGG AMBIENT #3 37
Figure 2-16. Time-series plot of historical groundwater levels from well 012797 CYPRESS PARK #1 – FLORIDAN 37
Figure 2-17. Time-series plot of historical groundwater levels from well 012769 JACKSON BLUE #2 - FLORIDAN 38
Figure 3-1. NCDM domain lateral extent and representative groundwater flow paths in the Upper Floridan aquifer 41
Figure 3-2. Estimated evaporation and transpiration (ET) from the plant canopy, soil surface, and unsaturated zone during the period from 2017 to 2019 51
Figure 3-3. Estimated average precipitation rates during 2017-2019 55
Figure 3-4. Initial (conceptual model) estimate of average groundwater recharge rates during 2017-2019 56
Figure 4-1. NCDM Grid 63
Figure 4-2. Active and inactive area of the NCDM grid in model layer 1 65
Figure 4-3. Active and inactive area of the NCDM grid in model layer 2 66
Figure 4-4. Active and inactive area of the NCDM grid in model layer 3 67

Figure 4-5. Active and inactive area of the NCDM grid in model layer 4 68
Figure 4-6. Active and inactive area of the NCDM grid in model layer 5 69
Figure 4-7. Geographic distribution of groundwater withdrawals from wells. 74
Figure 5-1. Locations and names of NCDM head calibration targets. 86
Figure 5-2. Locations and names of NCDM horizontal head difference calibration targets. 88
Figure 5-3. Locations and names of NCDM vertical head difference calibration targets. ... 90
Figure 5-4. Locations of NCDM baseflow calibration target zones. 94
Figure 5-5. Locations of NCDM spring-flow calibration targets. 97
Figure 5-6. Plot of simulated versus calibration target values of hydraulic head. 107
Figure 5-7. Map of head calibration target residuals. 108
Figure 5-8. Plot of simulated versus calibration target values of spring flows 109
Figure 5-9. Map of spring-flow calibration target residuals 111
Figure 5-10. Plot of simulated versus calibration target values of horizontal head differences 113
Figure 5-11. Map of simulated versus calibration target values of horizontal head differences 114
Figure 5-12. Plot of simulated versus calibration target values of vertical head differences 117
Figure 5-13. Map of vertical head difference residuals. 118
Figure 5-14. Plot of simulated versus calibration target values of baseflows 120
Figure 5-15. Map of NCDM grid cells with simulated heads above land surface..... 122
Figure 5-16. Simulated head values from model layer 1 123
Figure 5-17. Simulated head contours from model layer 2 124
Figure 5-18. Simulated head contours from model layer 3 125
Figure 5-19. Simulated head contours from NCDM layer 4 126
Figure 5-20. Simulated head contours from model layer 5 127
Figure 5-21. Calibrated values of the surficial aquifer system horizontal hydraulic conductivity 129
Figure 5-22. Calibrated values of the horizontal hydraulic conductivity of the upper confining unit of the Upper Floridan aquifer 130
Figure 5-23. Calibrated values of Upper Floridan aquifer horizontal hydraulic conductivity 131
Figure 5-24. Calibrated values of middle confining unit horizontal hydraulic conductivity 132
Figure 5-25. Calibrated values of Lower Floridan aquifer horizontal hydraulic conductivity 133
Figure 5-26. Calibrated values of surficial aquifer system vertical hydraulic conductivity 134
Figure 5-27. Calibrated values of upper confining unit vertical hydraulic conductivity 135
Figure 5-28. Calibrated values of Upper Floridan aquifer vertical hydraulic conductivity . 136

Figure 5-29. Calibrated values of middle confining unit vertical hydraulic conductivity ... 137
Figure 5-30. Calibrated values of Lower Floridan aquifer vertical hydraulic conductivity . 138
Figure 5-31. Calibrated values of recharge 140
Figure 5-32. Simulated groundwater evapotranspiration 141
Figure 5-33. Composite scaled sensitivity values for the head calibration target group ... 145
Figure 5-34. Composite scaled sensitivity values for the horizontal head-difference calibration target group 146
Figure 5-35. Composite scaled sensitivity values for the vertical head difference calibration target group 147
Figure 5-36. Composite scaled sensitivity values for the spring flow calibration target group 148
Figure 5-37. Composite scaled sensitivity values for the baseflow calibration target group 149
Figure 5-38. Composite scaled sensitivity values for the flooding penalty function calibration target group 150

List of Tables

Table 3-1. Estimates of hydraulic properties of hydrogeologic units prior to calibration 43
Table 3-2. Sources of water use data in the NCDM domain. 45
Table 3-3. Groundwater Use Estimates in the NCDM domain in years 2017-2019..... 49
Table 3-4. Estimated Domain-Averaged Water Budget Components for the NCDM Conceptual Model..... 60
Table 5-1. Parameters groups and number of adjustable parameters used in the NCDM calibration. 81
Table 5-2. Upper and lower bounds assigned to NCDM calibration parameters[1]. 82
Table 5-3. Stream and river reaches corresponding to conductance multiplier parameters used to construct and calibrate the NCDM. 83
Table 5-4. PEST observation (calibration target) group names used in the NCDM calibration 85
Table 5-5. Number of head targets by layer 87
Table 5-6. Horizontal Head Difference Targets..... 87
Table 5-7. Vertical head difference targets and associated observation wells 89
Table 5-8. Names and descriptions of NCDM baseflow observation reaches, including calibration target reaches 93
Table 5-9. NCDM spring flow calibration target names, values and associated spring names and site identifiers..... 96
Table 5-10. Relative contributions of calibration target groups during the final stages of the NCDM calibration..... 101
Table 5-11. Statistical summary of calibration target residuals of the NCDM..... 105
Table 5-12. Values of head calibration targets, simulated equivalents of targets, and target residuals 106
Table 5-13. Values of spring flow calibration targets, simulated equivalents of targets, and target residuals. 110
Table 5-14. Values of horizontal head difference calibration targets, simulated equivalents of targets, and target residuals 112
Table 5-15. Values of vertical head difference calibration targets, simulated equivalents of targets, and target residuals 116
Table 5-16. Values of baseflow calibration targets, simulated equivalents of targets, and target residuals 119
Table 5-17. Simulated water budget for the NCDM domain 139
Table 6-1. Estimated annual groundwater withdrawals in the NCDM for years 2000, 2005, 2010, 2015, 2020, and 2045 152

Table 6-2. Simulated pumping impacts on groundwater discharge to Jackson Blue Spring and Merritts Mill Pond in years 2000, 2005, 2010, 2015, 2020, and 2045. 157

List of Acronyms and Abbreviations

AG	agricultural water use
AOWR	Alabama Office of Water Resources
cfs	cubic feet per second
ET	evapotranspiration
ET_{uz}	evaporation and transpiration from the plant canopy, soil surface, and unsaturated zone
ET_{sat}	evaporation from areas where the land-surface is inundated or the shallow subsurface is saturated
FAS	Floridan aquifer system
FSAID	Florida Statewide Agricultural Irrigation Demand program
DSS	domestic self-supplied water use
GIS	Geographic information system
GWCA	Groundwater Contribution Area
ICI	industrial-commercial-institutional water use
IWUP	Individual Water Use Permit
LFA	Lower Floridan aquifer
LiDAR	Light detection and ranging
LISAPCU	Lisbon-Avon Park Composite Unit
MCU	middle confining unit of the Floridan aquifer system
MODFLOW	Modular Groundwater Flow Model
NCDM	North Central District Groundwater Flow Model
NWFWMD	Northwest Florida Water Management District
PS	public supply water use

REC	recreational self-supplied water use
SAS	surficial aquifer system
UFA	Upper Floridan aquifer
UCU	upper confining unit of the Floridan aquifer system
USGS	U.S. Geological Survey

Executive Summary

A steady-state, groundwater flow model was developed to support regional water supply planning, minimum flow and minimum water levels evaluations, and water use permitting evaluations for waterbodies in the north-central area of the Northwest Florida Water Management District (District or NWFWMD). In particular, the model is intended primarily to support the establishment of a minimum flow for Jackson Blue Spring as a tool that can estimate changes in the flows of the spring in response to changes in groundwater withdrawals from wells. This model is referred to as the North-Central District Model (NCDM) and was implemented using the U.S. Geological Survey MODFLOW-NWT (Niswonger and others, 2011) computer program for solving the three-dimensional groundwater-flow equation.

The NCDM extends across an approximately 1,600 square mile area that includes parts of Jackson, Calhoun, Holmes, and Washington Counties in Florida, and parts of Houston and Geneva Counties in Alabama. The northern extent of the NCDM coincides with the approximate updip limit of the productive part of the Floridan aquifer system as delineated by Williams and Kunianski (2015). The eastern boundary of the NCDM coincides with the Chattahoochee and Apalachicola Rivers, and most of the western and southwestern boundaries coincide with regional groundwater flow paths that define no-flow boundaries at distances intended to be sufficient to minimize their effect on simulated changes in flow at and near Jackson Blue Spring. Limited areas of the western and southern boundaries are defined by constant head boundaries, where water flows out of the NCDM domain.

The NCDM actively simulates groundwater levels and flows within each of the major hydrogeologic units in this region: the surficial aquifer system, the upper confining unit of the Floridan aquifer system, the Upper Floridan aquifer, the middle confining unit of the Floridan aquifer system, and the Lower Floridan aquifer. The NCDM is discretized vertically into five layers that generally correspond to these hydrogeologic units, and horizontally into square grid cells that are 2500 feet on each side.

The NCDM was developed as a steady-state model and calibrated to average conditions occurring from January 1, 2017, through December 31, 2019. Model calibration consisted of adjusting initial estimates of hydraulic conductivity, conductance of subsurface connections with river, stream, and spring features, recharge rates, and maximum rates of direct evapotranspiration from the water table to better match calibration targets defined by groundwater levels, groundwater level-differences, spring flows, and stream and river baseflows during the calibration period, as well as to minimize the occurrence of cells where groundwater levels exceeded land surface. Summary statistics of differences between these target values and their model-simulated equivalents indicated a relatively unbiased, well-fit

model, particularly for the head and spring flow targets, which were treated as higher-priority targets during the NCDM development. Calibration targets were generally most sensitive to parameters associated with the hydraulic conductivity of the Upper Floridan aquifer and groundwater recharge.

The NCDM was used to estimate the effects of historical and projected pumping from groundwater wells on groundwater discharge to Jackson Blue Spring and Merritts Mill Pond. These pumping effects were estimated by executing a series of NCDM simulations, including a 'no-pumping' simulation and individual simulations using pumping estimates from years 2000, 2005, 2010, 2015, 2020, and 2045. Estimates of pumping impacts based on these simulations ranged from about 3.3 cubic feet per second (cfs) in 2000 to 5.8 cfs in 2045 for Jackson Blue Spring, and from 3.5 cfs in 2000 to 6.7 cfs in 2045 for Merritts Mill Pond (excluding the impacts from Jackson Blue Spring).

The NCDM was developed primarily as a tool for simulating changes in groundwater flow to Jackson Blue Spring and nearby features such as Merritts Mill Pond. The model can also be used for other purposes, but certain limitations should be acknowledged. For example, simulations of changes in groundwater levels (for example drawdown from pumping wells) with the NCDM should be carried out with caution and with an understanding of the horizontal resolution of the NCDM grid (2,500 feet) and the regional nature of the model and associated variations in hydraulic properties. These types of simulations are often used to evaluate local impacts, such as drawdown under wetland features or evaluating the potential for interference with existing wells. Therefore, site specific or more localized information, such as specific capacity or aquifer performance testing, can provide more direct information than a regional model in these situations. Simple site-specific numerical models or analytical methods like the Theis or Thiem equations (Stahlman, 1971) can also be implemented to estimate an expected range for drawdown based on more local estimates of aquifer characteristics.

The NCDM only includes the western parts of groundwater contributing areas to the reaches of the Chattahoochee and Apalachicola Rivers in the NCDM, so suitable baseflow targets were not available for these river reaches that define the eastern boundary of the NCDM. Similarly, stream reaches near the western boundary (Econfina, Holmes, or Wrights Creek) and southern boundary (Chipola River downstream from the gage near Altha) did not have baseflow targets because these reaches were ungaged. Simulated changes in groundwater flow to the above reaches are therefore expected to have greater uncertainty.

The NCDM was not developed to estimate the movement and transformation of chemicals in the subsurface. Although the NCDM can be used to calculate groundwater flow paths and travel times using tools like MODPATH (Pollock, 2016), these or similar tools should not be

used with the current version of the NCDM to simulate the time of travel of chemicals within the subsurface because the NCDM was not calibrated for this purpose. Transport simulations typically depend on finer-scale variations in hydraulic conductivity and other properties, so development of models capable of simulating chemical transport should ideally include calibrating the model with historical chemical concentration data, historical and time-varying chemical loading rates, and independent estimates of travel time or groundwater age information. The karstic nature of most of the NCDM model domain further complicates this process and makes simulating chemical transport and time of travel very challenging.

1. Introduction

A steady-state, groundwater flow model was developed to support regional water supply planning, minimum flows and minimum water levels evaluations, and water use permitting evaluations for waterbodies in the north-central area of the Northwest Florida Water Management District (District or NWFWMD). Water Management Districts in Florida are required to establish Minimum Flows and Minimum Water Levels (MFLs) for selected waterbodies within their boundaries under Section 373.042 (1), Florida Statutes. The model is intended primarily to support the establishment and implementation of a minimum flow for Jackson Blue Spring by serving as a tool for estimating changes in the flows of the spring in response to changes in groundwater withdrawals from wells. This model is referred to as the North Central District Model (NCDM). The purpose of this report is to document the development of the NCDM, as well as an initial application of the model.

The main body of this report is organized into four main sections. The first section is a description of the hydrogeologic setting and essential hydrologic features of the area represented by the numerical mode. The second section briefly describes the conceptual model that forms the basis for the numerical model. The third section of the report describes how the model is constructed and includes a description of the extent of the model domain and its discretization, as well as the assignment of system properties and boundary conditions. The fourth main section of the report describes the history-matching (model calibration) process used to improve initial estimates of hydraulic property and boundary condition values. These four main sections of the report are followed by shorter sections describing an application of the model to estimate the effect of historical and future pumping on the flow from Jackson Blue Spring, and limitations of the model.

2. Study Area Hydrology and Hydrogeology

The geographic extent of NCDM is shown in Figure 2-1 and was defined so that it would be large enough to include the areas and the features that have significant effect on the flow from Jackson Blue Spring. The NCDM extent (also referred to the NCDM domain or active domain) was also defined so that it extends beyond these areas and features to logical boundaries defined by hydrologic or hydrogeologic features that are at a sufficient distance to not unreasonably limit the use of the model to predict changes in flow at the spring. Further description of the definition of the NCDM domain is provided later in this report.

This section of the report describes the hydrologic and hydrogeologic characteristics of the area within the NCDM domain. The physiography and essential aspects of geology and hydrostratigraphic units are described, along with a description of study area springs and groundwater levels, including key groundwater flow paths in the Upper Floridan aquifer that can be inferred from its potentiometric surface. The section concludes with a brief description of surface water features present in the NCDM domain.

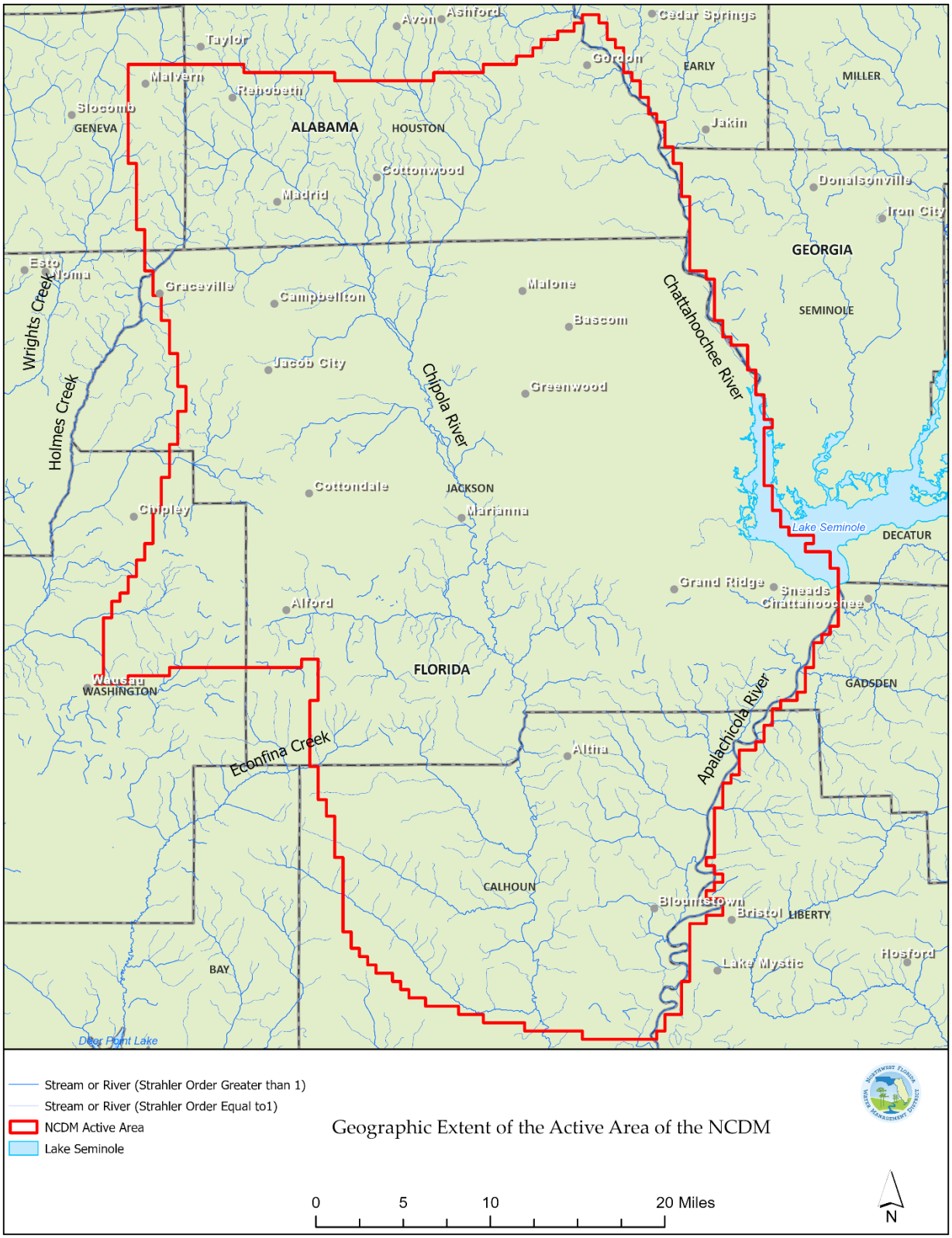

Figure 2-1. Geographic extent of the NCDM

2-1. Physiography and Hydrostratigraphy

The NCDM domain overlaps two physiographic districts: the Dougherty Karst Plain District and the Apalachicola Delta District. Most of the area that the NCDM encompasses is within the Dougherty Karst Plain, which is characterized by karst terrain, including sinkholes, caves, springs, and sinking streams (Figure 2-2; modified from Ebersole, 2019, Clark, 1976, Williams, 2022).

Land-surface elevations in the Dougherty Karst Plain District range from approximately 50 feet to 240 feet NAVD 88. The topography is generally flat in the northern portion of the Dougherty Karst Plain District, with steeper terrain to the south where streams and rivers have incised through surficial sediments or where karst landforms have developed.

The geologic units underlying the Dougherty Karst Plain District and represented in the North-Central District Model include (in descending age) Quaternary age alluvium, the Plio-Pleistocene age Citronelle Formation, the Miocene age Alum Bluff Group and Bruce Creek Limestone (where present), the Oligocene-aged Suwannee Limestone, and the Eocene-aged Ocala Limestone. Throughout the Dougherty Karst Plain District, Miocene, Oligocene, and Eocene age sediments are overlain by a residuum consisting of younger, weathered, carbonate and siliciclastic sediments.

The Apalachicola Delta District is characterized by sands and clays deposited by fluvial and coastal processes. The Apalachicola Delta District extends from the boundary of the Dougherty Karst District to the north to the Gulf of America to the south. The Apalachicola Delta District is also an area within the NCDM domain where there is a significant confining unit overlying the upper Floridan aquifer.

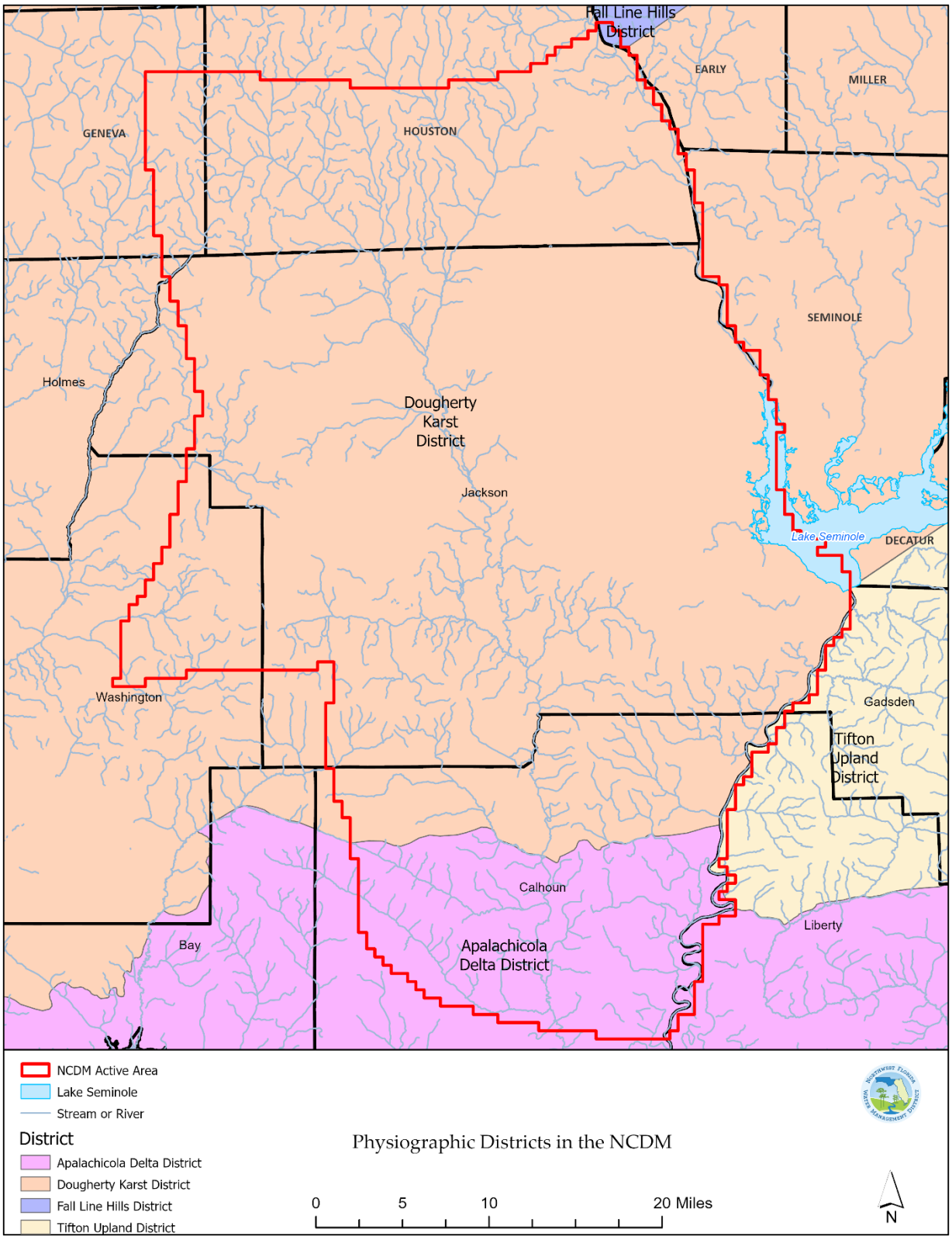

Figure 2-2. Physiographic Districts in the NCDM

The area within the North-Central District Model (NCDM) domain contains five major hydrostratigraphic units: the surficial aquifer system (SAS), the Upper Confining Unit (UCU), the Upper Floridan aquifer (UFA), the Lisbon-Avon Park Composite Unit (LISAPCU; also referred to as the middle confining unit (MCU) in this report), and the Lower Floridan aquifer (LFA).

The Surficial Aquifer System (SAS) generally consists of Citronelle Formation and undifferentiated clastic deposits of Plio-Pleistocene to Holocene age. In the Dougherty Karst District, the surficial aquifer can be thin or absent and comprised of limestone residuum consisting of weathered carbonate rocks. The surficial aquifer system is generally considered to be an insignificant source of water for most uses in the Dougherty Karst District. The thickness of the SAS varies throughout the NCDM domain, ranging from approximately 50 feet in northern Calhoun County to less than 10 feet in the Dougherty Karst Physiographic District (Williams and Kuniansky, 2015).

The Upper Confining Unit (UCU) is generally classified as a confining unit in the NCDM domain, where present. The UCU overlies the Upper Floridan aquifer system and is comprised of low permeability sediments of middle to late Miocene age. In the Dougherty Karst District, the UCU is thin to absent and frequently breached by karst features. Limestone residuum may create localized semi-confining conditions in areas within the Dougherty karst District (Crandall et al., 2013). In the Apalachicola Delta District, the thickness of the UCU can range from approximately 50 to 150 feet (Williams and Kuniansky, 2015).

The sediments that comprise the UCU generally consist of low permeability clastic deposits with interbedded carbonates and coarser grained sediments of Miocene age. Where the UCU is present, these beds of higher permeability sediments can provide relatively minor amounts of water and are primarily used for domestic use (NWFWMD, 1996).

The Upper Floridan aquifer (UFA) consists of permeable carbonates of Eocene to Oligocene age and is present across the NCDM domain. Within the Dougherty Karst Plain District, the Upper Floridan aquifer has well developed secondary porosity where the UCU is thin or absent. The UFA crops out in southern Alabama and continues to thicken and become more confined from north to south due to the transition from the Dougherty Karst Plain to the Apalachicola Embayment Region (NWFWMD, 1996).

The lithostratigraphic units that make up the Upper Floridan aquifer within the NCDM domain are the Oligocene-aged Suwannee Limestone and the Eocene-aged Ocala Limestone (Williams and Kuniansky, 2015). The thickness of the UFA ranges from approximately 50 feet in the northernmost region of the NCDM domain to approximately 500

feet near the southernmost region. Estimated transmissivities of the Upper Floridan aquifer in the region range from approximately 5,000 ft^2/day to 25,000 ft^2/day based on interpolation of aquifer performance tests but can vary locally especially where there is significant development of secondary porosity (Kuniansky et al., 2012). The transmissivity of the Upper Floridan aquifer can also be much higher than estimates from aquifer tests over larger spatial scales because of the limitations in aquifer testing in highly transmissive, karstic areas.

The Lisbon-Avon Park Composite Unit (LISAPCU; Williams and Kuniansky, 2015) is a lower permeability hydrogeologic unit that separates the Upper Floridan aquifer and the lower Floridan aquifer in northern Florida, southern Georgia, and southern Alabama. In this region the LISAPCU is equivalent to the Middle Confining Unit (MCU) described in Miller (1986). The LISAPCU is middle Eocene-aged and generally consists of well-indurated sand and clays and fine-grained carbonate rocks. The LISAPCU is laterally continuous across the entire NCDM domain and acts as a confining or semi-confining unit between the upper and lower Floridan aquifer.

There is minimal information regarding the aquifer properties of the LISAPCU in the NCDM domain. In January 2018, the NWFWMD performed a 14-day multiple well aquifer performance test in Malone, FL (northern Jackson County) to characterize the properties of the lower Floridan aquifer and the extent to which the UFA and LFA are hydraulically connected. The results of the APT indicated effective confinement between the UFA and LFA at the location of the test (Tetra Tech, 2018).

The lower to middle Eocene-aged Lower Floridan aquifer (LFA) in the NCDM domain consists of undifferentiated carbonate rocks such as limestone and dolomite and is generally lower permeability than the Upper Floridan aquifer. The Lower Floridan aquifer crops out in southern Alabama and represents the northern extent of the Floridan aquifer system in this region. The thickness of the Lower Floridan aquifer ranges from approximately 400 feet in the northern part of the NCDM domain and approximately 550 feet to the south (Williams and Kuniansky, 2015).

In southern Alabama and southwestern Georgia, the lower Floridan aquifer equivalent is the Claiborne aquifer. The Claiborne aquifer is defined as the permeable portions of the Lisbon and Tallahatta Formations and are part of the Claiborne Group of middle Eocene age (Williams and Kuniansky, 2015).

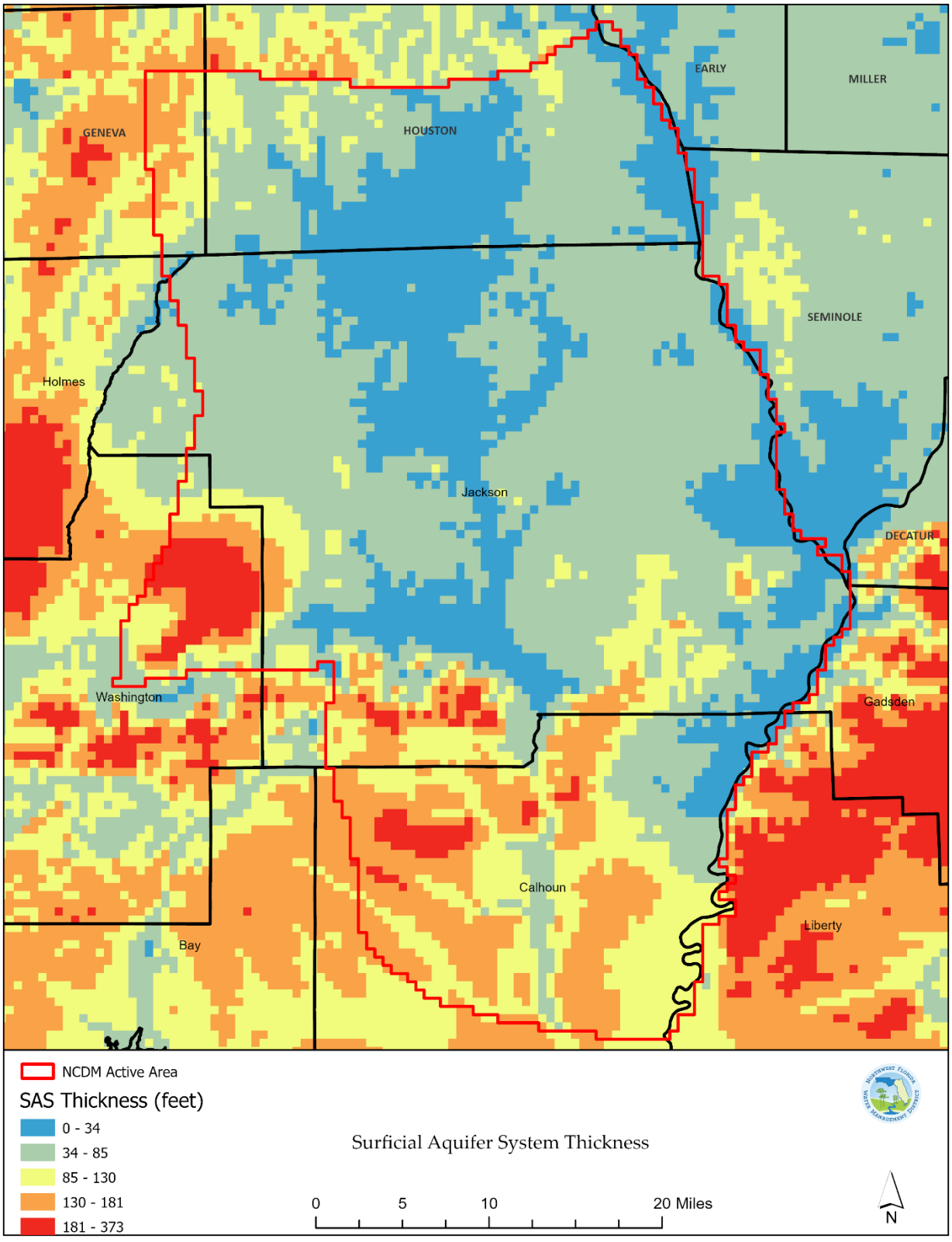

Figure 2-3. Thickness of the Surficial Aquifer System (SAS) in the NCDM domain.

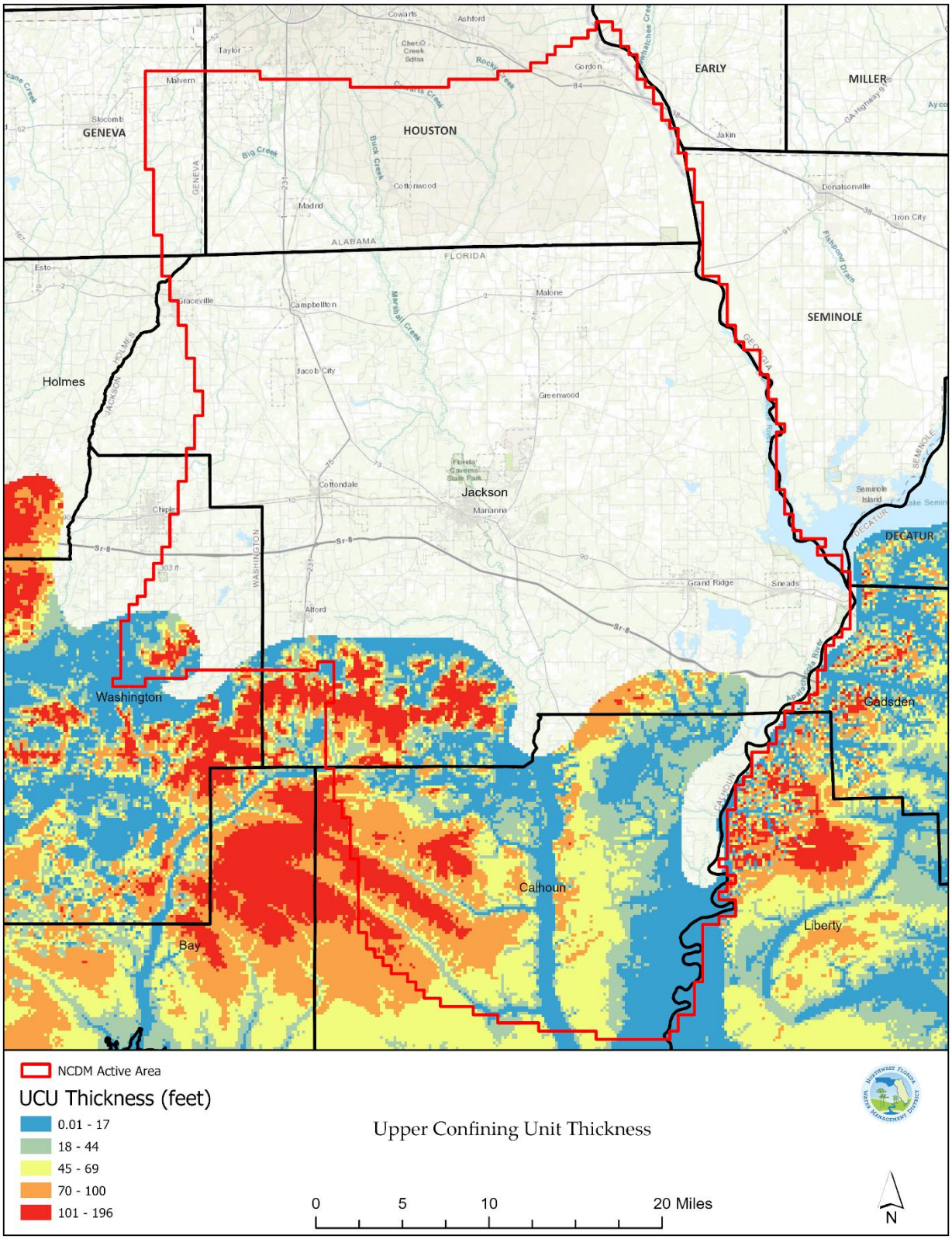

Figure -2-4. Thickness of the Upper Confining Unit (UCU) in the NCDM domain.

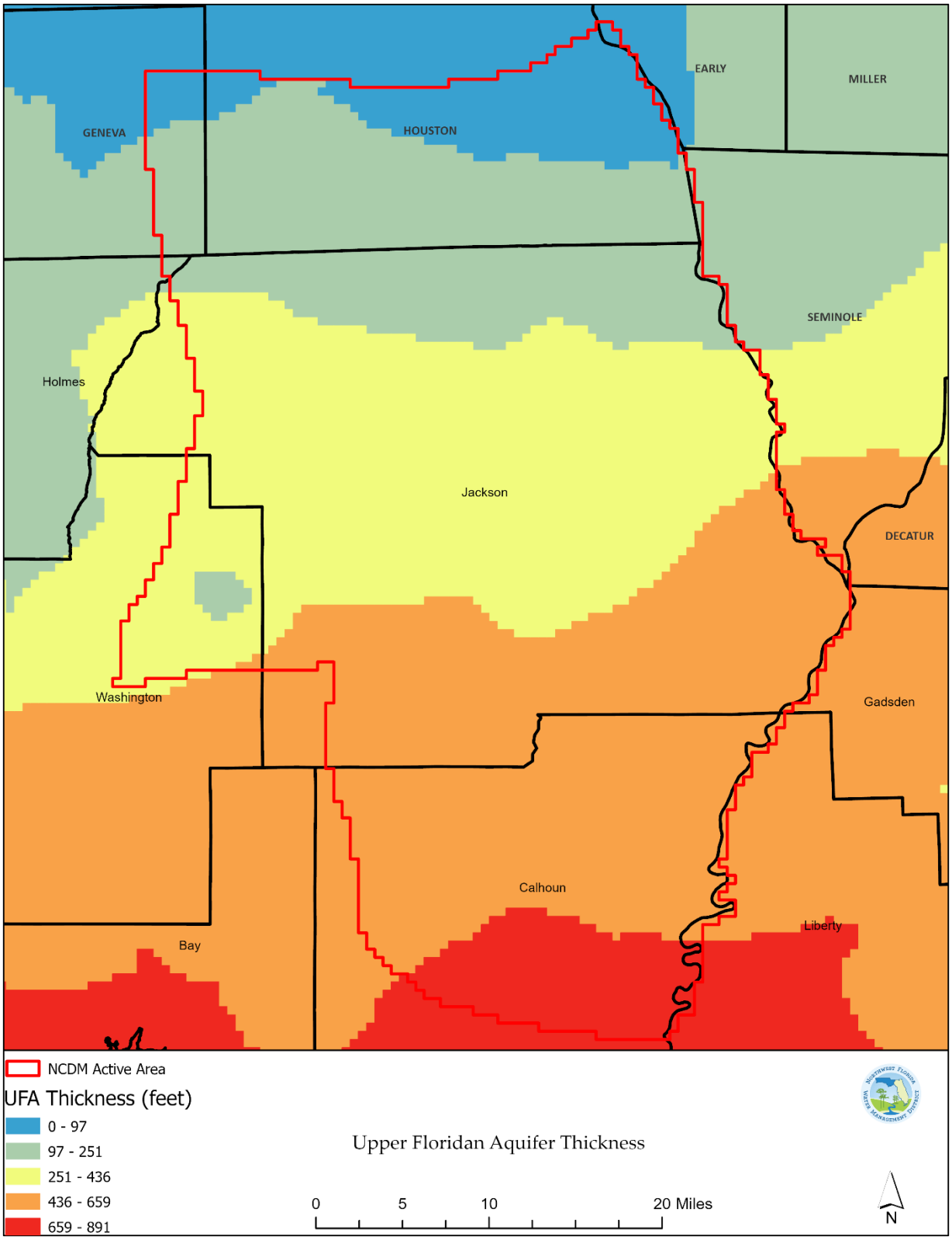

Figure 2-5. Thickness of the Upper Floridan Aquifer (FAS) in the NCDM domain.

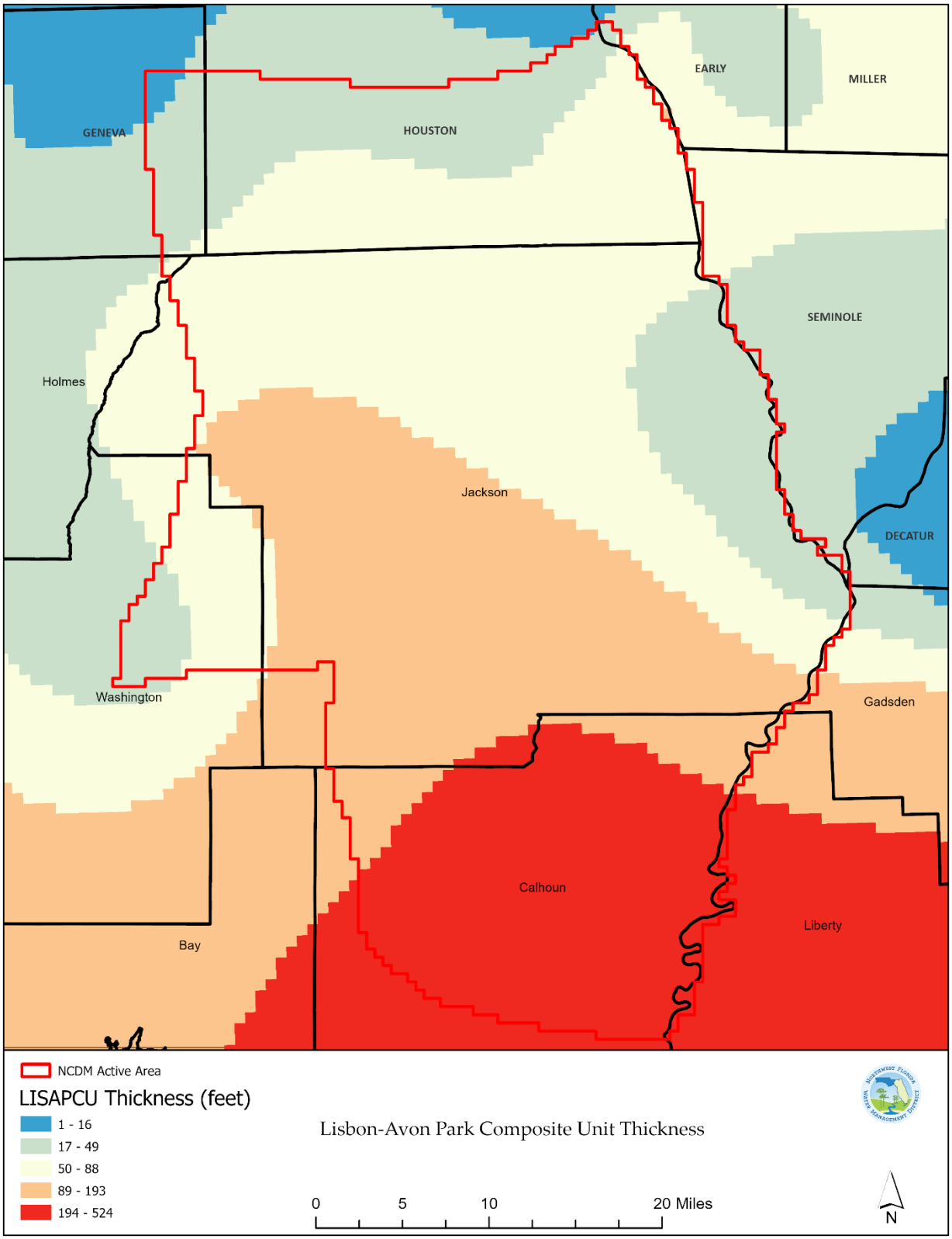

Figure 2-6. Thickness of the Lisbon-Avon Park Composite Unit in the NCDM domain.

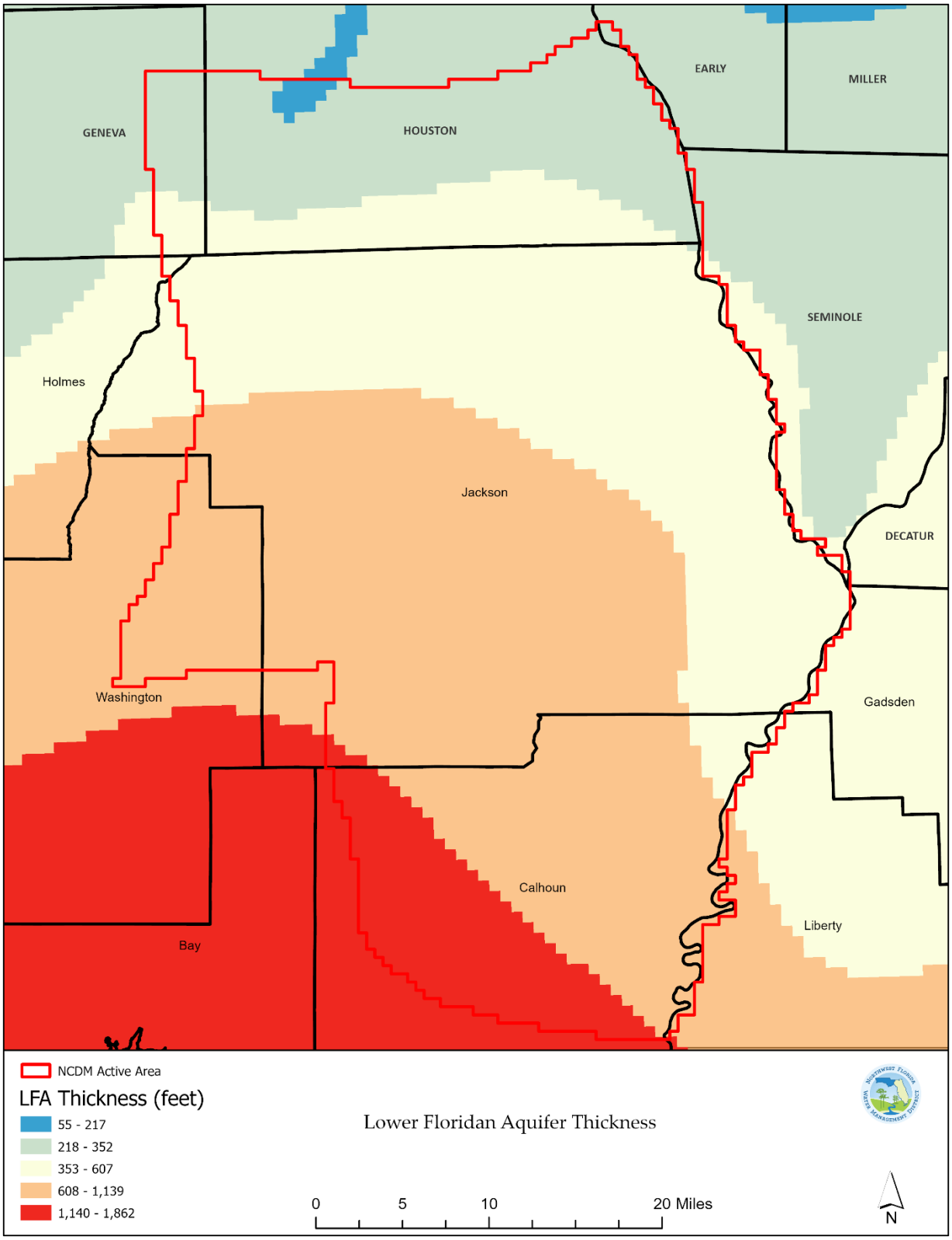

Figure 2-7. Thickness of the Lower Floridan Aquifer (LFA) in the NCDM domain.

2-2. Springs

The majority of the NCDM domain is located within the Dougherty Karst Plain, a geographic region characterized by karst terrain where the underlying carbonate rocks of the Upper Floridan aquifer are near land surface and the Upper Floridan aquifer is semiconfined or unconfined. In this region springs have developed through the dissolution of carbonate rocks and act as locations of concentrated discharge from the Upper Floridan aquifer.

Jackson Blue Spring is a first magnitude spring located near Marianna in Jackson County, Florida within the Dougherty Karst District and is the only first magnitude spring within the NCDM domain. The District previously delineated a groundwater contribution area (GWCA) extending over an approximately 130 square mile area from slightly south of Marianna, Florida to the southern part of Houston County, Alabama (Northwest Florida Water Management District, 2011). Jackson Blue Spring discharges directly into Merritts Mill Pond, a 270-acre impoundment that flows approximately 4 miles and terminates at a low-head dam at US Highway 90. Water from Merritts Mill Pond discharges over the dam (and occasionally through gates in the dam) at Highway US 90, forming the headwaters of Spring Creek, a tributary of the Chipola River (Figure 2-8. Merritts Mill Pond and Springs).

Jackson Blue Spring is a karst spring with an extensive cave network that originates in the Oligocene-aged limestones of the Upper Floridan aquifer. Jackson Blue Spring is a popular location for cave diving, with approximately 30,000 feet of mapped caves (AECOM, 2017). There are numerous karst features throughout the GWCA that result in a direct connection from the surface to the underlying Floridan aquifer. Due to the nonuniform nature of the distribution of these karst features, the rate of recharge from the surface to the Floridan aquifer can be spatially variable. Field measurements of discharge from Jackson Blue Spring made from 2002 to 2025 ranged from approximately 22 cubic feet per second (cfs) to approximately 262 cfs and averaged 106 cfs.

There are at least seven minor springs that directly discharge into Merritts Mill Pond. These submerged springs discharge water directly into the waterbody through fractures or conduits in the adjacent exposed limestone (Figure 2-8). There is limited information about the rate of discharge from each of the Merritts Mill Pond springs due to the limited accessibility and the vents being submerged. Barrios and DeFosset (2007) document a set of discrete discharge measurements for the seven known minor springs on Merritts Mill Pond. The discharge measurements from the minor springs in Merritts Mill Pond documented in Barrios and DeFosset (2007) range from 0.16 cfs to 3.87 cfs and were all measured in July 2007. Differences between concurrent (same day) flows measured at Jackson Blue Spring and at the outflow from Merritts Mill Pond indicate a substantial (greater than 100 cfs), diffuse groundwater discharge to the Merritts Mill Pond.

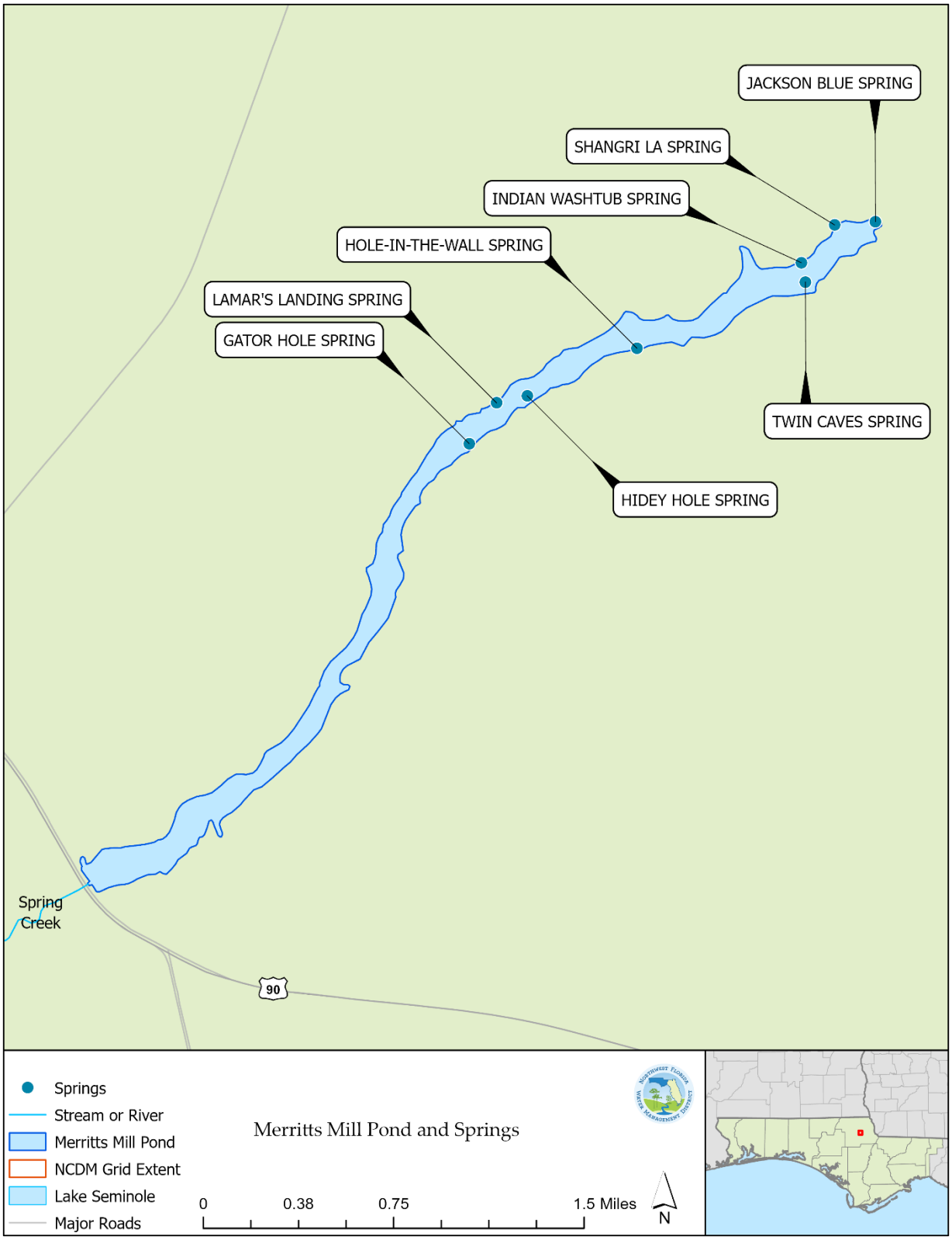

Figure 2-8. Merritts Mill Pond and Springs

There are 23 other known minor springs or spring groups within the NCDM domain with observed spring flows ranging between 0.08 cfs and 70 cfs for the period of record (Barrios and Chelette, 2004). This set of minor springs and springs groups with spring flow measurements collectively comprise 39 individual springs. The largest spring group, based on the period of record in the NCDM domain, is Lower Dry Creek Spring Group with an average flow of approximately 70 cfs. Many of these minor springs are located near the Chipola River where there is a strong hydraulic connection between surface water and groundwater due to the incision of the river into limestone of the Upper Floridan aquifer.

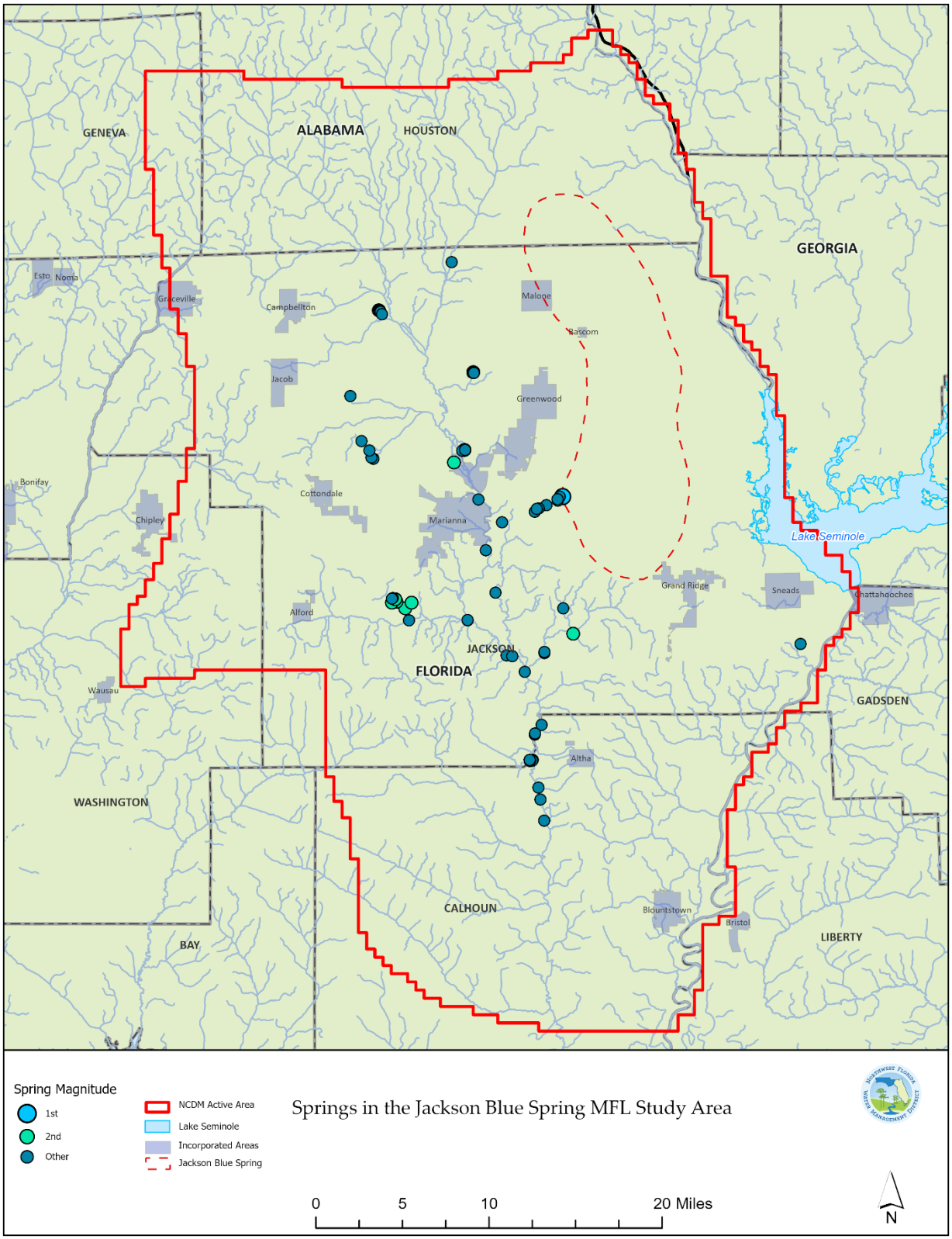

Figure 2-9. Spring locations within the NCDM domain

2-3. Groundwater Levels

As noted previously, the primary objective in developing the NCDM was to produce a tool capable of simulating changes in the flow from Jackson Blue Spring in response to changes in the locations and rates of groundwater withdrawals from wells. Jackson Blue Spring discharges water from the Upper Floridan aquifer, so understanding key spatial and temporal patterns in Upper Floridan aquifer groundwater levels can provide important information about the groundwater flow system in the region surrounding the Jackson Blue Spring and the factors that affect flow to the spring. These patterns can be evaluated using potentiometric surface maps and time-series plots of groundwater levels.

The potentiometric surface map of groundwater levels in the Upper Floridan aquifer during May and June of 2010 (Kinnaman and Dixon, 2011) is shown in Figure 2-10, and exhibits some general spatial patterns that have consistently appeared in similar maps developed prior to and since. The map shows a general pattern of north-to-south directed groundwater flow. An area of closely-space contour lines is evident in the northernmost part of the study area, which is consistent with the fact that the Upper Floridan aquifer is thinner and perhaps less permeable in this area, factors which reduce the transmissivity of the aquifer. Conversely, contour lines are more widely spaced in areas to the south, indicating a more transmissive system. These areas include: (1) those in Jackson County west of the Chipola River, the area surrounding Jackson Blue Spring, and southeastern Jackson County, and a broad, ridge-shaped area of the potentiometric surface extending south from southwestern Jackson County into northwestern Calhoun County (Figure 2-10).

Areas of groundwater discharge from the Upper Floridan aquifer are also indicated in the Upper Floridan aquifer potentiometric surface map of Kinnaman and Dixon (2011). These areas coincide with ‘valley-shaped’ sets of contour lines in the surface, where the surface slopes downward toward stream features, indicating groundwater flow toward these features. These areas include: (1) the area adjacent to the Chipola River near Merritts Mill Pond and extending southward into Jackson and Gulf Counties, (2) the area adjacent to the Chattahoochee River, at and upstream from the point where Jackson (Florida), Houston (Alabama), and Seminole (Georgia) Counties meet, (3) the area adjacent to the Apalachicola River, and (4) the areas near the border of Jackson and Washington Counties where the potentiometric surface indicates southwesterly groundwater flow, towards the spring-fed reach of Holmes Creek.

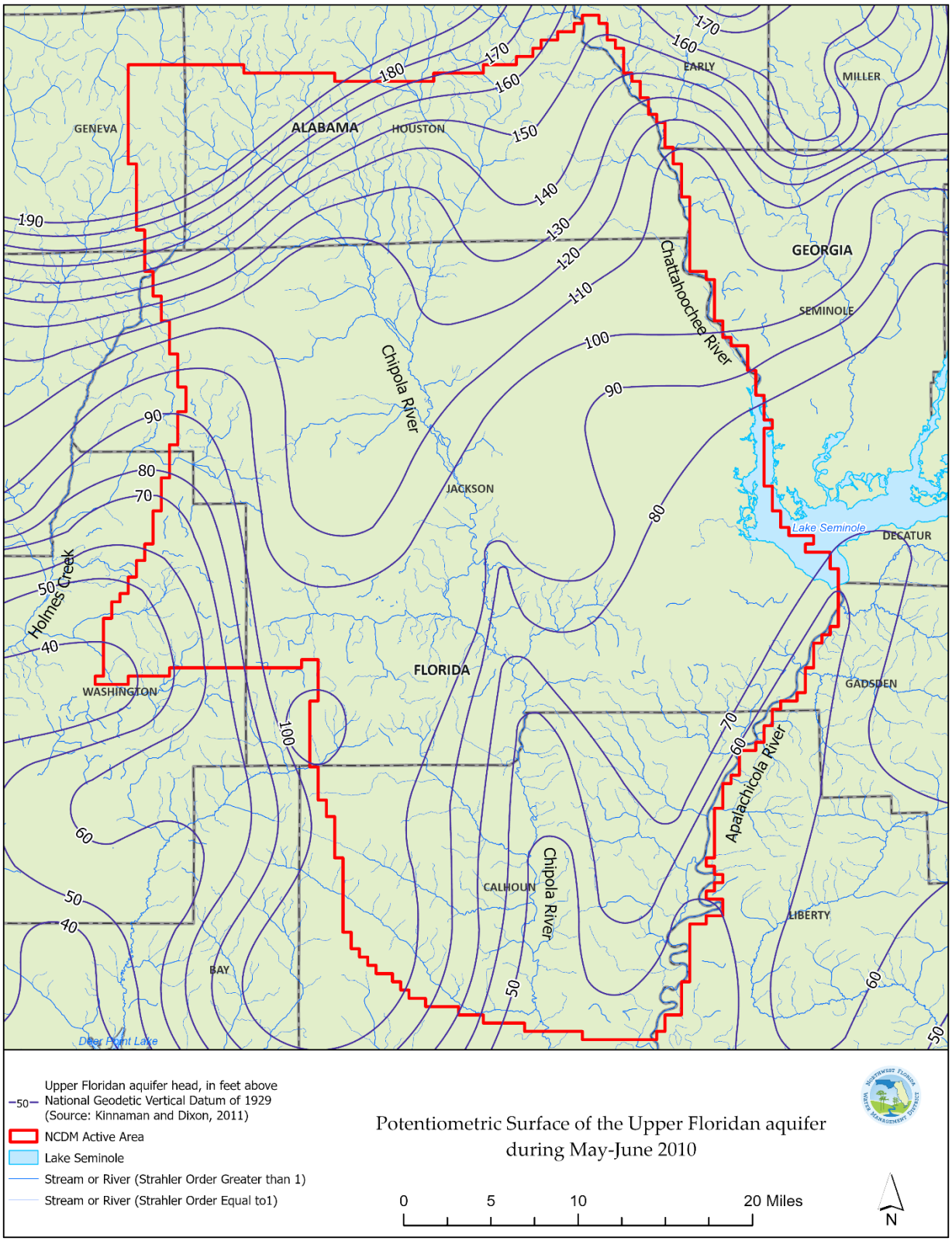

Figure 2-10. Potentiometric surface map of groundwater levels in the Upper Floridan aquifer during May and June of 2010

The locations of Upper Floridan aquifer monitoring wells with daily, historical data in the region near Jackson Blue Spring are shown in Figure 2-11, and time-series plots of these historical groundwater levels are shown in Figure 2-12 through Figure 2-17. The 005266 NWFWMD-PITTMAN VISA/S661 well had the longest period of record, beginning in December 2004. Groundwater levels varied over a range of about 20 feet at this well during its period of record and about 15 feet during the period from January 1, 2017, through December 31, 2019 (Figure 2-13). Note that the latter period was used to define the calibration period for the NCDM because of the similarity of the groundwater levels at the beginning and end of this period at this and other wells in the region surrounding Jackson Blue Spring, indicating minimal changes in groundwater storage during this period. The period of groundwater level records at other wells with daily, historical records in this region began in the latter half of 2016. The ranges in groundwater levels during the period from January 1, 2017, through December 31, 2019, at these wells were about 16, 28, and more than 25 feet at the 005408 NWFWMD-2 Egg Ambient #3 (Figure 2-15), 004795 International Paper @ Cypress (Figure 2-13), and 012797 Cypress Park #1 – Floridan (Figure 2-16) wells, respectively. The ranges in groundwater levels were lower during this period at the 05226 NWFWMD-Baxter Sand Pit Visa (8 feet; Figure 2-14) and 012769 Jackson Blue #2 – Floridan wells (4 feet; Figure 2-17), respectively, suggesting that the transmissivity of the Upper Floridan aquifer near these wells may be higher than near the other wells. The variability in historical groundwater levels exhibited in these monitoring wells also indicates the potential for variability in rates of groundwater discharge to receiving surface water bodies.

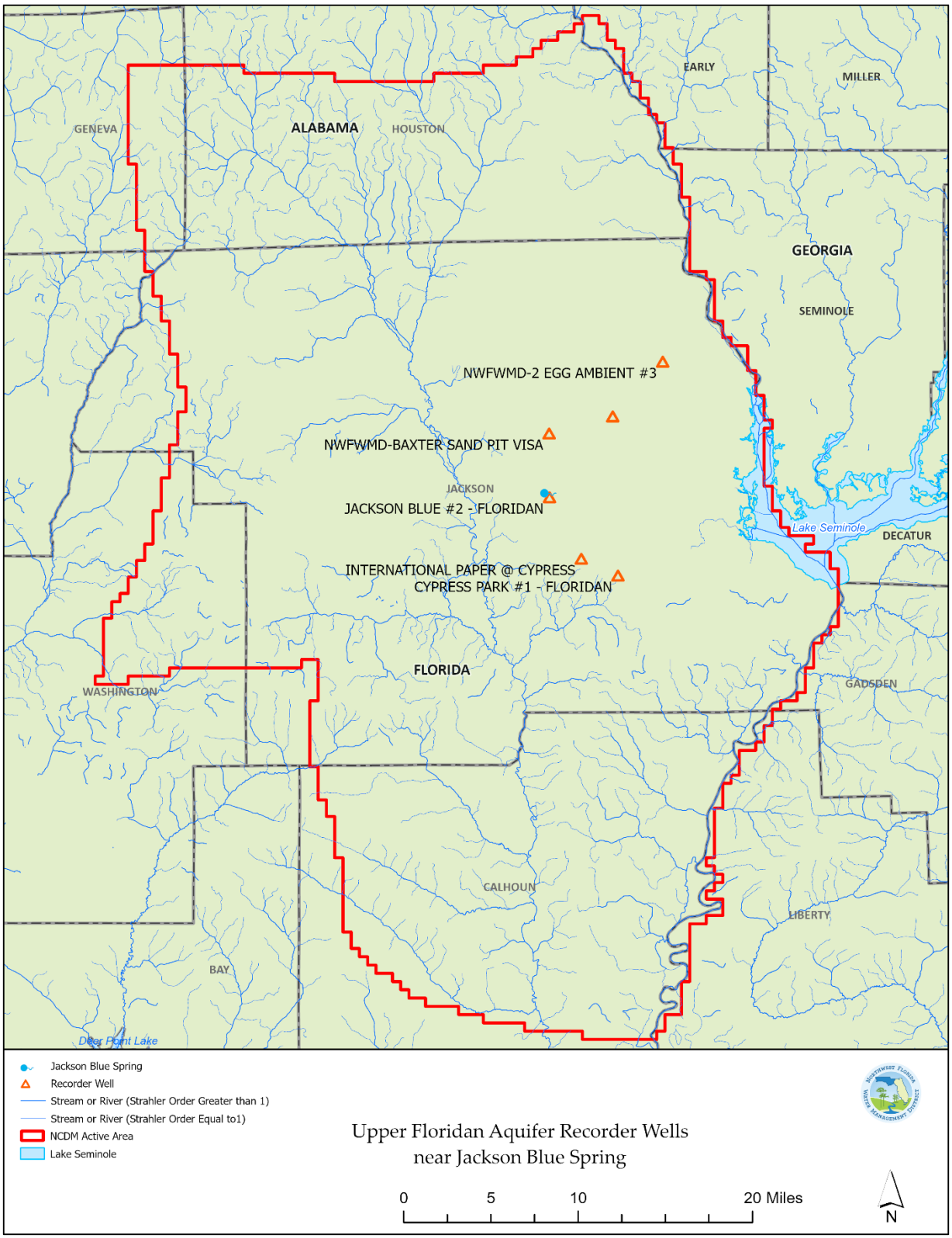

Figure 2-11. Locations of Upper Floridan aquifer monitoring wells with daily historical data in the region near Jackson Blue Spring

A high degree of connectivity between Jackson Blue Spring and the Jackson Blue #2 – Floridan well is indicated by the similarity of levels in this well and concurrent Jackson Blue Spring pool elevations. During the period from January 1, 2017, through December 31, 2019, the mean difference between the groundwater level at this well and the Jackson Blue Spring pool elevation (groundwater level minus spring pool elevation) was only 0.35 foot, with upper and lower quartile values of 0.40 and 0.28 foot, respectively. This similarity in spring pool and groundwater levels also included a 'drawdown period' in October 2020 when the gates at the Merritts Mill Pond control structure were opened for a longer period to allow the pond level to fall, exposing most of the sediments at the bottom of the pond. The difference between groundwater levels at the Jackson Blue #2 – Floridan well and concurrent, daily Jackson Blue Spring pool elevations during this drawdown period ranged between about 0.5 and 0.75 foot, with mean, upper quartile and lower quartile differences between groundwater and spring pool levels of 0.63, 0.70, and 0.55 feet, respectively.

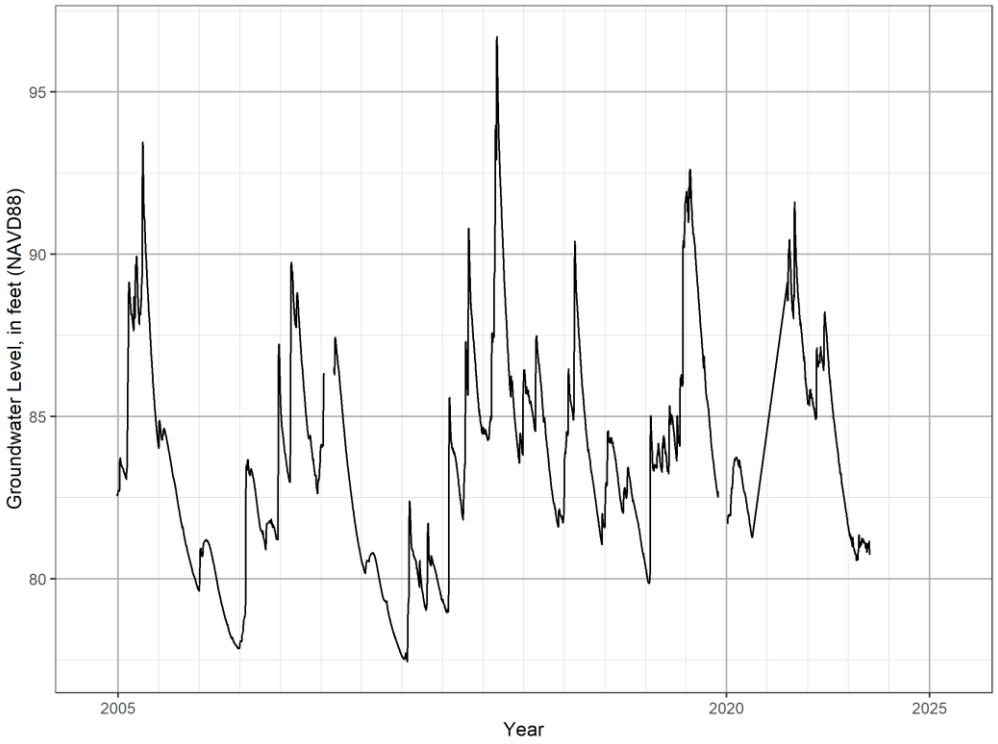

Figure 2-12. Time-series plot of historical groundwater levels from well 005266 NWFWMD-PITTMAN VISA/S661

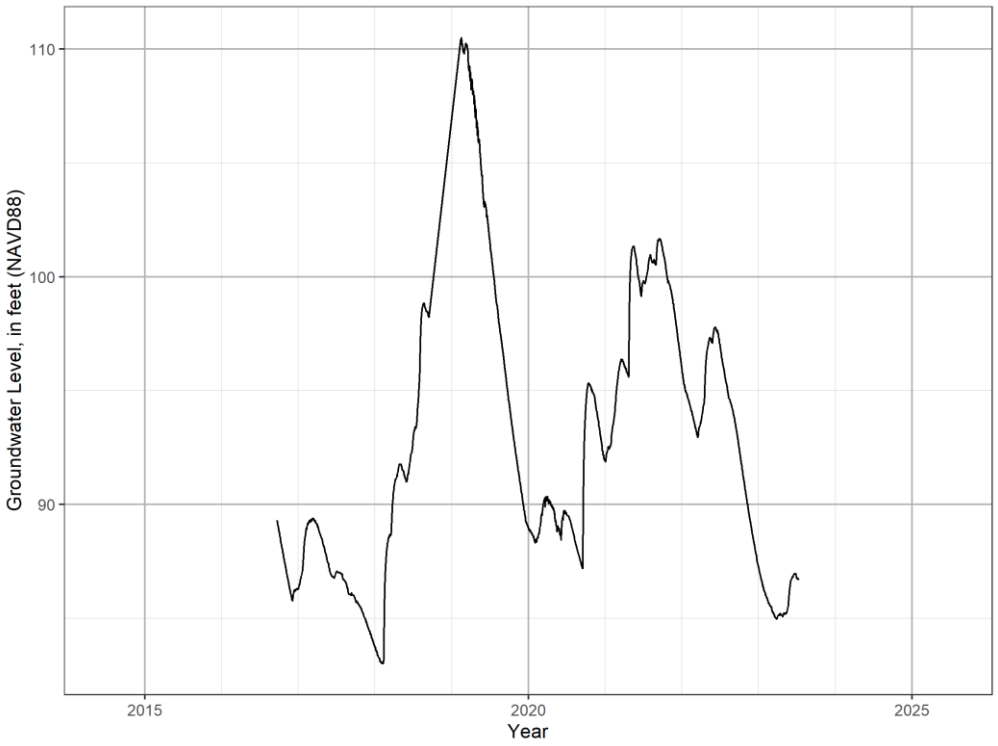

Figure 2-13. Time-series plot of historical groundwater levels from well 004795 INTERNATIONAL PAPER @ CYPRESS

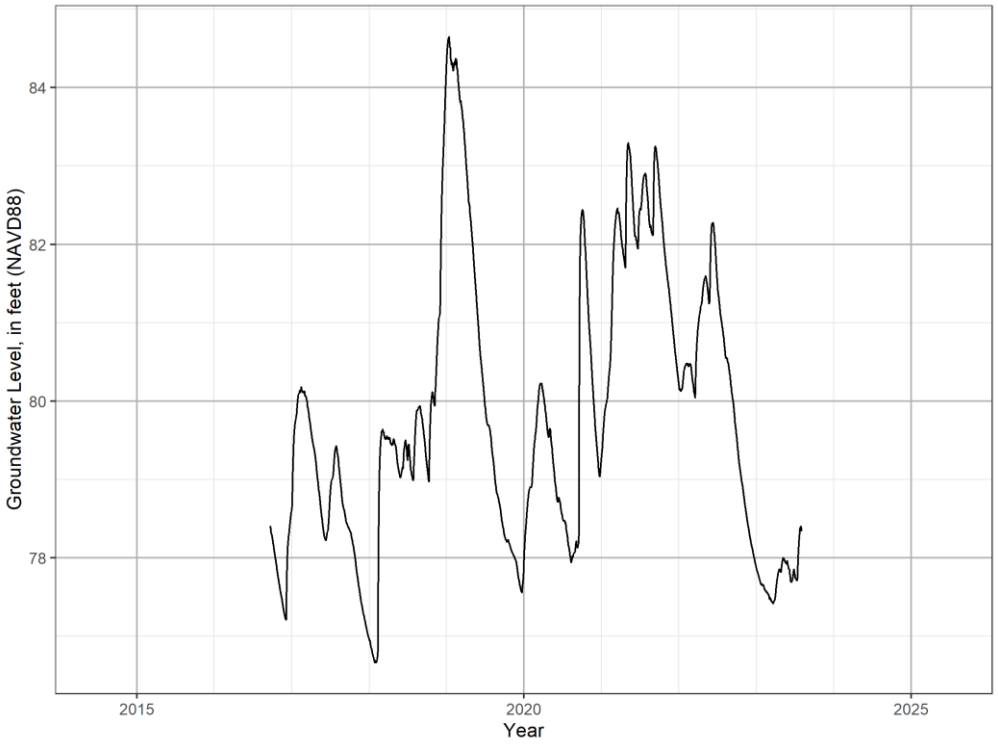

Figure 2-14. Time-series plot of historical groundwater levels from well 005226 NWFWMD-BAXTER SAND PIT VISA

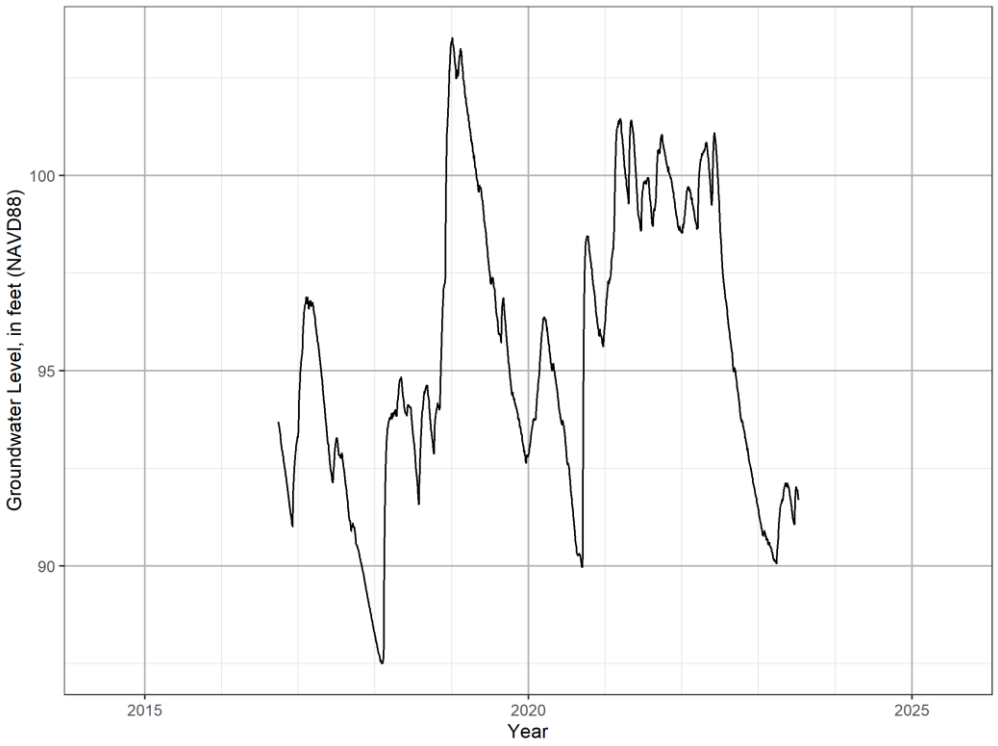

Figure 2-15. Time-series plot of historical groundwater levels from well 005408 NWFWMD-2 EGG AMBIENT #3

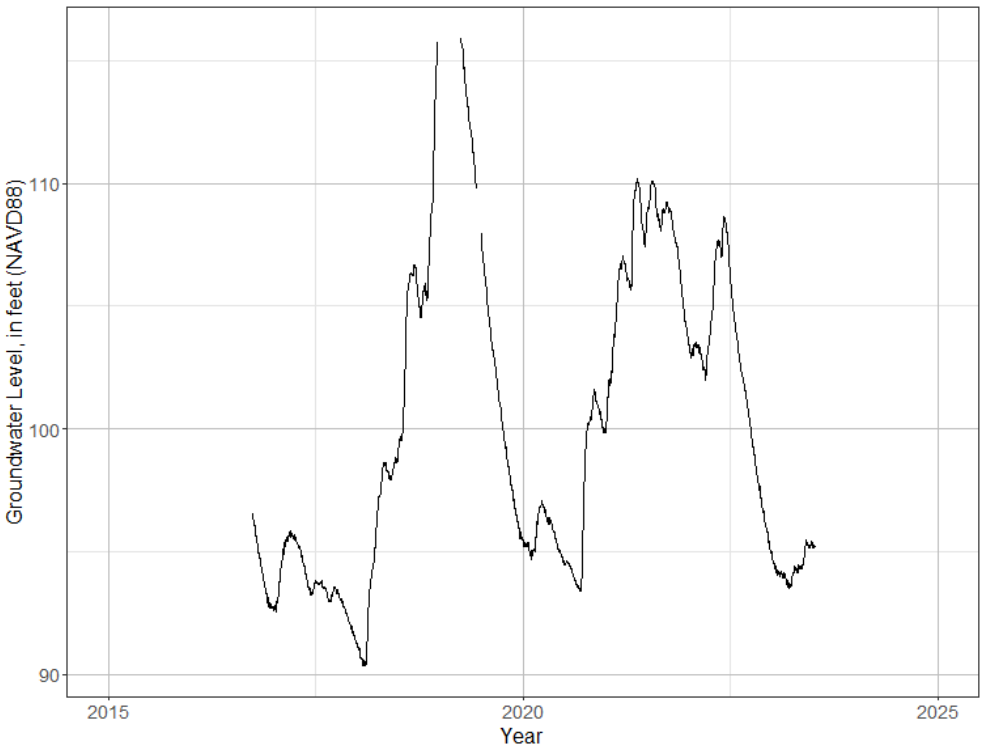

Figure 2-16. Time-series plot of historical groundwater levels from well 012797 CYPRESS PARK #1 – FLORIDAN

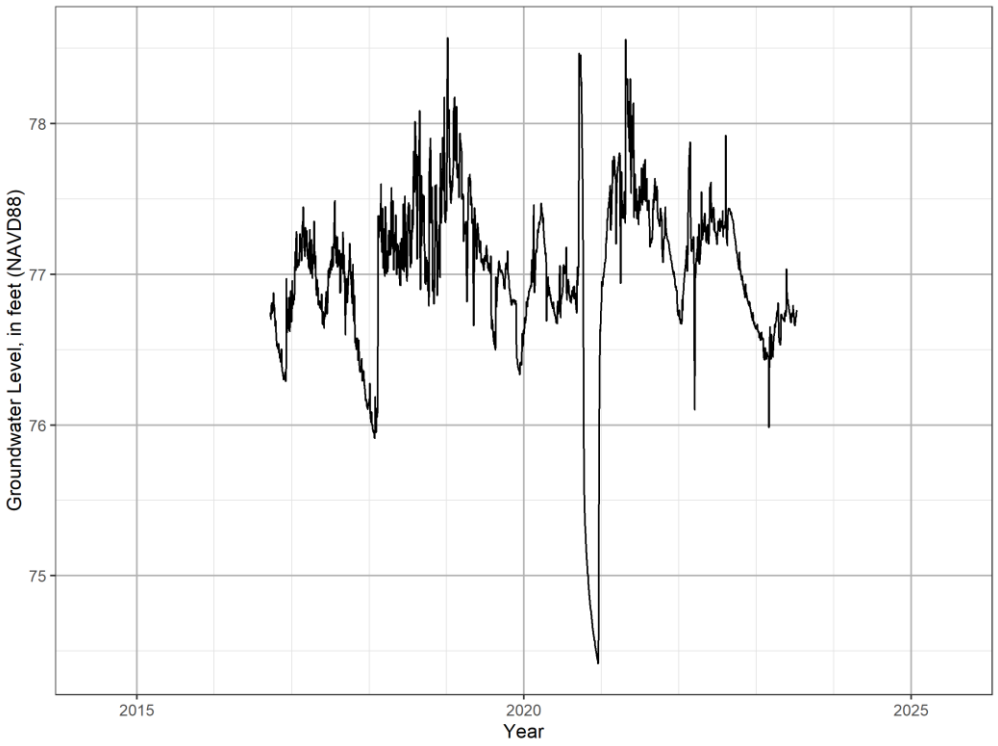

Figure 2-17. Time-series plot of historical groundwater levels from well 012769 JACKSON BLUE #2 - FLORIDAN

2-4. Surface Water Features

Streams, rivers, lakes, and wetlands are all present in the NCDM domain. The Chipola River and its numerous tributaries cover much of the area and are its primary means of surface drainage (Figure 2-1). A substantial portion of this channelized surface drainage is sustained by groundwater outflow from the surficial aquifer system or Upper Florida aquifer. Groundwater outflow to the Chipola River system is facilitated by several factors. Much of the Chipola River system is either incised directly into the Upper Floridan aquifer or drains areas where the Upper Floridan aquifer is unconfined, which eases the exchange of water between the streams and the aquifer. The numerous springs that occur along and near the banks of the Chipola River and its tributaries also provide a means for direct, concentrated discharge of groundwater to the river and tributaries. High annual rainfall rates (approximately 5 feet per year) result in relatively high recharge rates, which sustain groundwater levels sufficiently to create hydraulic gradients toward the streams and rivers in the NCDM domain. An example of this can be seen in the concave shape of the contour lines that define the Upper Floridan aquifer potentiometric surface near the Chipola River in the central and southern parts of the NCDM domain (Figure 2-10).

The Chattahoochee and Apalachicola Rivers occur along the eastern boundary of the NCDM and are also features that receive groundwater discharged from the Upper Floridan aquifer.

This is evident in the concave shape of the contours that define the Upper Floridan aquifer potentiometric surface along the Chattahoochee River in the northern part of the NCDM domain and along the Apalachicola River (Figure 2-10). Limited sections of the upper reaches of Econfina, Holmes and Wrights Creeks occur near the western boundary of the NCDM domain and also exchange water with the contiguous surficial aquifer.

Large lakes are generally absent from the NCDM domain. The exception is Lake Seminole, which occurs along the central part of the eastern boundary of the domain, at the confluence of the Chattahoochee, Flint, and Apalachicola Rivers, and intersection of the boundaries of Alabama, Florida, and Georgia. Smaller lakes also occur in some areas of the NCDM domain. Merritts Mill Pond is sustained by groundwater discharge from the Upper Floridan aquifer (including flow from Jackson Blue Spring), and its level is maintained by a small dam at its downstream extent. Wetlands are generally found along floodplain corridors and headwater areas adjacent to rivers and streams. An area of wetland features also occurs in an area west of Marianna, roughly between the towns of Cottondale, Alford, and Chipley. These wetlands occur within an area where the surficial aquifer system is less permeable, and therefore shallow water tables may be more likely. Surface water features are generally absent east and north of Jackson Blue Spring. This is a classic characteristic of karst areas, where dissolution of rock in the subsurface has created a highly transmissive aquifer capable of draining the system through the subsurface, rather than through a stream network.

3. Conceptual Model

A conceptual model of the groundwater flow system was developed to provide a basis for constructing and calibrating the numerical model of the system. Development of the model begins with a definition of a 'control volume' or active 'model domain' defining the volume of the subsurface to be conceptualized and ultimately represented numerically. Initial estimates of hydraulic properties can then be developed for this domain, along with estimates of stresses on the system, such as pumping from wells, groundwater recharge, and groundwater-surface water exchanges. These aspects of the conceptual model are described in the text that follows.

3.1 Model Domain

Definition of the NCDM conceptual and numerical model domain was based primarily on the hydrogeologic and hydrologic characteristics of the study area, as well as the intended use of the numerical model as a tool for estimating pumping effects on groundwater discharge from Jackson Blue Spring. A description of the lateral and vertical extent of the NCDM is described below.

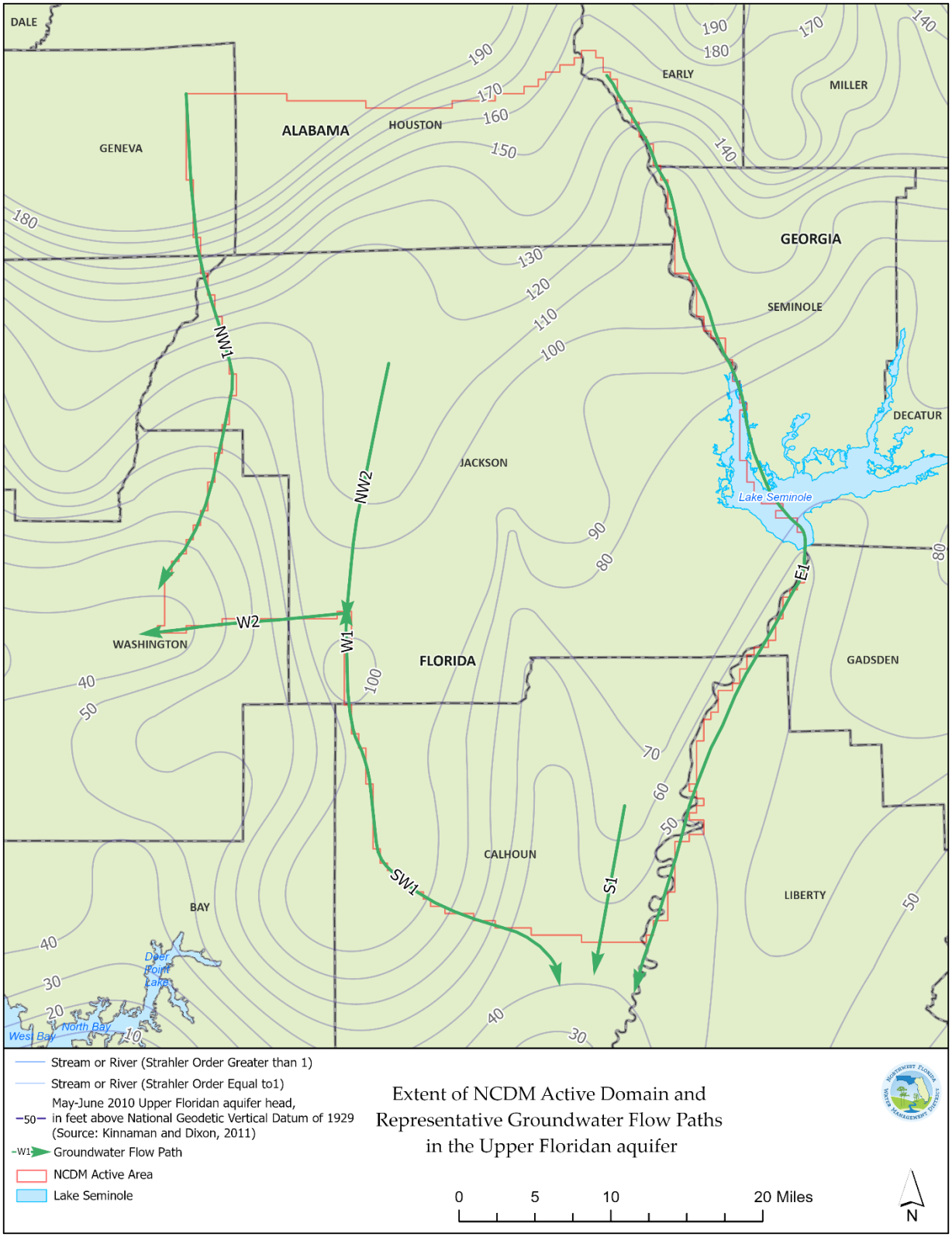

Figure 3-1. NCDM domain lateral extent and representative groundwater flow paths in the Upper Floridan aquifer

The lateral extent of the NCDM is defined almost entirely by features that approximate no-flow boundaries (Figure 3-1) along groundwater flow paths along historically persistent features in the potentiometric surface of the Upper Floridan aquifer. The exception is the northern extent of the model, which coincides with the up-dip limit of the productive part of the Upper Floridan aquifer, as defined by Williams and Kuniansky (2015), and is therefore also conceptualized as a no-flow boundary. This location also coincides with the "... approximate up dip limit of the carbonate facies" of the gradational sequence of carbonate and clastic facies within the Floridan aquifer system (Williams and Kuniansky, 2015). With a few exceptions, the eastern, western, and southern boundaries coincide with no-flow boundaries defined by groundwater flow paths that can be defined from consistent geographic patterns in Upper Floridan aquifer (UFA) historical groundwater level data and potentiometric surfaces. These were defined for the most part from the most recent aquifer-wide potentiometric surface map for the Upper Floridan aquifer (Kinnaman and Dixon, 2011). The groundwater flow paths associated with the eastern and western boundaries of the NCDM originate near the northern extent of the FAS. The eastern boundary (associated with the flow path labeled as E1 in Figure 3-1) coincides approximately with the Chattahoochee and Apalachicola rivers. Note that the eastern boundary of the NCDM (based on flow paths delineated from the potentiometric surface map) has been adjusted slightly in some areas to more closely align with the Chattahoochee and Apalachicola rivers. This was considered appropriate because flow path locations are subject to some degree of uncertainty because of limited spatial coverage of groundwater levels, and also because of the degree of interaction between these rivers and the UFA indicated by the shape of the potentiometric surface along this boundary.

The northern part of the western boundary of the NCDM coincides with a groundwater flow path (labeled as flow path NW1 in Figure 3-1) that is directed southward from the northern boundary of the NCDM, extending downgradient towards springs that discharge into Holmes Creek. It also includes another flow path (labeled as W2 in Figure 3-1) directed towards these springs that originates in southwestern Jackson County, at the intersection of two flow paths (labelled as NW2 and W1 in Figure 3-1) that coincide with a 'ridge' in the Upper Floridan aquifer potentiometric surface. The southwestern part of the lateral NCDM boundary is defined by a flow path (labeled as flow path SW1) that is directed along the southern part of this ridge, before turning toward eastward towards the lower reaches of the Chipola River, where it forms part of the southern lateral boundary.

There are two segments of the western and southern lateral boundaries that are not defined by persistent historical groundwater flow paths. The first of these is in the part of the western boundary closest to the springs along Holmes Creek (between flow paths NW1 and W2 in Figure 3-1), where groundwater within the UFA and NCDM flows westward out of the NCDM

towards those springs. The other segment is along the southern boundary roughly between the Chipola and Apalachicola Rivers (between flow path SW1 and E1 in Figure 3-1), where groundwater within the UFA flows out of the NCDM domain in a southerly direction (roughly parallel with flow path S1), towards the Gulf of America.

3-2. Hydraulic Properties

Development of a steady-state groundwater flow model like the NCDM requires specifying values of horizontal and vertical hydraulic conductivity (K_h and K_v, respectively). K_v can also be calculated as the product of K_h and the ratio, K_h divided by K_v. This ratio is referred to as hydraulic conductivity anisotropy, or simply as anisotropy. Prior to model calibration, initial estimates of hydraulic properties of a given hydrogeologic unit at a given location were assigned using one of two methods. The first method was to assign a uniform value to a given hydrogeologic unit throughout the model domain. This approach was used to assign initial estimates of anisotropy in all hydrogeologic units, and K_h in all hydrogeologic units except for the UFA. The values assigned to K_h were estimated based on the lithology of a particular hydrogeologic unit and corresponding literature values, or previous experience with models in Florida and the Coastal Plain (Table 3-1).

Table 3-1. Estimates of hydraulic properties of hydrogeologic units prior to calibration

Hydrogeologic Unit	Horizontal Hydraulic Conductivity, in feet per day			Anisotropy (Ratio of Horizontal to Vertical Hydraulic Conductivity)		
	Initial Estimate	Lower Bound Estimate	Upper Bound Estimate	Initial Estimate	Lower Bound Estimate	Upper Bound Estimate
Surficial Aquifer System	10	1.00E-01	2.00E+02	10	1	100
Upper Confining Unit	0.01	1.00E-04	1.00E-01	10	1	100
Upper Floridan Aquifer	2 - 233	1	1.00E+04	10	1	100
Middle Confining Unit	1	1.00E-02	1.00E+02	10	1	100
Lower Floridan Aquifer	25	0.5	1.00E+03	10	1	100

A second method was used to estimate initial values of K_h in the part of the NCDM domain representing the UFA and was based on the results from specific capacity and aquifer performance tests (collectively referred to as APT results in this report). This method was implemented by first creating a regular grid of point locations, spaced every 20 cells (47,500 ft apart) in the row and column directions and spanning the NCDM domain. Values of UFA K_h

were then estimated at each of these point locations based on the nearest APT-derived K_h values, which were calculated by dividing the APT-derived transmissivity values by the estimated thickness of the UFA at a given APT location. Note that in a number of instances, transmissivity (and therefore K_h) values from clusters of APT tests might exhibit considerable variability, so the values assigned to the regular grid of point locations described above represented a smoothed (spatially-averaged) estimate based on these APT results. A final set of initial K_h estimates was then computed at a denser grid of points, spaced approximately 14,600 feet apart in the row and column directions and spanning the NCDM domain. This second set of points are referred to as pilot points in this report and were the points at which K_h values were updated during the calibration phase of NCDM development, and from which K_h values at NCDM model-grid cells were interpolated during calibration. Additional implementation details are provided in later sections of this report that describe the construction and calibration of the numerical model.

These initial estimates of hydraulic conductivity served two purposes. First, they were necessary to construct a working version of the NCDM that could then be improved to better fit historical observations during model calibration. Second, they served as initial estimates of expected values of hydraulic conductivity that were used as 'preferred-value prior information' during the earlier phase of the calibration. These initial values were subsequently adjusted as the calibration process matured, reflecting knowledge gained during that process and an understanding of the limitations of these initial estimates. For example, APT-derived estimates of transmissivity and hydraulic conductivity typically are lower than the broader-scale values represented by a regional model like the NCDM. Values were also adjusted in some cases to be more consistent with previous modeling efforts in highly karstic areas of Florida.

3-3. System Stresses

The state of any groundwater flow system is represented by the spatial distribution of groundwater levels and flows at any given point in time and is a function of the hydraulic characteristics of that system, as well as the stresses acting on this system. These stresses typically include withdrawals or injections of water, groundwater recharge, losses from direct evapotranspiration from shallow groundwater, and exchanges between a given hydrogeologic unit and surface water body (groundwater-surface water interactions), as described in the sections that follow.

3-3-1. Pumping from Wells

Pumping from wells supplies groundwater to meet the needs for public supply (PS), industrial/commercial/institutional (ICI), domestic self-supply (DSS), recreational self-supply (REC), and agriculture (AG) uses within the NCDM domain. The rates and locations of

groundwater withdrawals in the NCDM domain were compiled and estimated for calendar years 2017 through 2019 (Friedman, May 2022), which is the time span that defines the calibration period of the NCDM. The sources of those data are listed in Table 3-2

Table 3-2. Sources of water use data in the NCDM domain.

Water Use Category	Region	Source	Description
PS, ICI	NWFWMD	NWFWMD	Based on reported pumpage from NWFWMD database
DSS	NWFWMD	NWFWMD	Based on methods used for 2018 NWFWMD Water Supply Assessment
REC	NWFWMD	NWFWMD	Based on reported pumpage from NWFWMD database and estimates from the 2018 NWFWMD Water Supply Assessment
AG	NWFWMD	NWFWMD/ FSAID	Based on reported pumpage from NWFWMD database and FSAID estimates
PS, ICI, REC, AG	Alabama	USGS/ Alabama Office of Water Resources Division	Based on USGS county level estimates and withdrawal locations provided by the Alabama Office of Water Resources
DSS	Alabama	USGS/ U.S. Census	Based on USGS county level estimates and U.S. Census block data

[PS, public supply; ICI, industrial-commercial-institutional; DSS, domestic self-supplied; REC, recreational; AG, agricultural; FSAID, Statewide Agricultural Irrigation Demand; NWFWMD, Northwest Florida Water Management District; USGS, U.S. Geological Survey]

Locations and rates of withdrawals of groundwater for PS and ICI uses in the Florida part of the NCDM domain were based on well-construction reports and groundwater withdrawals reported from District Individual Water Use Permits (IWUPs). These data are reported and stored in the District's well construction and IWUP databases at the station level, where a station generally represents an individual well. Locations and rates of withdrawals for REC uses were also obtained from reported data stored in the District's databases for REC users with permitted rates of 0.1 million gallons per day (MGD) or greater. REC users falling below this threshold are not required to report their withdrawals to the District. Withdrawals for these unreported uses typically represent withdrawals from private landscape irrigation wells and were estimated to be 76 gallons per day per well, which was the estimated rate used in the District's 2018 Water Supply Assessment (NWFWMD, 2018). The locations of these wells were obtained from the District's well construction database, after eliminating REC wells that had been previously accounted for in the set of REC wells with reported groundwater withdrawals or wells with abandonment permits. Groundwater withdrawals for

PS, ICI, and REC uses were assigned to layers based on individual well construction information.

Locations of withdrawals of groundwater for agricultural uses in the Florida part of the NCDM domain were obtained from District well-construction and IWUP databases whenever possible. The locations and withdrawal rates of wells that are below reporting thresholds can generally be estimated from geospatial datasets from the Florida Statewide Agricultural Irrigation Demand project (FSAID; Balmoral Group, 2019; Balmoral Group, 2020; Balmoral Group, 2021). Starting in 2013, the FSAID project was initiated as a joint effort between Florida Department of Agricultural and Consumer Services (FDACS) and all five Water Management Districts to estimate and project agricultural water demands throughout the entire state of Florida. Estimates are developed and updated on an annual basis providing baseline estimates and projections every five years for a 20-year horizon. The end-product of the FSAID project is a GIS dataset of irrigated areas with attributes specifying crop type and with baseline and projected water use. Aggregate information by county and WMD is also provided.

Areas with agricultural water uses below reporting thresholds were defined by selecting polygon features from the FSAID Irrigated Lands dataset that did not contain an agricultural well with reported withdrawal data within a 0.5-mile buffer radius of a given polygon. Withdrawals from these selected polygon features were then assigned to the centroid of these irrigated lands polygons. Groundwater withdrawals for agricultural use were assigned to the Upper Floridan aquifer, as there are no known large agricultural withdrawals from the surficial aquifer system or the lower Floridan aquifer within the model domain. Yields from the surficial and intermediate aquifers are typically insufficient to operate center pivots that are typically used in agricultural operations in this area.

Withdrawals of groundwater for domestic self-supplied (DSS) uses in the Florida part of the NCDM were based on annual, county-level DSS use totals estimated by District planning staff. Locations of DSS wells in Florida were determined by selecting DSS wells from the District's well construction database. Groundwater withdrawal at individual DSS wells were then estimated by uniformly distributing the county-level DSS totals for a given year among all active DSS well in a given county. The status (active or inactive) of a given DSS well was determined based on the date that a well was constructed and whether an abandonment permit had been issued for that well. County-level DSS totals were uniformly distributed to the subset of DSS wells determined to be actively used for a given calibration year and county. Groundwater withdrawals for each year were distributed to model layers based on available well construction information. In the Floridan portion of the NCDM domain, DSS withdrawals occurred in the SAS, UFA, with some minor use from the MCU.

Estimated groundwater withdrawals within the Alabama portion of the NCDM domain are apportioned to model layers based on well construction information that was available at 33 wells. The fraction of a well's open interval that was exposed to each hydrogeologic unit was calculated at each of these 33 wells, and an average value of this fraction was then calculated for each hydrogeologic unit. The result of this analysis showed that, on average, 71 and 29 percent of the wells' open intervals were exposed to the UFA and LFA, respectively. Accordingly, withdrawals from wells in Alabama were apportioned to the UFA and LFA using these averages.

Groundwater withdrawal rates for all water use categories within the Alabama portion of the NCDM domain for were based on USGS water use data for years 2010 and 2015 (U.S. Geological Survey, 2016). USGS estimates were not available for year 2020 at the time the NCDM was being developed. Groundwater withdrawals for public supply and domestic self-supply uses in Alabama were based on county-level total withdrawal rates that were estimated for each year within the 2017-2019 calibration period by linearly extrapolating from the 2010 and 2015 county totals. Groundwater withdrawals for agriculture uses in Alabama in 2017-2018 were assigned the average of USGS reported values for 2010 and 2015 in Houston and Geneva counties, respectively. ICI, REC, and power generation uses were insignificant within the Alabama portion of the domain.

County-level USGS DSS groundwater withdrawal estimates were distributed to centroids of U.S. Census blocks in Houston and Geneva County based on population density (U.S. Census Bureau, 2010). The ratio of census block 2010 population to county-total 2010 population was calculated and multiplied by total county DSS groundwater withdrawal for each year of analysis for each block within Houston and Geneva County and assigned to the centroid of the census blocks.

The locations of withdrawals for non-DSS and agriculture use categories were obtained from withdrawal locations provided by the Alabama Office of Water Resources (AOWR) (AOWR, 2023). This dataset included latitude, longitude, source/aquifer, well and casing depth, average pumpage per well, and monthly pumpage for select years for 543 wells within southeastern Alabama. Wells in this dataset were assigned to a water-use category based on a District staff review of well owner information and Alabama certificate category (public, non-public, or agriculture). No ICI use was assumed in the Alabama portion of the NCDM domain. County-level USGS public supply withdrawal values were spatially distributed to withdrawal locations provided by the AOWR, based on values of the "average use per well" variable in the dataset provided by the AOWR (AOWR, 2023). Although monthly pumpage for the NCDM calibration years was not directly available from the AOWR data set, the monthly pumpage values were similar to county totals in USGS reports. Additionally, the USGS

reported no withdrawals of groundwater for recreation or landscape uses in Houston or Geneva counties.

Total county USGS groundwater use for public supply in Alabama was distributed to public supply wells within each county by prorating the total county use based on average reported use per well. County-level estimates of groundwater withdrawals for agricultural water use derived from the USGS datasets were distributed spatially to irrigated agricultural areas identified from two different sources. In Houston County, irrigated agricultural areas were identified using the areas mapped by Marella and Dixon (2014). Since Marella and Dixon's (2014) study area did not include the northern 30 percent of Houston County, the county level irrigation rates assigned to agricultural irrigation wells in Houston County were reduced by 30 percent. In Geneva County, the National Land Use Cover (NLCD; Dewitz and U.S. Geological Survey, 2021) was used to spatially distribute county USGS totals to features within Geneva Count with NLCD codes 81 and 82 (representing agriculture land use). The USGS agricultural irrigation groundwater withdrawals for Geneva County were multiplied by a factor of 0.05 to approximate withdrawal totals within the study area, since roughly 5 percent of Geneva County is within the NCDM domain. This adjusted total was distributed to irrigated area polygons in Geneva County based on the ratio of a given polygon's area to the sum of all agricultural irrigation polygon areas in Geneva County. A summary of the groundwater withdrawal estimates in the NCDM domain for years 2017-2019 is shown in Table 3-3. The geographic distribution of these withdrawal estimates are shown later in this report, in Figure 4-7 (in the section describing the construction of the numerical model).

Table 3-3. Groundwater Use Estimates in the NCDM domain in years 2017-2019

Water Use Category	Region	Groundwater Withdrawal, in millions of gallons per day		
		2017	2018	2019
Agriculture	Alabama	4.30	4.30	4.30
	Florida	21.62	19.13	24.92
Domestic Self Supplied	Alabama	0.19	0.18	0.17
	Florida	4.04	3.79	3.39
Industrial-Commercial-Institutional	Alabama	0.00	0.00	0.00
	Florida	0.01	0.00	0.00
Public Supply	Alabama	0.71	0.72	0.74
	Florida	4.07	3.82	4.04
Recreational Self Supplied	Alabama	0.00	0.00	0.00
	Florida	0.03	0.04	0.05
Total	**Alabama**	**5.20**	**5.20**	**5.21**
	Florida	**29.77**	**26.78**	**32.40**
	Alabama and Florida	**34.97**	**31.98**	**37.61**

3-3-2. Evapotranspiration

The combined effect of evaporation and transpiration (evapotranspiration; ET) is an important component of the water budgets of hydrologic systems. The upper boundary of the NCDM domain is the water table, and ET affects the amount of water flowing across this boundary. Evaporation and transpiration from the plant canopy, soil surface, and unsaturated zone (collectively referred to as ET_{uz} in this report) reduce the amount of rainfall that ultimately reaches the water table as groundwater recharge. In areas where the water table is shallow enough to saturate shallower depths in the subsurface or inundate the land surface, outflows across the water table boundary can occur as water evaporates directly from exposed or shallow groundwater. The additional amount of ET that can occur (beyond that estimated for ET_{uz}) from these extractions of near-surface groundwater by ET are referred to as referred to as ET_{sat} in this report. In areas where the water table is deep enough so that no ET_{sat} can occur, actual ET rates (ET) are equal to ET_{uz}. In areas where the water table is shallow enough so that ET_{sat} can occur, actual ET rates equal the sum of ET_{uz} and ET_{sat}. In this study, it is assumed that the maximum value of ET_{sat} ($ET_{sat,max}$) occurs when the water table is at or near the land surface. Under these conditions, water is available in sufficient quantities to satisfy atmospheric demands, and the ET rate is assumed to be equal potential evapotranspiration (ET_p) rate.

Average rates of ET_{uz} were estimated in the NCDM domain during the 2017-2019 calibration using spatially-distributed potential ET (ET_p) datasets developed by the U.S. Geological Survey (2019). The ET_p datasets have a daily temporal resolution, a 2-kilometer spatial resolution, and span the state of Florida. However, these data were not available in Alabama for the 2017-2019 calibration period, so the first step in this process was to compute a consistent set of ET_p values that spanned the entire NCDM domain, including the part of the domain in Alabama. ET_p is largely a function of incoming solar radiation and therefore lattitude. Therefore, the first step in this estimation process was to fit a linear regression model to the ET_p dataset that estimates ET_p as a function of latitude and then using this regression model to estimate average ET_p during 2017-2019 at every cell in the NCDM. Estimates of average ET_{uz} during 2017-2019 were then computed using a linear relation between actual evapotranspiration (ET) and ET_p using the equation $ET_{uz} = ET = -0.045 + 0.54ET_p$, where the intercept and slope coefficients (-0.045 and 0.54, respectively) in this equation represent the average of the intercept and slope coefficients from the Lake Wales Ridge and Lyonia Preserve actual versus potential evapotranspiration equations described in O'Reilly (2007). Note that both sites had very deep water tables, so ET_{sat} at these sites should be negligible and the ET rates therefore represent ET_{uz}. Average $ET_{sat,max}$ during 2017-2019 was then estimated at each NCDM grid cell as ET_p minus ET_{uz}.

The average ET_{uz} during 2017-2019 estimates varied (spatially) over a range of about 26.4 to 28.9 inches per year, with a mean value of 27.6 inches per year. The average $ET_{sat,max}$ during 2017-2019 estimates varied spatially over a range of about 21.7 to 23.6 inches per year, with a mean value of 22.7 inches per year. Given their underlying relation between latitude and PET, the estimated rates of ET_{uz} exhibited an expected north-south trend (Figure 3-2), as did $ET_{sat,max}$. Note that ET_{uz} and $ET_{sat,max}$ are based on the simplifying assumption that ET_p is a simple function of latitude; whereas, in the real world, ET_o (and therefore ET_{uz} and $ET_{sat,max}$) will exhibit more spatial variability and a larger range (and uncertainty) than that implied by Figure 3-2 because ET_p also depends on variables that are not necessarily dependent on latitude. Nevertheless, the ET_{uz} and $ET_{sat,max}$ values computed in this analysis are considered useful for the purposes of NCDM development because they are intended provide reasonable, initial estimates of variables necessary for construction of the initial (pre-calibration) numerical version of the NCDM.

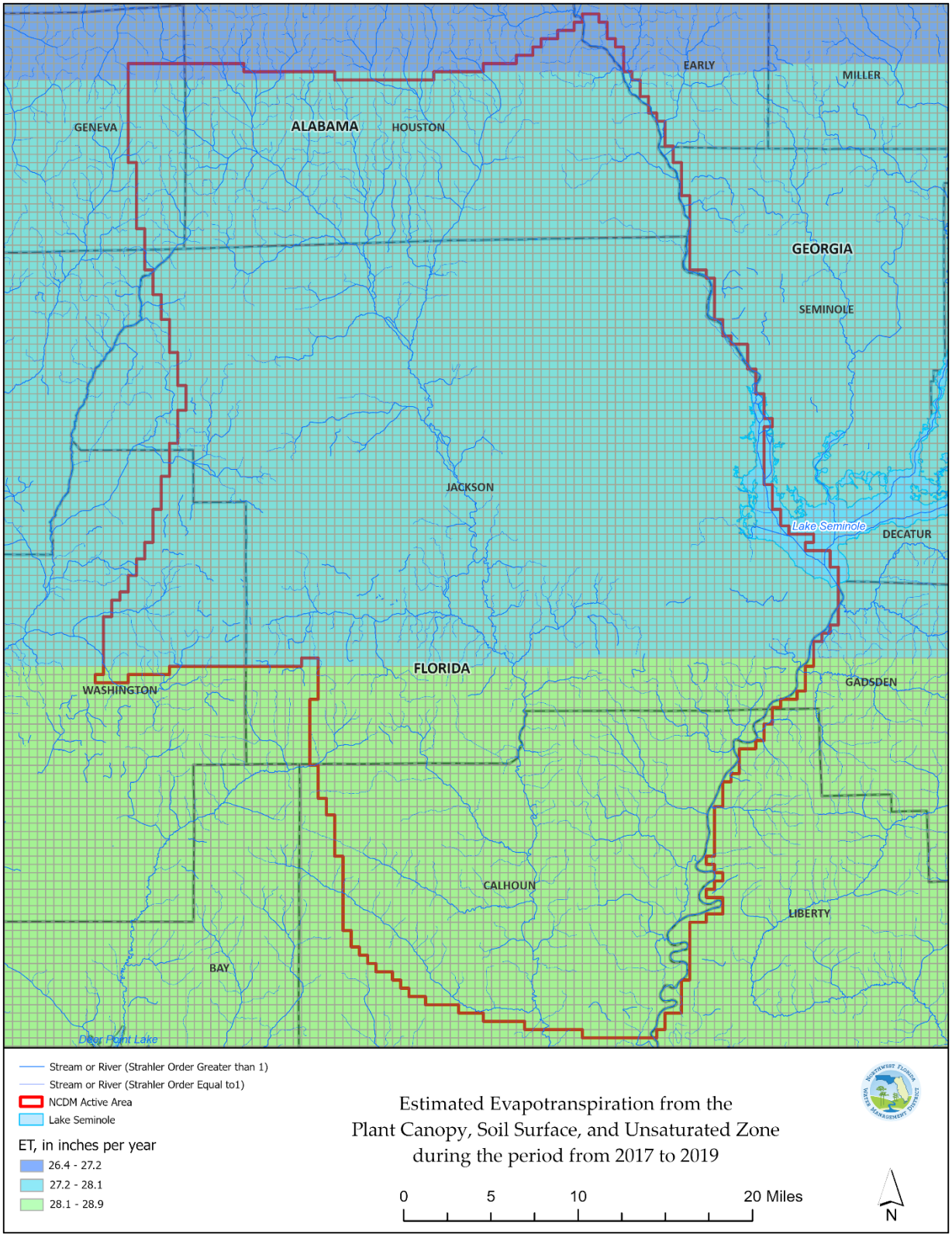

Figure 3-2. Estimated evaporation and transpiration (ET) from the plant canopy, soil surface, and unsaturated zone during the period from 2017 to 2019

3-3-3. Groundwater Recharge

Groundwater recharge to the upper-most active layer in the NCDM was estimated using a water balance approach, expressed with the following equation:

$$R = P - ET_{uz} - Q_d \quad (1)$$

where R represents groundwater recharge to the water table,

P represents precipitation (rainfall),

ET_{uz} represents evaporation and transpiration from the plant canopy, soil surface, and unsaturated zone (unsaturated zone ET), and

Q_d represents direct (storm) runoff.

Spatially-distributed ET_{uz} rates during the NCDM calibration period were estimated using the method described in the previous section of this report. Spatially-distributed precipitation rates during the NCDM calibration period were based on National Weather Service Surveillance Radar (WSR-88D) Doppler radar rainfall data that have been adjusted with rainfall estimates from District rainfall stations (Vieux, 2020). These data were produced at a daily time step and at a 2 kilometer by 2 kilometer resolution. Average recharge values were computed for the 2017-2019 calibration period at each cell in the Vieux (2020) rainfall grid and then used to compute corresponding 2017-2019 average precipitation rates for each cell in the NCDM grid using the QGIS (QGIS Development Team, 2024) software Zonal Statistics command.

Urban development is largely absent in the NCDM domain, and the primary mechanism for generating direct runoff most likely through saturation excess runoff in (floodplain and riparian) areas adjacent to streams where water tables are at shallower depths and soil moisture content is generally higher. In these areas, soils can reach saturation or near saturation levels readily during storms, leading to storm runoff that can be easily conveyed to (and away by) adjacent streams and rivers. Accordingly, areas of the NCDM that were not in close proximity to a receiving stream or river were assumed to have negligible rates of storm runoff in the conceptual model. Areas in close proximity were defined as those coinciding with NCDM grid cells (see later section describing the discretization of the NCDM domain) containing stream or river features. Storm runoff was estimated at the two stream gages in the NCDM domain that have long-term, continuous records: the USGS 023258789 Chipola River at Marianna, Florida gage and the downstream gage, USGS 02359000 Chipola

River near Altha, Florida. These storm runoff estimates were computed for the 2017-2019 calibration period at both sites by subtracting the estimated average baseflow during this period at each of these gages from the corresponding average total streamflow at the gage during that period. Baseflow estimates were computed using the approach described later in this report.

Once the direct runoff was estimated at each gage, the values were distributed to NCDM grid cells coincident with stream features represented in the 1:100,000 scale National Hydrography Dataset Plus (NHDPlus) dataset (McKay and others, 2012). The direct runoff at the Chipola River at Marianna gage was distributed evenly across all NCDM cells containing stream features that contribute flow to this gage. This was accomplished by dividing volumetric rate of direct runoff during the 2017-2019 calibration period (in units of volume per unit time) at the Chipola River at Marianna gage by the total area of NCDM cells containing stream features that contribute flow to that gage. This resulted in an estimated average rate of direct runoff of 15.5 inches per year over these cells during 2017-2019. A similar procedure was used for cells that coincide with stream features that contribute to the Chipola River near Altha, but do not contribute flow to the upstream gage on the Chipola River at Marianna. The (volumetric) average direct runoff from this set of cells was estimated using the following formula:

$$\Delta Q_d = Q_{d,Altha} - Q_{d,Marianna} = Q_{Altha} - Q_{Marianna} - (Q_{b,Altha} - Q_{b,Marianna}) \quad (2)$$

where ΔQ_d represents the volumetric rate of direct runoff between the Chipola River near Altha and Chipola River near Marianna gages,

$Q_{d,Altha}$ direct runoff to the Chipola River near Altha gage,

$Q_{d,Marianna}$ direct runoff to the Chipola River at Marianna gage,

Q_{Altha} total flow to the Chipola River near Altha gage,

$Q_{Marianna}$ total flow to the Chipola River at Marianna gage,

$Q_{b,Altha}$ baseflow to the Chipola River near Altha gage,

$Q_{b,Marianna}$ baseflow to the Chipola River at Marianna gage.

This resulted in an estimated average rate of direct runoff of 19.4 inches per year over the cells contributing flow to the Chipola River near Altha gage (but not the Chipola River at Marianna gage) during 2017-2019. Direct runoff to cells coinciding with stream features that

did not contribute to either of these two gages was estimated as 17.45 inches, which is the average of the direct runoff estimates at the two gages.

The result of applying equation 1 to compute an initial estimate of average recharge rates for the NCDM domain during the 2017-2019 period is shown in Figure 3-4. It should be noted that uncertainties in values of the hydrologic variables represented by the terms on the right sides of equations 1 and 2 propagate and contribute to the uncertainty of the spatially-distributed recharge estimates.

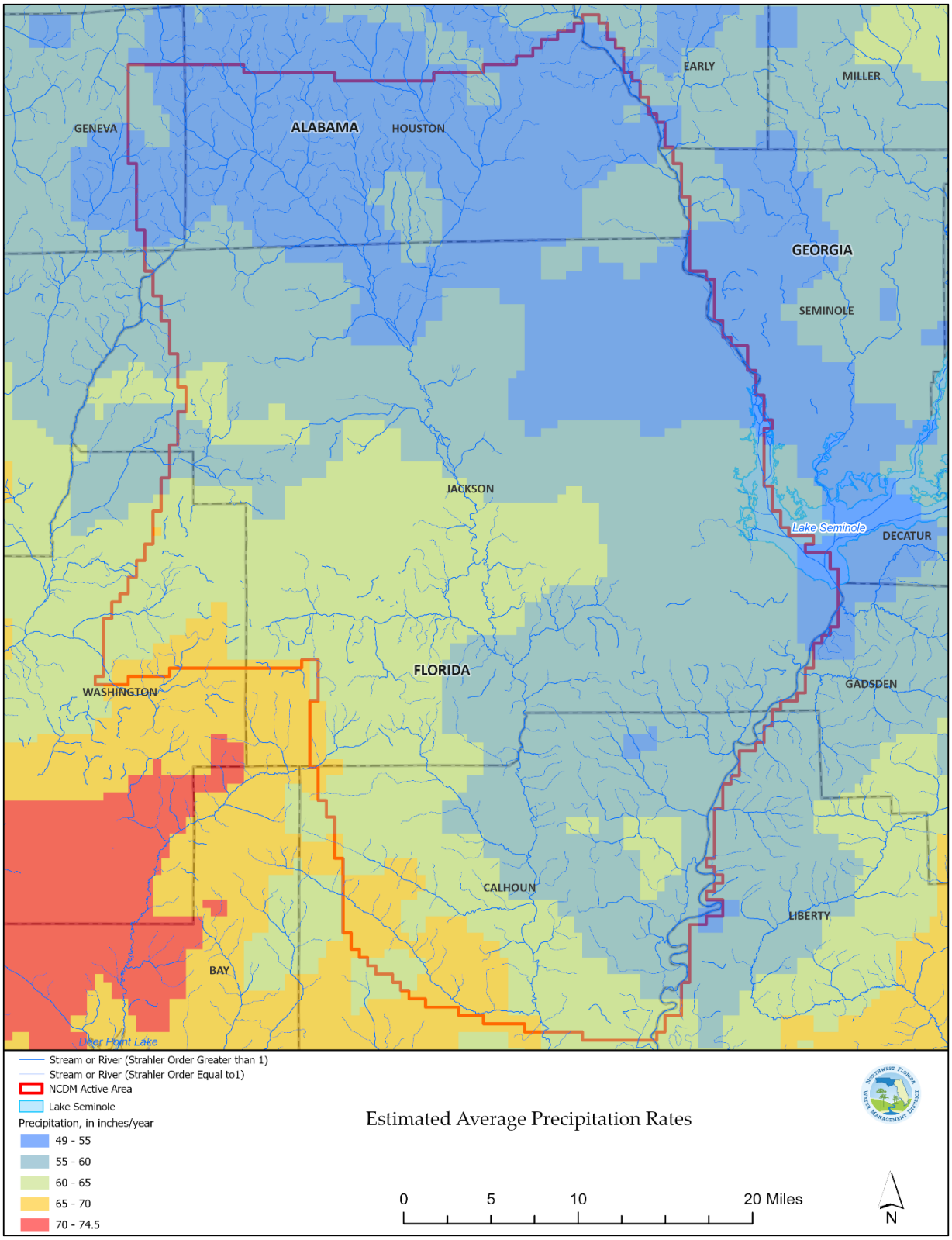

Figure 3-3. Estimated average precipitation rates during 2017-2019

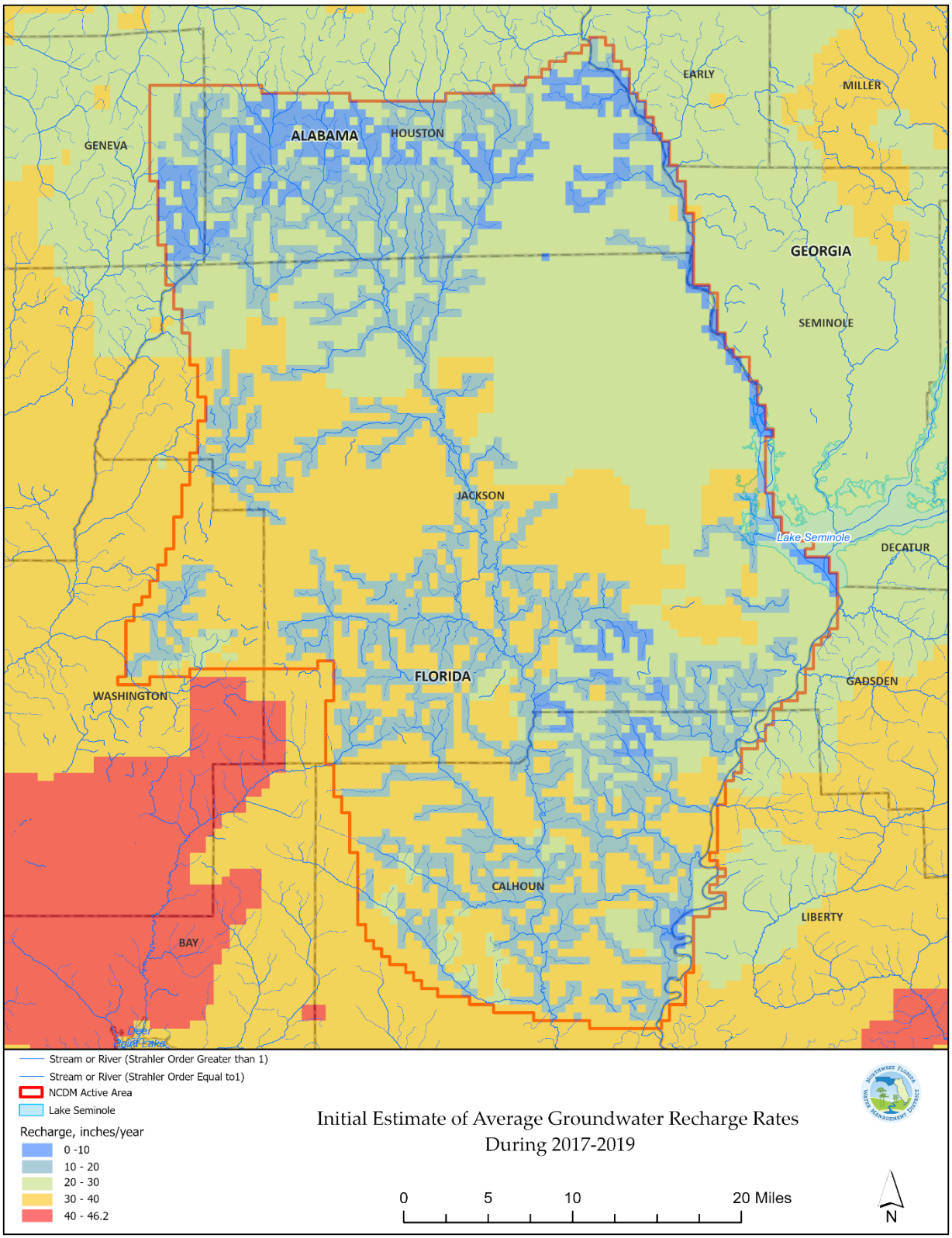

Figure 3-4. Initial (conceptual model) estimate of average groundwater recharge rates during 2017-2019

3-3-4. Groundwater-Surface Water Interactions

Streams, rivers, and spring features represent important boundary conditions within the groundwater flow system. Groundwater-surface water exchanges occur throughout the NCDM, wherever these features occur. These features often act important outlets or 'sinks' for the groundwater system, receiving groundwater outflows (discharges) from aquifers and conveying them downstream and ultimately out of the NCDM domain as stream and river flows. Most of the groundwater discharge from the groundwater flow system represented in the NCDM is expected to occur along the Chipola River and lower reaches of its tributary streams, where these features are typically more deeply incised into contiguous aquifers or where aquifer confinement (if present) is thinner or less continuous. Springs represent locations of concentrated groundwater discharge along the Chipola River and its tributaries and also serve as 'headwater features' for some tributaries. Stream-to-aquifer leakage can also be a source of water for the groundwater flow system. This generally occurs in topographically higher areas and upper reaches of streams, where stream stages can sometimes exceed groundwater levels in contiguous aquifers.

Two USGS gages with historical, continuous daily time series of stream flow exist along the Chipola River: USGS 02358789 Chipola River at Marianna, Florida, and USGS 02359000 Chipola River near Altha, Florida. Groundwater contributions to streamflow were estimated using baseflow-separation techniques at both sites for the 2017-2019 period, using methods described later in this report. Groundwater contributions to the Chipola River at Marianna were estimated to be about 550 cfs during this period. Fifteen springs with historical discharge measurements occur along this reach, and their collective flow contributions to this reach were estimated from these measurements to be about 90 cfs. Groundwater contributions to the Chipola River near Altha gage were estimated to be about 1,150 cfs, indicating a roughly 600 cfs groundwater contribution to the tributaries and section of the river that define the reach between Marianna and Altha gages. Twenty-three springs with historical flow measurements exist in the reach between these two gages, and their collective flow contributions to this reach were estimated from these measurements to be about 330 cfs (or roughly half of the total groundwater flow to the reach).

The lower reaches of the Chipola River (downstream from the Altha gage) and many of its tributaries are deeply incised into the surrounding topography, although still well above the top of the Upper Floridan aquifer, which is overlain by the upper confining unit in this part of the domain. Accordingly, the lower part of the Chipola River basin would be expected to receive groundwater contributions from the surficial aquifer system. Historical potentiometric surface maps of the Upper Floridan aquifer also indicate the likelihood of upward leakage of groundwater from the Upper Floridan aquifer to this lower reach of the Chipola River. However, the presence of the upper confining unit limits the rate of this

leakage, so the surficial aquifer system is most likely the primary source of groundwater discharge to the lower Chipola River and its tributaries.

Stream-aquifer exchanges of water also occur in reaches not associated with the Chipola River system. The eastern NCDM boundary generally coincides with the Chattahoochee and Apalachicola rivers and these river reaches are incised (or nearly so) into the Upper Floridan aquifer along much of these reaches. Historical potentiometric surface maps of the Upper Floridan aquifer also indicate that groundwater flows from the Upper Floridan aquifer into these reaches from the easternmost parts of the NCDM domain.

Two other smaller drainage systems exist in the NCDM domain. The first of these are the tributaries draining the northwestern and western area of the NCDM domain and that ultimately flow into Holmes Creek, which is west of the NCDM domain. The other drainage system is the uppermost reaches of Econfina Creek. Both systems are small headwater drainages in topographically higher areas, so groundwater inflow to these systems may be lower and the potential for stream to aquifer leakage may be greater.

3-3-5. Groundwater Discharge Across the Domain Boundary

As described previously, groundwater discharges across the NCDM domain in two locations. The first location is in the central part of the western boundary between flow paths labelled NW1 and NW2 in Figure 3-1. Groundwater flows in a westerly direction at this location, towards springs that sustain the flow of Holmes Creek. Historical potentiometric surface maps of the Upper Floridan aquifer indicate that a large fraction of the flow to the springs along Holmes Creek is derived from flow across this part of the NCDM boundary. Much of this spring flow is measured at the stream gaging station 02366000 Holmes Creek at Vernon, Florida. The historical stream flow hydrograph of Holmes Creek suggests that the base flow of Holmes Creek is probably within a range of about 300 to 600 cubic feet per second during the period from January 1, 2017, through December 31, 2019. Therefore, it is likely that flow across this part of the western boundary of the NCDM is on the order of a few hundred cubic feet per second.

The other location where groundwater discharges across the NCDM domain boundary is along part of the southern boundary, between flow paths labelled SW1 and E1 in Figure 3-1. Flow across this part of the boundary is difficult to estimate; however, the magnitude of flow is likely to be fairly small. For example, the groundwater flow rate across this part of the southern NCDM boundary would be about 1 cubic foot per second, assuming a hydraulic gradient in the UFA of about 1×10^{-4} (based on the May- June 2010 UFA potentiometric surface map by Kinnaman and Dixon (2011)), the combined thickness of the UFA and LFA of about 750 feet, horizontal hydraulic conductivity in the UFA on the order of 10 feet per day, and the approximately 8 mile length of this part of the boundary.

3-3-6. Domain Water Budget

The various system stresses described in the previous paragraphs represent the component fluxes of water across the boundaries that define the domain of the NCDM. This domain can be thought of as a 'control volume' within which any change in the amount of water stored in the domain is equal to the difference between inflows to and outflows from the domain. This statement can be represented by the following water budget equation, which is essentially a conservation of mass equation, since variations in the density of groundwater within the NCDM domain are expected to be negligible:

$$\Delta S = R - ET_{gw} - W - Q_{gw \leftrightarrow sw} - Q_{bnd} \quad (1)$$

where:

ΔS represents the change in the volume of water stored in the domain,

R represents recharge to the water table,

ET_{gw} represents evapotranspiration from the water table,

W represents net groundwater withdrawals from wells

$Q_{gw \leftrightarrow sw}$ net groundwater discharge to streams, rivers, and springs

Q_{bnd} net groundwater flow out of the domain, across the NCDM boundary

The NCDM was developed as a steady-state model, and changes in storage under steady-state conditions are, by definition, zero. Therefore equation (1) can be rearranged with inflows equal to outflows as follows:

$$R = ET_{gw} + W + Q_{gw \leftrightarrow sw} + Q_{bnd} \quad (2)$$

Estimated values of these inflow and outflow terms for the period spanning calendar years 2017 through 2019 are shown in Table 3-4. The values shown represent average rate for the NCDM domain, expressed as volume per unit area per unit time (length per unit time). It should be noted that estimating the terms of real-world water budget equations are generally subject to a considerable degree of uncertainty and the NCDM is no exception. As such, the values shown in the table are presented as a ranges. The ranges shown assume a 25 percent variation from the expected value for the model domain and are just a rough approximation. These values represent ranges in the domain-wide average for each component, so budget-component values are expected to exceed these ranges within more localized areas of the domain, depending on local factors.

Table 3-4. Estimated Domain-Averaged Water Budget Components for the NCDM Conceptual Model

Budget Term	Estimated Value, inches per year
Recharge	18 to 30
Evapotranspiration from the water table	3 to 5
Groundwater withdrawal from wells	0.4 to 0.6
Net groundwater discharge to streams, rivers, and springs	14 to 22
Net groundwater flow out of the NCDM domain	2 to 3

4. Numerical Model Construction

Construction of the initial, uncalibrated version of the NCDM consisted of four components: (1) selecting the model code to solve the appropriate system of equations that constitute the model, (2) defining the spatial extent of the model and its discretization, (3) hydraulic property assignment, and (4) boundary condition assignment. Each of these components are discussed in the following sections.

4-1. Model Code and Governing Equation

As noted previously, the primary objective driving development of the NCDM was that it be used to support establishing a minimum flow for Jackson Blue Spring. Specifically, the model should be a useful tool for estimating how much the flow from Jackson Blue Spring would be expected to change in response to changes in the magnitude and spatial distribution of groundwater withdrawals from wells. Historically, tools used to address this type of problem in Florida and elsewhere have been implemented using one of the various computer programs from the Modular Groundwater Flow (MODFLOW) set of programs from the U.S. Geological Survey that solve the equation for saturated, constant-density flow of liquid water through a porous medium. This equation is derived by combining the equations describing the conservation of fluid volume and momentum, the latter expressed as Darcy's Law.

The NCDM is implemented using the MODFLOW-NWT (Niswonger and others, 2011) version of the MODFLOW set of computer programs for simulating groundwater flow (U.S. Geological Survey, 2022). This version was selected because of its successful implementation for similar applications in Florida and elsewhere, its widespread use and support, open-source distribution, and robust performance when "… solving problems involving drying and rewetting nonlinearities of the unconfined groundwater-flow equation" (Niswonger and others, 2011). The groundwater flow system is represented in the NCDM by discretizing the model domain into structured grid of 'cells.' The MODFLOW-NWT software computes hydraulic head at each cell and flows between cells and associated boundary condition features, by (1) defining a groundwater flow equation for each of these cells based on their geometry, hydraulic properties and boundary conditions, (2) assembling these equations into a system of equations represented in matrix form, and (3) solving this system of equations is using numerical methods. The Newton solution method was used to solve the systems of equations for the NCDM, using the under-relaxation scheme and 'Complex' option described by Niswonger and others (2011).

4-2. Model Domain and Discretization

The next steps in model construction are the definition of the spatial extent (domain) of the model, as well as discretization of the domain vertically and horizontally into a grid of model cells. Definition of the extent of the NCDM domain was described previously in the Conceptual Model section of this report. As noted in that section, delineation of the lateral boundaries of the domain was based primarily on the location of the updip limit of the productive part of the Floridan aquifer system and typical patterns of groundwater flow in the study area, as well as the intended use of the model as a tool for estimating pumping effects on groundwater discharge from Jackson Blue Spring.

The NCDM is discretized horizontally as a structured, grid of square cells with sides 2,500 feet in length (Figure 4-1). There is no rotation of the grid with respect to the orthogonal, north-south, and east-west aligned axes. The grid consists of 215 rows oriented in an east-west direction, and 134 columns oriented in a north-south direction. The northwestern (upper left) corner of the grid is located at easting (x) and northing (y) coordinates of 622399.587 meters and 3500697.366 meters, respectively, in the following coordinate reference system (CRS):

- CRS Name: EPSG:26916 - NAD83 / UTM zone 16N
- Units: meters
- Map Projection System: Universal Transverse Mercator (UTM)
- Reference: Static (relies on a datum which is plate-fixed)

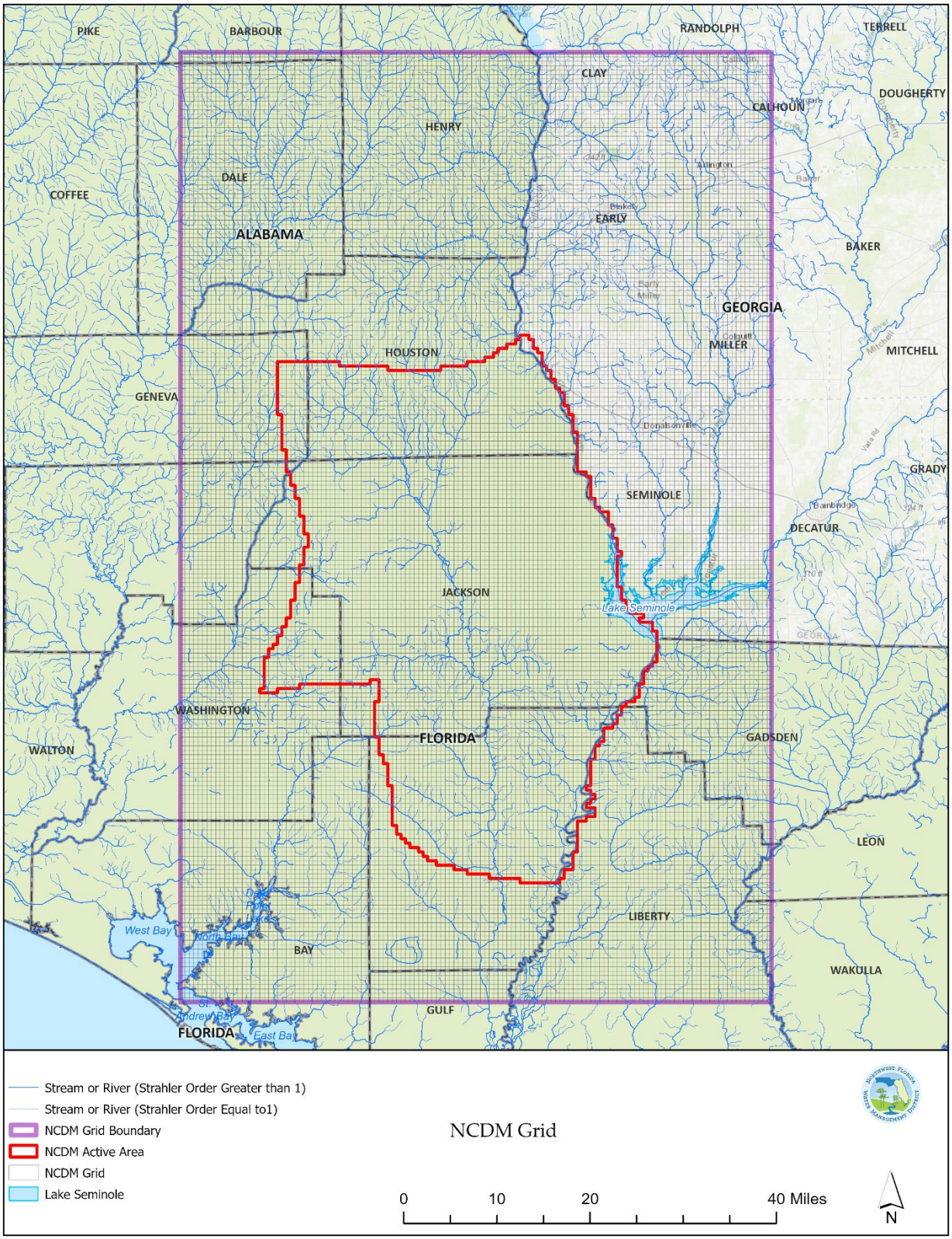

Figure 4-1. NCDM Grid

The vertical extent and discretization of the NCDM is similar to other models representing the Floridan aquifer system. The upper boundary of the model coincides with land surface, and the lower boundary of the model coincides with the base of the Floridan aquifer system. The NCDM is discretized vertically into five layers. In the southern part of the model domain where the upper confining unit (UCU, also known as the intermediate aquifer/confining unit) of the FAS is present, layer 1 generally corresponds to the surficial aquifer system (SAS) and layer 2 generally corresponds to the UCU. Elsewhere (where the UCU is generally absent), cells in layer 1 are inactive and layer 2 generally corresponds to the SAS. Layers 3, 4, and 5 generally correspond to the Upper Floridan aquifer (UFA), middle confining unit (MCU) of the Upper Floridan aquifer, and Lower Floridan aquifer (LFA), respectively. The top of the SAS coincides with land surface and the elevation of this surface was based on land-surface elevation values from a 2-meter resolution, LiDAR-derived digital elevation model (Kebart, January 2020). The elevations of the tops of the UCU and UFA were based on raster datasets described in Grubbs and others (August 2022). The elevations of the tops of the MCU and LFA and the base of the LFA were based on raster datasets from the U.S. Geological Survey (Williams and Dixon, 2015). The elevations of the bottoms of each layer (and therefore the top of the underlying layer, when applicable) were assigned model grid cells by computing the area-weighted, mean elevations over values from the above raster datasets for each NCDM grid cell.

Note that to minimize horizontal discontinuity with a given model layer, a minimum layer thickness of 30 feet was employed. In areas where the thickness of a given hydrostratigraphic unit was less than 30 feet parts of overlying and/or underlying hydrostratigraphic unit were included within a given cell. Calculation of the effective hydraulic conductivity values for these cells is described in the next section of this report.

This process of horizontal and vertical discretization results in a set of three-dimensional cubes (grid cells) representing a volume within the subsurface. This volume is divided into two parts. The first part consists of the ‘active domain’ of the NCDM that coincides with the subset of grid cells where simulated groundwater levels and flow directions and rates are calculated. This second part coincides with the ‘inactive’ part of gridded volume that surrounds the active NCDM domain. Active and inactive parts of the model domain are areas inside and outside (respectively) of the line delineating the NCDM Active Domain boundary shown in Figure 4-2 through Figure 4-6.

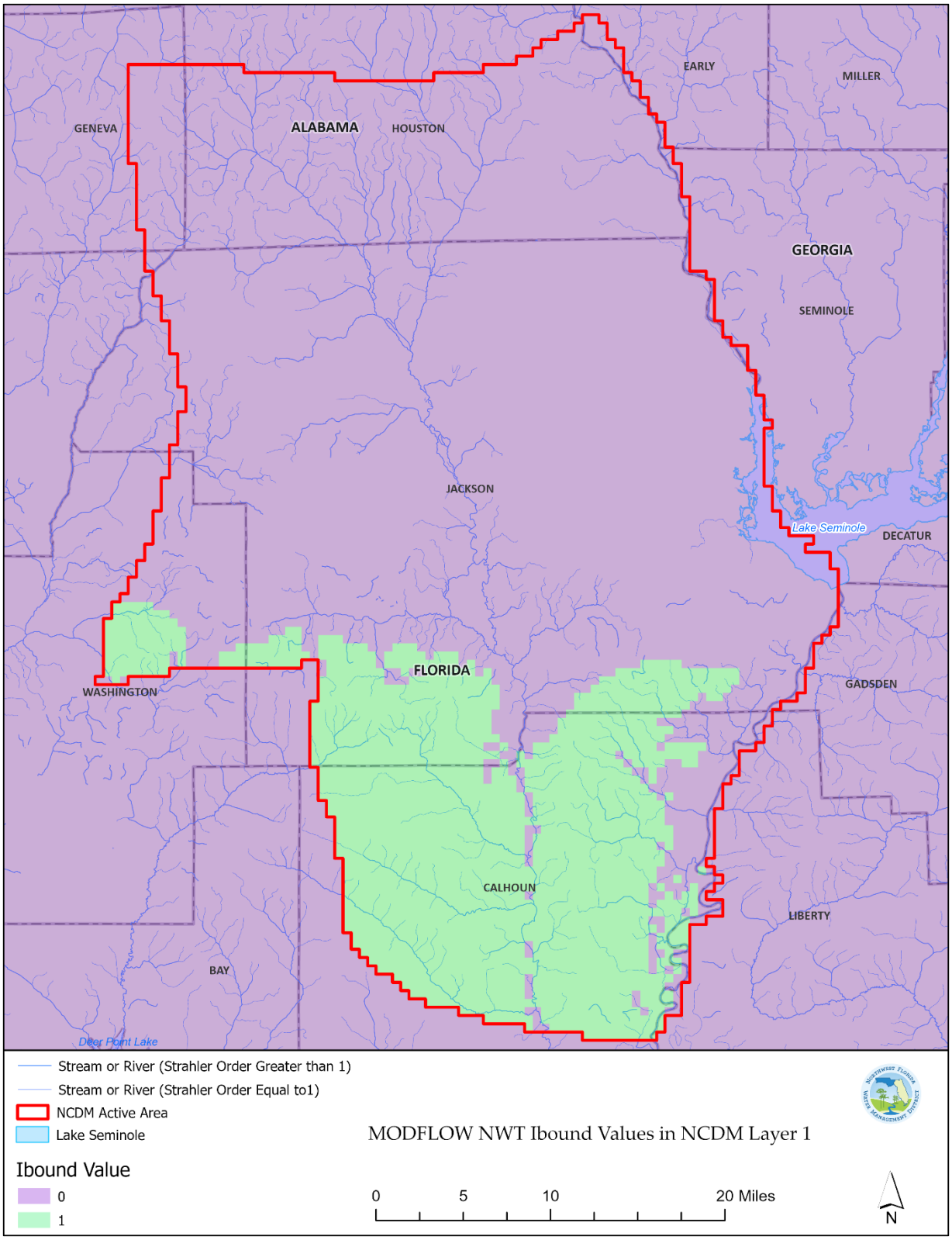

Figure 4-2. Active and inactive area of the NCDM grid in model layer 1

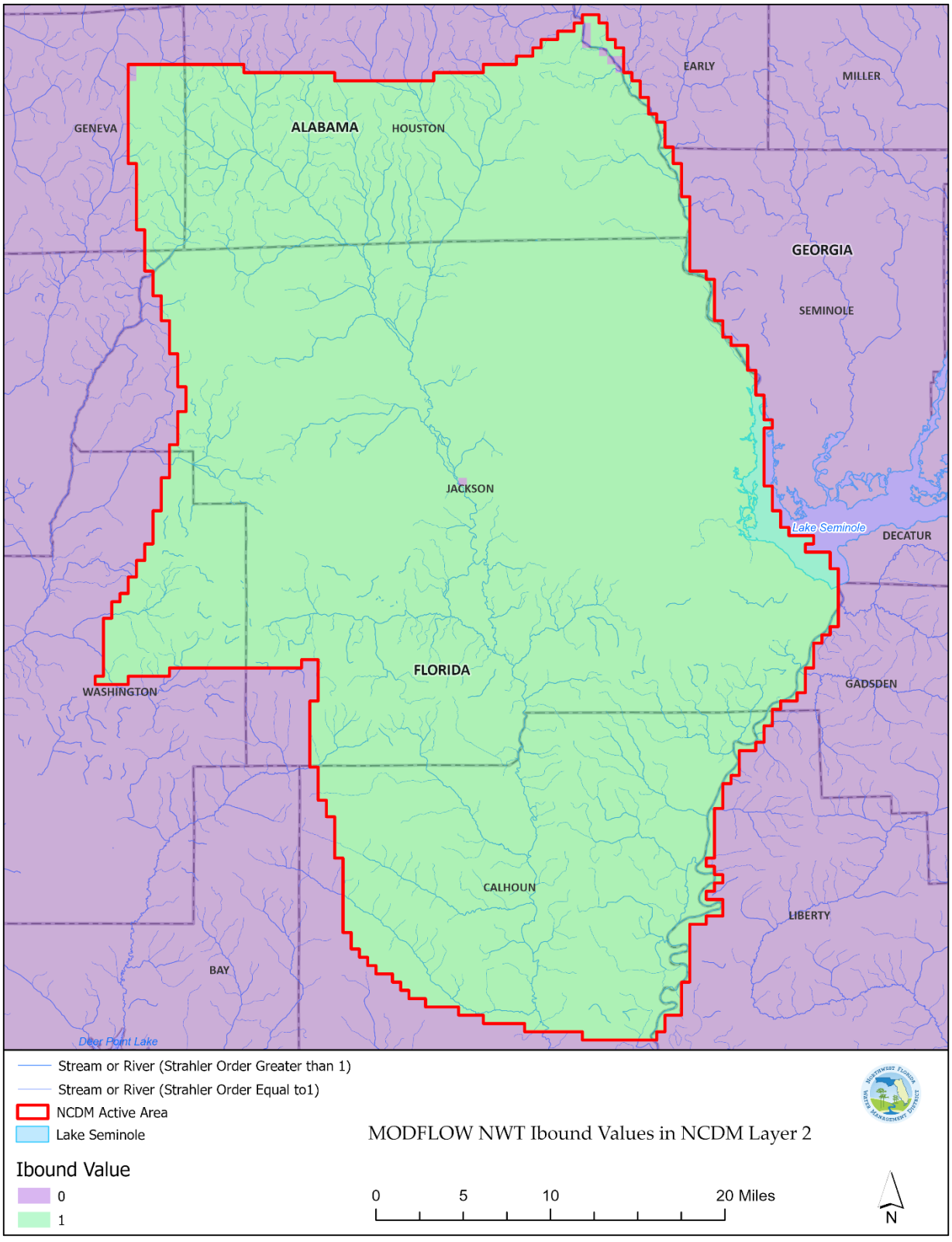

Figure 4-3. Active and inactive area of the NCDM grid in model layer 2

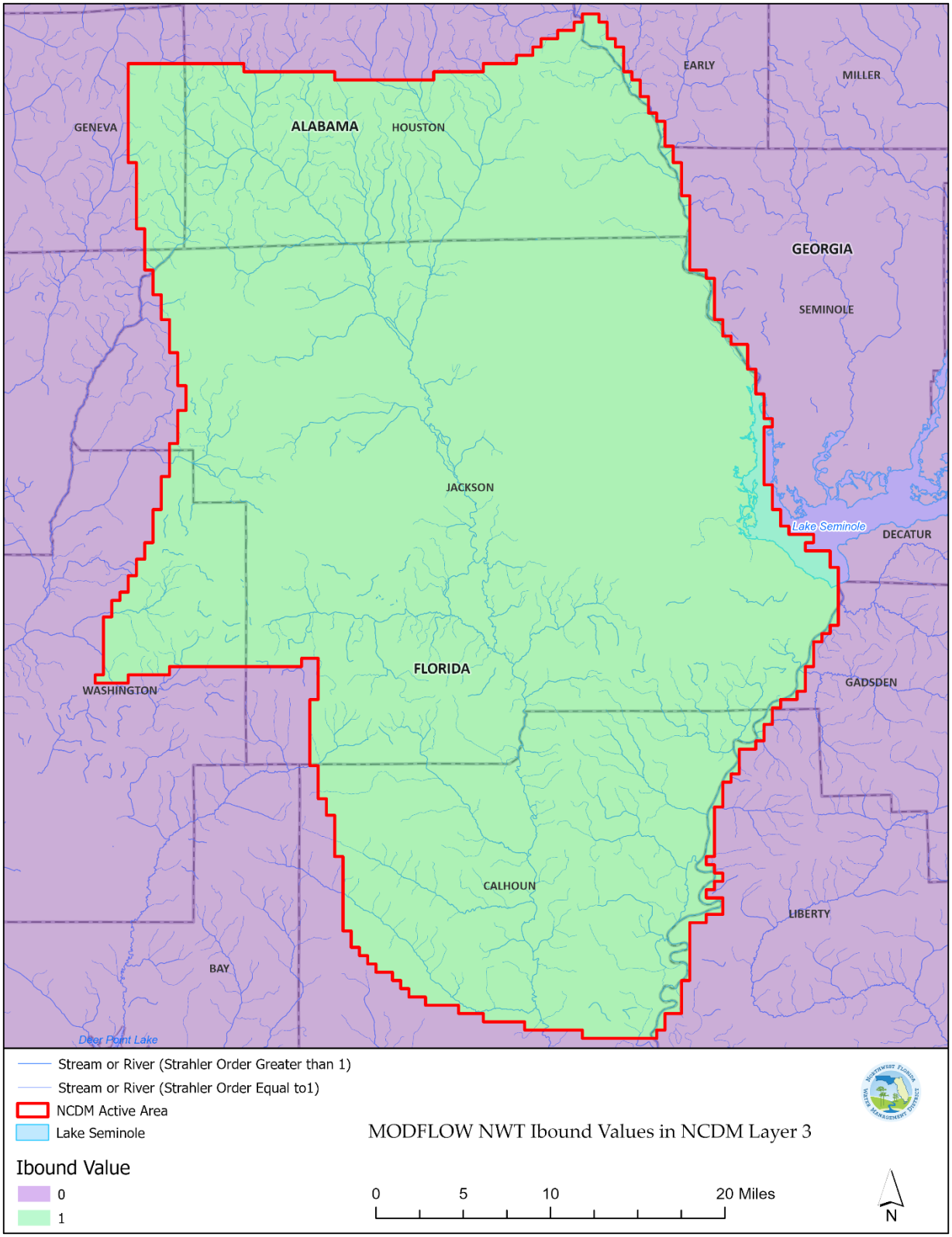

Figure 4-4. Active and inactive area of the NCDM grid in model layer 3

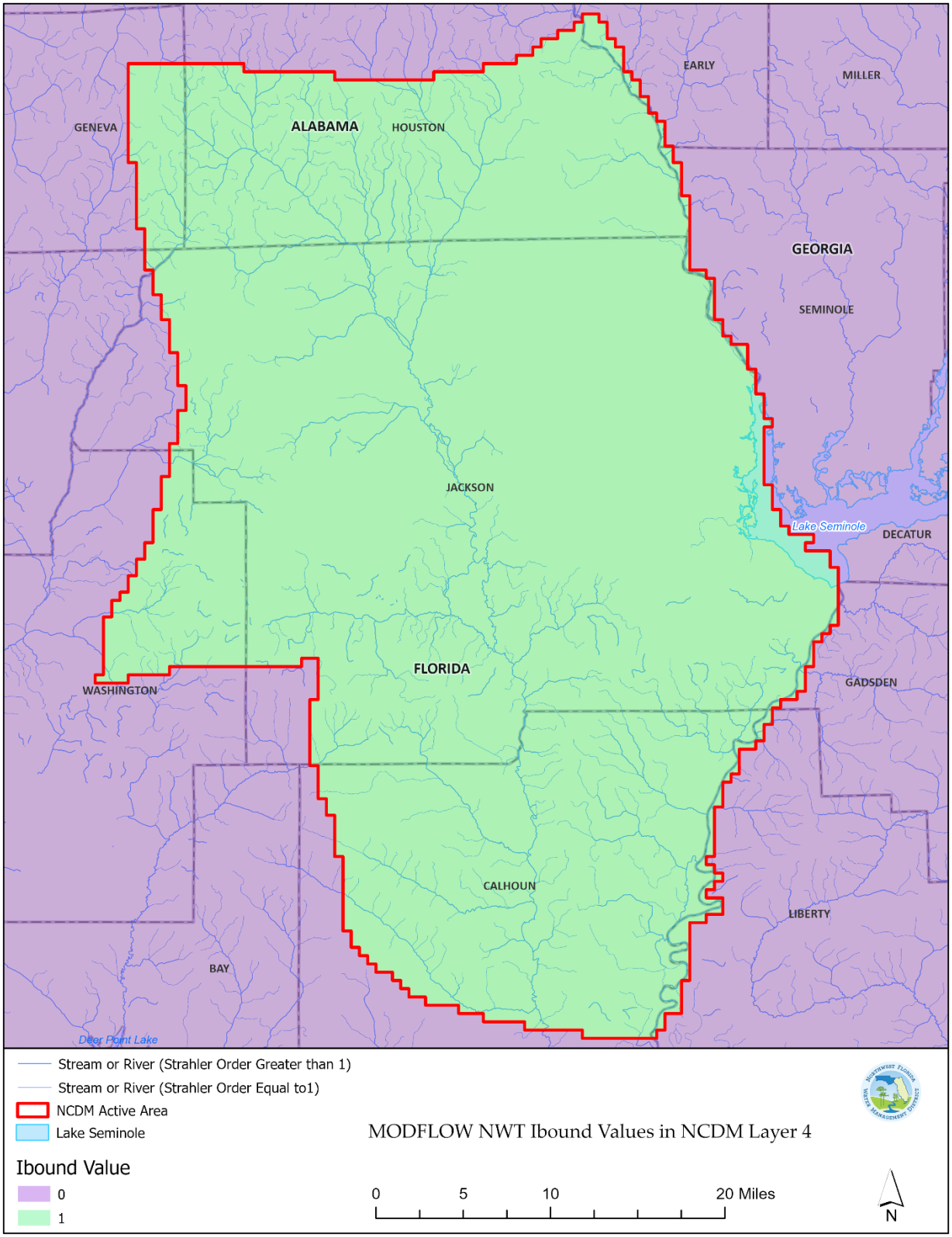

Figure 4-5. Active and inactive area of the NCDM grid in model layer 4

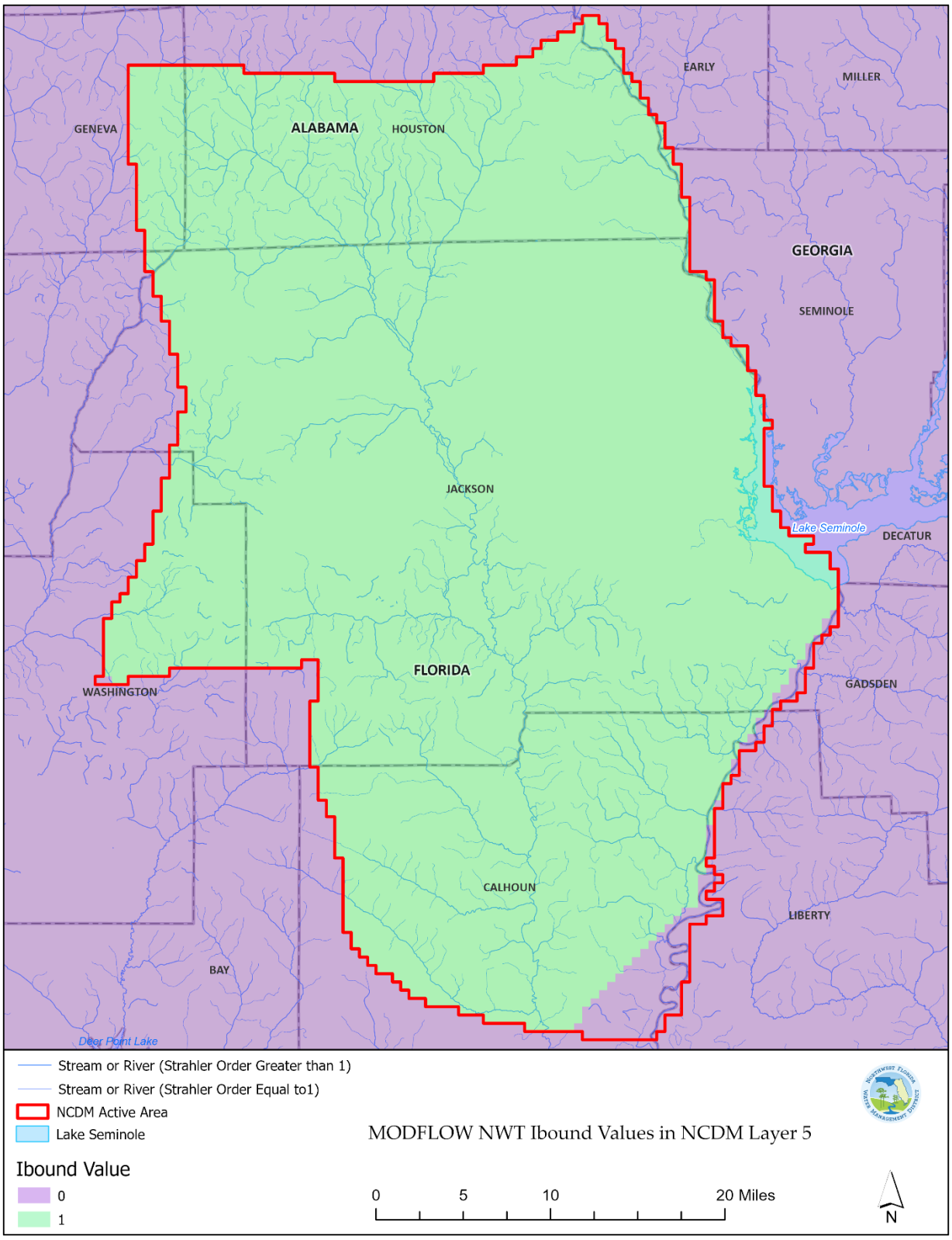

Figure 4-6. Active and inactive area of the NCDM grid in model layer 5

4-3. Hydraulic Properties

The construction of any steady-state numerical groundwater flow model requires that two hydraulic property values be assigned to every model grid cell: horizontal and vertical hydraulic conductivity (K_h and K_v, respectively). K_v can also be defined implicitly by specifying values of the ratio of K_h divided by K_v (anisotropy) at each grid cell in the input files associated with the MODFLOW-NWT Upstream Weighting Package and letting the MODFLOW-NWT software model calculate K_v as the product of anisotropy and K_h. This was the method employed by the NCDM.

Values of K_h and anisotropy are represented in the model as sets of discretized, two-dimensional, spatially-variable 'fields' and in the Upstream Weighting Package input file as 2-dimensional arrays of values (one array per model layer). Each value in the array is associated with a particular model grid cell (defined by a specific combination of row and column values). These values were assigned to individual model grid cells in a multi-step process, as described below.

In the first step, K_h or anisotropy values for a given hydrogeologic unit are assigned to pilot-point locations spaced approximately 14,600 feet apart and spanning the active NCDM domain. Values are then assigned to each 2-dimensional location (row and column address) on the NCDM grid by interpolating from these pilot-point locations. This interpolation was implemented using the calc_kriging_factors_auto_2d function in the software PLPROC (Doherty, April 2022), which employs ordinary kriging, but allows the variogram range to vary over the interpolation domain, based on the density of pilot points in a given area of the domain. This results in interpolated hydraulic property fields that are smoother in areas of the domain where pilot points are sparser, and more heterogeneous in areas of the domain where points are denser. Although the spacing of the pilot points used in the NCDM was consistent throughout the NCDM domain, this approach would have provided the flexibility to easily change the density of pilot points during the calibration phase of NCDM development had that need arisen. Calculation of the kriging factors is a function of the locations of the pilot points and does not depend on their actual values. Therefore, it was only necessary to calculate the kriging factors once, at the outset of the calibration effort. Once these factors were computed, K_h or anisotropy values for a given hydrogeologic unit were interpolated from pilot point locations to each row and column address in the model. This process was carried out using the "PLPROC krige_using_file" function, which read the previously computed kriging factors. K_v values at these addresses were then calculated as the product of corresponding anisotropy and K_h values at each address.

In the first step described above, each of the five hydrogeologic units occurring in the NCDM domain (SAS, UCU, UFA, MCU, and LFA) was assigned a corresponding set of K_h and K_v

values for each NCDM row and column address. This resulted in a 2-dimensional array of K_h or K_v values for each hydrogeologic unit. The NCDM is a 3-dimensional model, so an additional step was needed to assign K_h or K_v values to individual NCDM model grid cells based on their 3-dimensional (row, column, and layer) address. In most cases, a given model grid cell contained only one of these hydrogeologic units, so in these cases the value of K_h or K_v in the cell would just be the value obtained through kriging-based interpolation at the cell's row and column address and for the hydrogeologic unit contained within that cell.

There were cases where multiple hydrogeologic units might occur within a given model grid cell, however. This was particularly the case in areas where a given hydrogeologic unit was pinching out, or otherwise very thin. In these cases, a final processing step was required in which the K_h or K_v values in the cell were based on effective values that were computed based on the concepts of 'resistors in parallel' or 'resistors in series,' respectively (Freeze and Cherry, 1979). With the resistors in parallel analogy, the effective K_h value assigned to a given cell is equal to the mean of the interpolated values K_h of each hydrogeologic unit present in the cell, weighted by their corresponding thickness within the cell:

$$\overline{K_h} = \frac{1}{d}\sum_{i=1}^{n} K_h d_i$$

where d_i represents the thickness of hydrogeologic unit i within a given cell, d represents the total thickness of that cell, and n represents the number of hydrogeologic units within that cell.

Similarly, with the 'resistors in series' analogy, the effective K_v value assigned to a given cell is computed as the *inverse*, thickness-weighted mean of the interpolated values K_v of each hydrogeologic unit present in the cell:

$$\overline{K_v} = d\sum_{i=1}^{n} \frac{1}{d_i/K_h}$$

Anisotropy values for cells containing multiple hydrogeologic units were then calculated by dividing the values of $\overline{K_h}$ by $\overline{K_v}$.

4-4. Boundary Conditions

Stresses on the groundwater flow system like groundwater recharge or withdrawals from pumping wells are represented in numerical and analytical models as boundary conditions. Their locations and values determine (in combination with the spatial distribution of hydraulic property values) the state of the system: the spatial distribution of hydraulic heads and associated groundwater flows and exchanges of flows with surface features like springs

and streams. The boundary conditions implemented in the NCDM represent the following stresses: groundwater recharge, evapotranspiration from shallow groundwater, groundwater withdrawals from pumping wells, groundwater-surface water exchanges between streams, rivers, lakes, and springs, and no-flow and constant boundaries defining the limits of the active NCDM domain.

The NCDM was developed as a steady-state model, which means that for any location in the model domain, stresses on the system are constant, the system is at equilibrium reflecting those constant stresses, and therefore there is no change in the amount of water stored in the system. During the initial stages of NCDM development historical groundwater levels at wells with continuous recorders were evaluated to identify a period of one year or longer when groundwater levels were reasonably similar at the beginning and end of the period, indicating that changes in storage in the system over the period were minimal. The three-year period beginning January 1, 2017, through December 31, 2019. was identified as being a good approximation of this criterion and was therefore selected as the calibration period for the model. Accordingly, average values of relevant boundary conditions, such as recharge and groundwater withdrawals from wells, were estimated for this calibration period.

Groundwater recharge and evapotranspiration from shallow groundwater (ET_{gw}) are represented in the NCDM using the MODFLOW-NWT Recharge and Evapotranspiration Packages, respectively (Niswonger and others, 2011). Recharge and ET_{gw} are represented in these packages as discretized, two-dimensional fields, and their values were assigned using NCDM model grid cells using the essentially the same pilot point and kriging-based approach as that was previously described for horizontal hydraulic conductivity and anisotropy. The key difference in the approach for recharge and ET_{gw} is in the two-step process used to assign recharge and ET_{gw} values to NCDM grid cells. In the first step, recharge or ET_{gw} multiplier values are assigned to pilot locations, and values of recharge or ET_{gw} multipliers are interpolated at model grid cells using the same process as that used for K_h and anisotropy. These pilot point locations are also the same as those used to interpolate values of K_h and anisotropy. In the second step, the recharge or ET_{gw} values that are assigned to model grid cells (and corresponding elements of the arrays read by MODFLOW-NWT) are calculated as the product of the interpolated recharge or ET_{gw} multiplier value at that cell and the corresponding 'reference value' of recharge or ET_{gw} at that cell. These reference values correspond to the estimates of recharge or ET_{gw} described previously in the Conceptual Model section of the report. As such, they represent pre-calibration estimates of recharge and $ET_{gw.}$ Note that, unlike K_h and anisotropy, recharge or ET_{gw} values are only assigned to the uppermost active cells in the model.

Groundwater withdrawals from wells were represented using the MODFLOW-NWT Well Package (Niswonger and others, 2011). Average withdrawal rates during the model calibration period were estimated using the methods described by Friedman (May 2022) and which are summarized in the Conceptual Model section of this report. Withdrawals from individual wells were represented by corresponding entries in the Well Package input file, unless the open or screened interval of a given well intersected more than one model grid layer. In these cases, the withdrawal from that well was distributed across the intersected layers in proportion to the product of the K_h value in the cell containing that well and the length of the open or screened interval within the cell (Tetra Tech, September 2024), and withdrawals by that well from individual layer represented on individual entries (one per model layer per well) in the Well Package input file. The geographic distribution of groundwater withdrawals is shown in Figure 4-7. Note that negative values indicate the values shown in the figure are groundwater withdrawals, rather than injections.

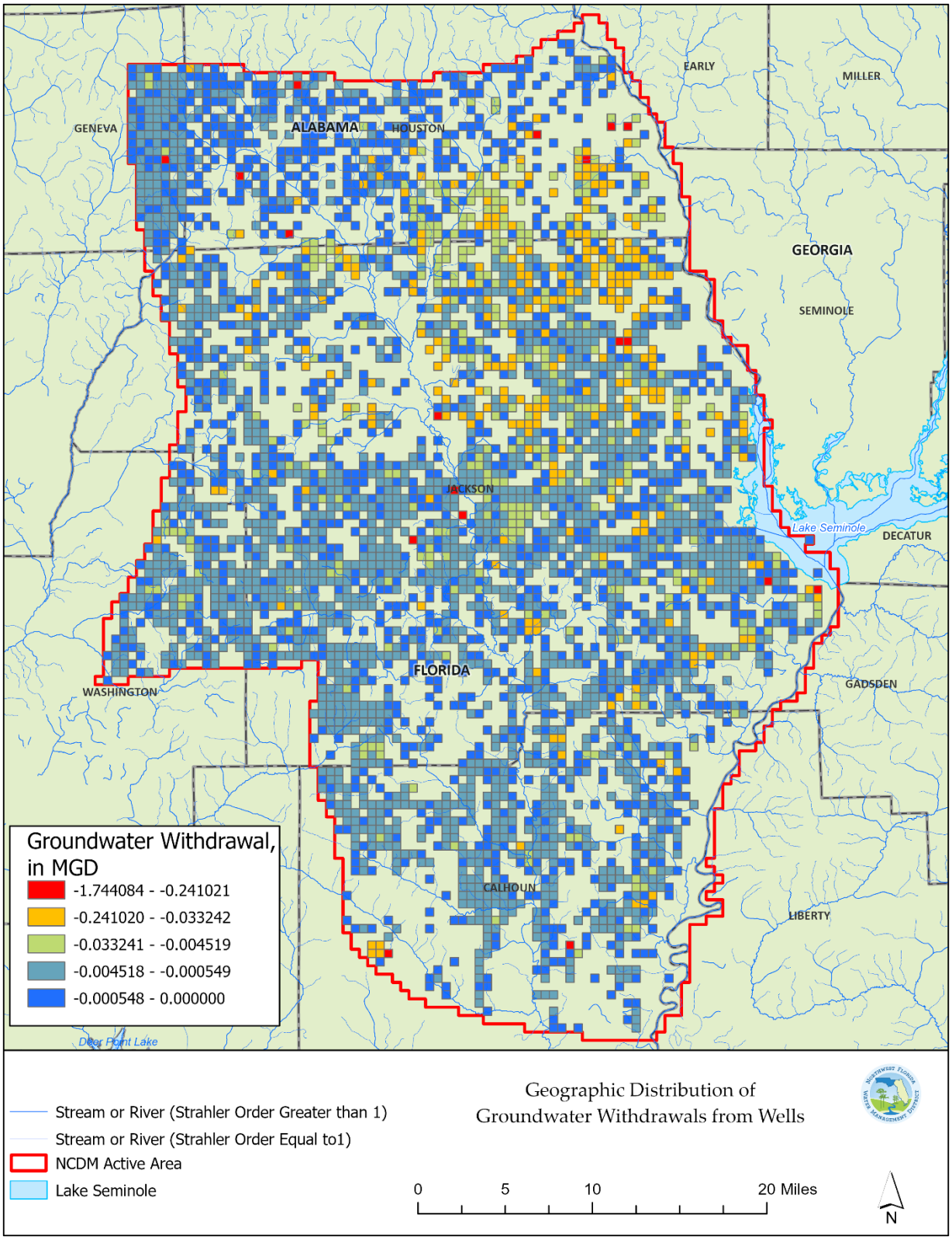

Figure 4-7. Geographic distribution of groundwater withdrawals from wells.

Streams, rivers, and Lake Seminole were represented using the River Package and Drain Package components of MODFLOW-NWT (Niswonger and others, 2011). Smaller tributaries, defined as streams classified with a Strahler order value of one in the NHDPlus dataset (McKay and others, 2012) were represented with the Drain Package. Streams and rivers classified with a Strahler order value greater than one in this NHDPlus dataset were represented using the River Package, as was Lake Seminole.

Stream water-surface (stage) or spring-pool elevations and conductance values are required to use the Drain Package, along with the address (layer, row, and column location in the model grid) of the grid cell containing the stream reach or spring being represented. The River Package requires the same information as the Drain Package and additionally requires that the stream- or lake-bed elevation be specified. Streambed elevations, and stream, river, and lake stages were estimated using high-resolution, LiDAR-derived, digital elevation model (DEM) data, and historical observations of stages and depths, using the methods and implementing software described in Tetra Tech (May 2017; September 2024). In some cases, these elevations were subsequently revised during the course of model development to eliminate 'short-circuiting' of flows from one boundary condition feature to another (by making the stages associated with all River and Drain Package features within a given cell equal) or to otherwise improve the consistency with available data, such as stages from stream gaging stations, topographic maps, or digital elevation models.

The conductance of stream or river reaches represented by the River or Drain Packages were based on the area (product of the length and estimated width) of a given reach within a model grid cell. In the case of Lake Seminole, this area is equal to the area of the cell covered by the lake. River or Drain conductance values were then computed by multiplying the reach or lake areas by a multiplier value. This multiplier is conceptually equivalent to an estimate of the hydraulic conductivity of the flow path between the top of the cell connected to the River or Drain Package feature and length of that flow path.

Initial values of spring-pool elevations were estimated and assigned to corresponding Drain Package features using high-resolution, LiDAR-derived DEM data and historical observations of stages and depths, using the methods, and implementing software described in Tetra Tech (May 2017). In some cases, these stages were subsequently revised during the course of model development to be more consistent with available data. For example, in some cases the tool would assign different stages to multiple springs discharging to a single spring pool (because of variations in DEM elevations across the pool), so the stages were subsequently assigned a common value to reflect the fact that the spring pool that they shared had an essentially flat-water surface. Initial Drain Package

conductance values associated with individual springs were estimated by dividing an estimate of the spring flow by a small head gradient value of 0.01.

The lateral boundaries of the NCDM are consistent with those previously described in the Conceptual Model section of this report and are largely defined as no-flow boundaries. The northern boundary of the model coincides with the approximate up dip limit of the productive part of the Upper Floridan aquifer, as defined by Williams and Kuniansky (2016). The eastern lateral boundary generally coincides with the centerline of Lake Seminole and the Chattahoochee River to the north and the Apalachicola River to the south. Nearly all of the western boundary coincides with regional groundwater flow lines with locations that are sufficiently west of the Chipola River and Jackson Blue Spring to minimize the effect of the boundary location on simulated flows from Jackson Blue Spring. The northern part of this western flowline boundary is interrupted by a segment where groundwater that has flowed in a generally southerly direction begins to flow westward, toward a group of springs along Holmes Creek. This section of the western boundary is represented in the NCDM in model layers 3 and 5 (representing the Upper and Lower Floridan aquifers) with specified head boundary conditions and implemented using the MODFLOW Time-Variant Specified-Head Package (Harbaugh and others, 2000). The heads assigned to these specified head boundary condition features were computed by averaging values interpolated from historical potentiometric surface maps representing May and September conditions (Albritton, 2021; Albritton, 2022; Fowler and Albritton, 2022a; Fowler and Albritton, 2022b).

Most of the remainder of the western boundary of the NCDM is associated with a groundwater flowline that originates on a high, dome-shaped area of the Upper Floridan aquifer potentiometric surface, about 3 miles southwest of the town of Alford. A short segment of the western boundary is oriented in an east-west direction about midway down the length of the western boundary and coincides with an east-to-west directed groundwater flowline (flowing towards the springs on Holmes Creek, just west of the active NCDM domain).

Much of the southwestern and southern part of the lateral NCDM boundary is also a no-flow boundary coinciding with the southern extension of the groundwater flowline originating near Alford that bends in a southeasterly direction toward the Apalachicola River. The easternmost part of this southern boundary is represented in Model layers 3 and 5 (representing the Upper and Lower Floridan aquifers, respectively) with specified head boundary condition features (also implemented using the MODFLOW Time-Variant Specified-Head Package), reflecting the southerly direction of groundwater flow in this area. The heads assigned to these specified head boundary condition features were also computed by averaging values that were interpolated from historical potentiometric surface

maps representing May and September conditions (Albritton, 2021; Albritton, 2022; Fowler and Albritton, 2022a; Fowler and Albritton, 2022b) during the calibration period (January 1, 2017, to December 31, 2019).

5. Model Calibration

Model calibration, also known as history matching, is a process in which hydraulic property and boundary condition values are varied within plausible ranges to improve the correspondence between historical observations (calibration targets) and their model-simulated equivalents. Modern best practices for model development require that this process of updating and evaluating candidate sets of hydraulic property and boundary condition values typically occur many thousands of times for a given model calibration effort and model-development project. The NCDM has five layers, 215 rows, and 134 columns, so each update entails assigning multiple values to more than 140,000 model grid cells. Therefore, sufficient computing resources and a well-structured, automated process are essential for efficiently generating new sets of hydraulic property and boundary-condition values to be tested, updating and running the model to reflect a given set of candidate values, and comparing the calibration target values (for example groundwater levels and spring flows) with corresponding model outputs.

This section of the report is organized into two subsections. The first section describes the process used to implement calibration of the NCDM. The second section describes the results of that calibration process.

5-1. Implementation of the NCDM Calibration

Calibration of the NCDM was implemented using the PEST-HP and the PEST software suite (Doherty, February 2020; Doherty, January 2023). This software provides a framework and means for efficiently updating the model with plausible values, running the updated model, and postprocessing results. In particular, the PEST-HP software makes it possible to efficiently execute hundreds of candidate versions of the NCDM simultaneously (in parallel), evaluate the results of those model runs, and generate new candidate versions of the NCDM that are most likely to improve the model fit while adhering to constraints specified by the user. Execution of the PEST software and associated model runs were carried out on the District's high-performance computing cluster, which includes 11 compute nodes (servers) that collectively have over 400 computing cores, each capable of independent execution of individual model runs.

Calibration of the NCDM (like most groundwater flow and transport models) occurs through minimizing the value of an objective function defined as the squared, weighted differences between user-specified, calibration target values and model simulated equivalents of these values. Examples of calibration targets include measurements or estimates of groundwater levels, groundwater discharge to streams (baseflow), and spring flows. The objective function also includes a 'Tikhonov regularization' component (Doherty, 2015) to help minimize overfitting of the calibration targets by penalizing excessive heterogeneity in the

two-dimensional hydraulic conductivity, recharge, and evapotranspiration fields represented in the model.

In a given calibration run, the calibration occurs as a series of iterations that are implemented with the PEST-HP software. Each iteration consists of two steps. In the first step, a matrix of derivatives (the Jacobian matrix) is constructed by running the model once (or twice if central differencing is being used to calculate derivative values) for each adjustable parameter, each time incrementally adjusting the parameter, calculating the change in each of the calibration-target and regularization equation values, and then calculating a value of the derivative of the target with respect to the parameter (the change in the each target's value divided by the incremental change in the parameter value).

Once this Jacobian matrix is constructed, a set of candidate 'parameter upgrades' are generated and evaluated. Each of these parameter upgrades is generated by constructing a system of equations intended to minimize the objective function based on the most recently-constructed Jacobian matrix, the target values and their respective weights, the regularization equation values and their respective weights, and a 'Marquardt lambda' value that improves the efficiency of the calibration for nonlinear problems (Doherty, 2015; Doherty, 2023). Once constructed, the system of equations is solved using the LSQR algorithm (Doherty, 2015; Doherty, 2023; Paige, C.C. and Saunders, M.A., 1982a, 1982b), which results in a set of new parameter values. The model is then reconstructed and run based on these values, and a corresponding objective function value is calculated. This second step is repeated multiple times with different candidate Marquardt lambda values, each time calculating a set of parameter values and corresponding objective function values. At the conclusion of this second step, the model with the set of parameter values that produced the smallest objective function value becomes the reference for computing a new Jacobian matrix and subsequent set of candidate parameter sets during the next iteration of a given calibration run.

Other aspects of the calibration are implemented with the PEST-HP software, other software in the PEST suite, and with custom Python programming language scripts. These aspects include the specification of parameter values and reasonable ranges for adjusting these values, translation of parameter values into model input files, execution of the model, and calculation of model-simulated equivalents of calibration targets from model outputs. Details of aspects of the NCDM calibration are provided in the text that follows. That discussion is organized into several subsections. The first subsection describes the parameters and associated preprocessing used to efficiently construct and modify the NCDM during a given calibration run. This is followed by subsections describing calibration

targets, target weighting, postprocessing of model outputs during calibration, as well as implementation of Tikhonov regularization.

5-1-1. Parameterization and Preprocessing

A key aspect of model calibration is defining parameters that can be specified and (in most cases) adjusted during the calibration process and translation of these parameters into model input values written to model input files in the required format for successful execution of the model. In this report, this translation of parameters into model inputs is referred to as parameterization, and the sequence of steps and software used to implement that translation process is referred to as preprocessing.

5-1-1-1. Parameterization

There were 3,523 parameters used to construct and calibrate the NCDM, and these were divided into fifteen parameter groups NCDM calibration (Table 5-1). All but 14 of these parameter groups were adjustable parameters that were varied during calibration. Most of these parameters were associated with pilot points representing K_h, anisotropy, or a multiplier used to scale pre-calibration estimates of recharge or the maximum rate of groundwater *ET* ($ET_{sat,max}$). Kriging-based interpolation of the values at the K_h, anisotropy, and recharge or ET multiplier pilot point locations was used to translate these pilot point parameters into corresponding model inputs, as discussed in the Numerical Model Construction section of this report. The same parameterization process used to construct the NCDM was used during the NCDM calibration, although during calibration this process was repeated thousands of times to evaluate thousands of different combinations parameter values and corresponding model inputs.

The upper and lower limits assigned to each set of adjustable parameters during the NCDM calibration are shown in Table 5-2. Note that two sets of limits are given for the K_h parameters for the surficial aquifer system (kh_sas). The lower and upper limits for most of the kh_sas pilot point parameters were 0.1 and 200, respectively. However, clay and clayey materials were present in lithologic logs from wells drilled near and east of Chipley, Florida, so the lower and upper limits of pilot point parameters are much lower in this area.

Table 5-1. Parameters groups and number of adjustable parameters used in the NCDM calibration.

Parameter Type	Hydrogeologic Unit	PEST parameter group name	Number of Adjustable Parameters
Horizontal Hydraulic Conductivity Pilot Points	Surficial Aquifer System	kh_sas	289
	Upper Confining Unit of the Floridan Aquifer System	kh_ucu	289
	Upper Floridan aquifer	kh_ufa	289
	Middle Confining Unit of the Floridan Aquifer System	kh_mcu	289
	Lower Floridan aquifer	kh_lfa	289
Ratio of Horizontal to Vertical Hydraulic Conductivity Pilot Points	Surficial Aquifer System	ak_sas	289
	Upper Confining Unit of the Floridan Aquifer System	ak_ucu	289
	Upper Floridan aquifer	ak_ufa	289
	Middle Confining Unit of the Floridan Aquifer System	ak_mcu	289
	Lower Floridan aquifer	ak_lfa	289
Recharge Multiplier Pilot Points	--	rch	289
Groundwater Evapotranspiration Multiplier Pilot Points	--	et	289
River Package Conductance Multiplier	--	rivc	9
Drain Package Conductance Multiplier	--	drnc	7
Spring Conductance	--	sprc	25

Table 5-2. Upper and lower bounds assigned to NCDM calibration parameters[1].

Parameter Type	*Hydrogeologic Unit*	*PEST parameter group name*	*Parameter Lower Limit*	*Parameter Upper Limit*
Horizontal Hydraulic Conductivity Pilot Points	Surficial Aquifer System	kh_sas	0.1 (1.0E-5 east of Chipley)	200 (0.1 east of Chipley)
	Upper Confining Unit of the Floridan Aquifer System	kh_ucu	1E-4	0.1
	Upper Floridan aquifer	kh_ufa	1	1E4
	Middle Confining Unit of the Floridan Aquifer System	kh_mcu	0.01	100
	Lower Floridan aquifer	kh_lfa	0.5	1000
Anisotropy Pilot Points	Surficial Aquifer System	ak_sas	1	100
	Upper Confining Unit of the Floridan Aquifer System	ak_ucu	1	100
	Upper Floridan aquifer	ak_ufa	1	100
	Middle Confining Unit of the Floridan Aquifer System	ak_mcu	1	100
	Lower Floridan aquifer	ak_lfa	1	100
Recharge Multiplier Pilot Points	--	rch	0.4	1.5
ET Multiplier Pilot Points	--	et	0.6	1.4
River Package Conductance Multiplier	--	rivc	0.01	100
Ephemeral Streams (Drain Package) Conductance Multiplier	--	drnc	0.01	100
Spring Conductance	--	sprc	1000	1E10

[1]*Units for horizontal hydraulic conductivity are feet per day and conductance units are in square feet per day. Units for anisotropy and multiplier parameters are dimensionless.*

As noted in the Numerical Model Construction section of the report, the conductance of boundary condition features representing ephemeral and perennial stream and river features were computed as the product of the area (length times width) of a stream or river segment intersected by a model grid cell and a conductance multiplier value. Nine of these conductance multiplier values were used in the construction and calibration of the NCDM and correspond to the stream and river reaches listed in Table 5-3.

Table 5-3. Stream and river reaches corresponding to conductance multiplier parameters used to construct and calibrate the NCDM.

River or Stream Conductance Parameter Name	Stream Reach Description
rivc1, drnc1	Reaches contributing to flow to the Chipola River at Marianna gage (02358789)
rivc2, drnc2	Reaches contributing flow to the Chipola River near Altha gage (02359000) but downstream from the Chipola River at Marianna gage (02358789)
rivc3, drnc3	Reaches contributing flow to the Chipola River downstream of the Altha gage (02359000)
rivc4, drnc4	Reaches contributing flow to the Apalachicola River, but downstream of the confluence of the Chattahoochee, Flint, and Apalachicola Rivers
rivc5, drnc5	Reaches contributing flow to the Apalachicola River, at and upstream of the confluence of the Chattahoochee, Flint, and Apalachicola Rivers
rivc6, drnc6	Reaches contributing to Holmes Creek
rivc7, drnc7	Reaches contributing to Econfina Creek
rivc8, drnc8	Merritts Mill Pond
rivc9, drnc9	Spring Creek

Thirty-nine spring conductance parameters were used in the NCDM calibration, each corresponding to an individual spring. Some of the springs did not have a corresponding historical measurement of flow but were part of a spring group that did have one or more historical measurements of the collective flow from all of the springs in the spring group. If none of the springs in a given spring group had an individual flow measurement, then the flow from each spring in the group was assumed to be an equal fraction of the aggregate flow from the spring group. Springs within a given spring group were assigned identical water surface elevations (stages). Accordingly, only one adjustable conductance parameter was necessary for calibration of flow from these springs if all of the springs were associated with only one model grid cell (because the simulated head difference would be identical for all of the springs, and simulated spring flow is calculated as the product of simulated head difference and spring conductance). Therefore, 14 of the 39 spring conductance parameters were not adjustable 4 and were instead 'tied' (set equal to) the value of an adjustable parameter assigned to one of the springs in the spring group.

5-1-1-2. Preprocessing

During model calibration, numerous candidate sets of parameter values are translated into corresponding model inputs. This translation process occurs as a sequence of preprocessing steps in which a series of computer programs and scripts are executed to create the model input files with values derived from a given set of parameter values being

evaluated, and in the format required by the MODFLOW-NWT software. Each of the programs executed during this preprocessing step has their own set of input files.

The sequence of preprocessing steps is defined in the initial part of a 'model batch file' that is executed by the PEST-HP software. Preprocessing begins with the execution of an NCDM-specific script (plproc_pp_interp.in) read by the PLPROC software (PLPROC, Doherty, April 2022) which performs the kriging-based interpolation and subsequent calculations and processing needed to translate sets of pilot point K_h, anisotropy, recharge multiplier, and groundwater ET multiplier values into corresponding K_h, anisotropy, recharge rate, and maximum groundwater ET rate arrays that are read by MODFLOW-NWT.

The next preprocessing step is the generation of a MODFLOW-NWT River Package input file for perennial stream and river features (defined as NHDPlus features with Strahler order values greater than 1). As described previously, hydraulic conductance values for these features are calculated by multiplying the value of the rivc parameter associated with that feature's river reach by the feature's area (calculated as the product of the feature's length and area). An NCDM-specific Python script (calc_riv_cond.py) calculates these hydraulic conductance values and creates a River Package input file containing these values and the other data associated with the perennial stream and river features.

In the next preprocessing step, a similar NCDM-specific Python script (calc_drn_cond.py) is executed, creating a MODFLOW-NWT Drain Package input file with records representing ephemeral stream (NHDPlus Strahler-order 1) features. Hydraulic conductance values of these ephemeral stream features are calculated from drnc parameter values assigned to stream reaches containing the features (by multiplying the area of a given stream feature by its respective drnc parameter value). This script also reads spring conductance parameters and includes corresponding records for each of the 39 springs in the Drain Package input file that it constructs.

The final preprocessing step in the NCDM calibration process is the creation of the NCDM MODFLOW-NWT Well Package input file, which defines the location and rate of groundwater withdrawals from wells during the NCDM calibration period. Data describing the location and rates of well withdrawals were translated into Well Package input files with an NCDM-specific Python script (Tetra Tech, September 2024). In cases where a well's open- or screened interval spanned more than one model layer, this script also distributed (disaggregated) a well's withdrawals to multiple model layers in proportion to the product of the length of the interval within the layer and the K_h of the grid cell containing the well in that layer.

5-1-2. Calibration Targets

A set of calibration target values were developed for the NCDM using a variety of data. The targets are organized into target groups (PEST observation groups) that were given specific names to implement the NCDM calibration with the PEST model development software (Table 5-4). These calibration target groups included groundwater level (head) targets at specific locations (typically observation wells) and targets based on differences in groundwater levels (head difference targets) at different locations. Also included were targets associated with estimated groundwater discharge to streams and rivers (baseflow targets), spring flows, and targets intended to minimize the occurrence of simulated heads exceeding land surface (flooding penalty function targets).

Table 5-4. PEST observation (calibration target) group names used in the NCDM calibration

Calibration Target Group Name	Description
dhh_obs	Horizontal head difference targets
dhv_obs	Vertical head difference targets
h_obs	Head targets
pen_fxns	Flooding penalty-function targets
qspring_obs	Spring flow targets
qstream_obs	Stream and river baseflow targets

5-1-2-1. Head Targets

Head targets for the NCDM were developed by averaging aquifer heads in wells within the NCDM domain during the period of January 1, 2017, to December 31, 2019. Head data for wells were available for all hydrogeologic units except for the Middle Confining Unit (NCDM layer 4). A summary of the number of available head measurements by model layer can be found in Figure 5-1. Locations and names of NCDM head calibration targets.

Much of the head data used to develop head targets were manually measured by NWFWMD staff or from water level recorders maintained by the District. Additional water level measurements of water level data from loggers from Individual Water Use Permit (IWUP) permittees were used where available.

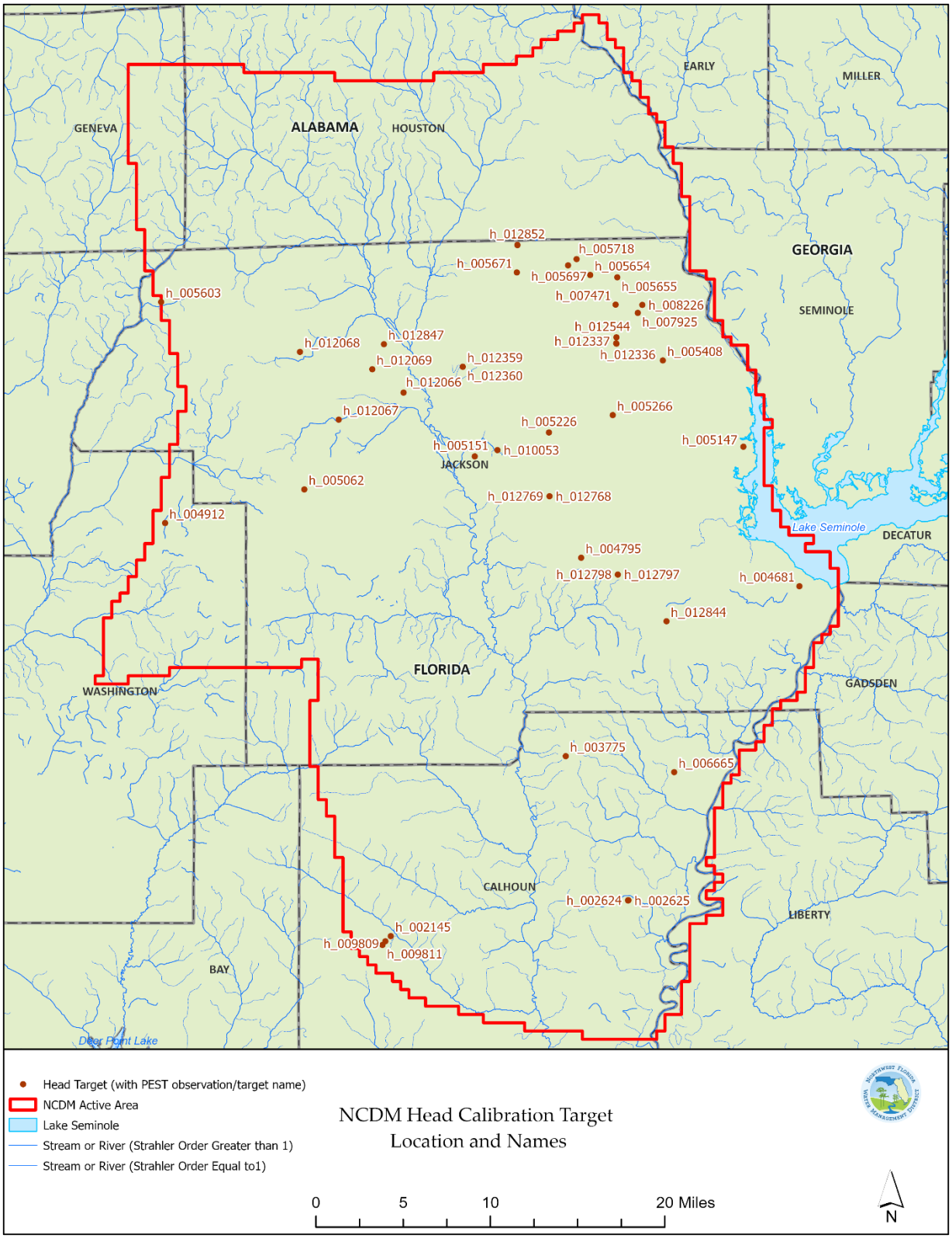

Figure 5-1. Locations and names of NCDM head calibration targets.

Table 5-5. Number of head targets by layer

Model Layer	Number of Head Targets
1	4
2	1
3	38
4	0
5	2
Total	**45**

5-1-2-2. Horizontal Head Difference Targets

Horizontal head difference targets were developed using the same dataset as the head targets described previously. Horizontal head difference targets for the NCDM were computed as the difference in heads at observation wells open to the same hydrogeologic unit in different geographic locations. The well pairs were selected to create head difference targets representing areas with lower and higher head gradients. Six horizontal head difference targets were developed for the NCDM calibration, but one target (dhh_5) was ultimately not used in the calibration because it did not have any concurrent observations at the wells that constitute its well pair. The locations of the horizontal head difference targets are shown in Figure 5-2.

Table 5-6. Horizontal Head Difference Targets

Target Name	Well 1			Well 2		
	District ID	Hydrogeologic Unit	Head	District ID	Hydrogeologic Unit	Head
ddh_1	NWF 12797	Upper Floridan aquifer	98.85	NWF 12769	Upper Floridan aquifer	77.00
ddh_2	NWF 12797	Upper Floridan aquifer	98.09	NWF 4681	Upper Floridan aquifer	73.98
ddh_3	NWF 5266	Upper Floridan aquifer	84.58	NWF 12769	Upper Floridan aquifer	77.10
ddh_4	NWF 12854	Upper Floridan aquifer	125.77	NWF 5671	Upper Floridan aquifer	121.30
ddh_5	NWF 12359	Upper Floridan aquifer	82.29	NWF 5151	Upper Floridan aquifer	75.46
ddh_6	NWF 12068	Upper Floridan aquifer	103.88	NWF 12069	Upper Floridan aquifer	88.44

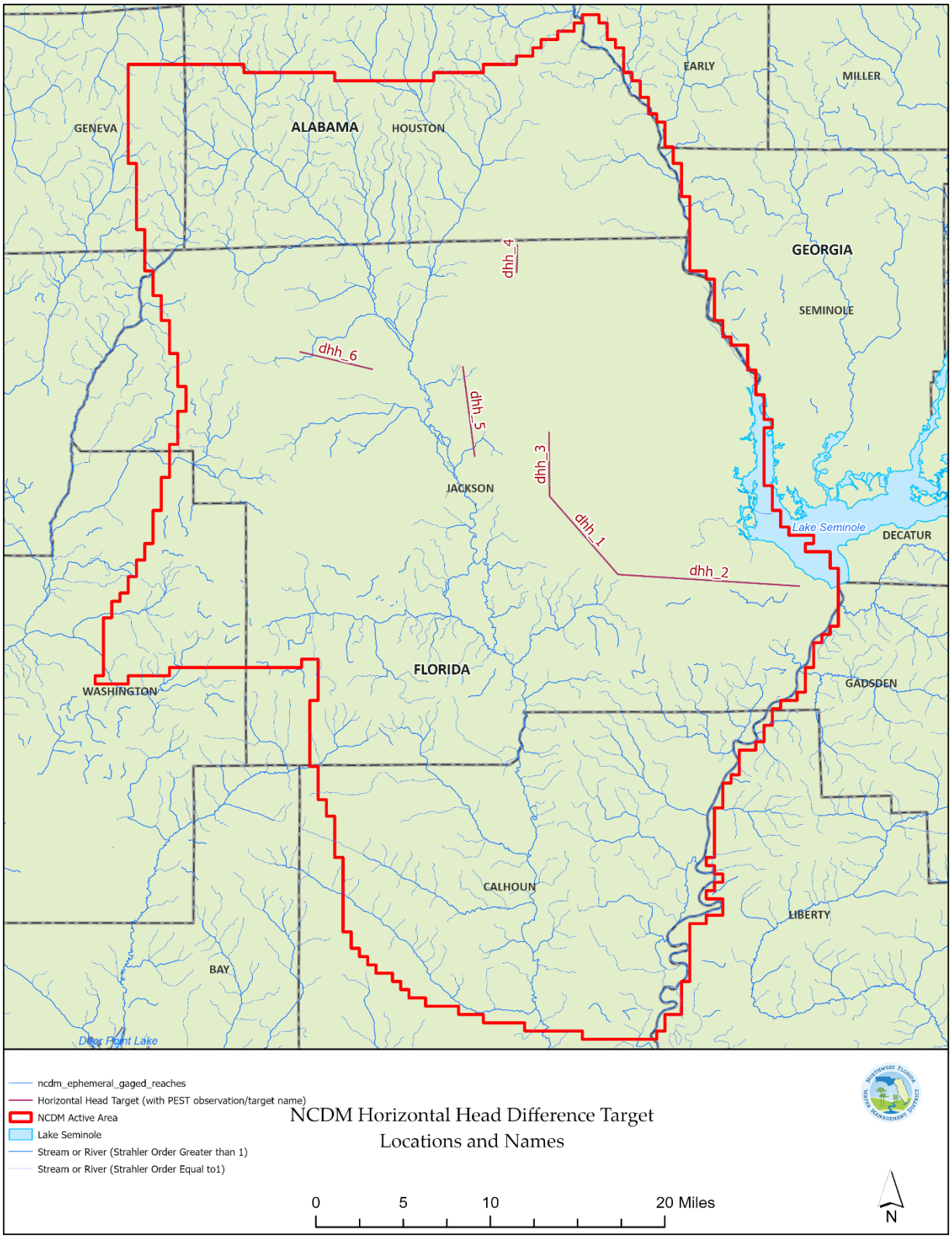

Figure 5-2. Locations and names of NCDM horizontal head difference calibration targets.

5-1-2-3. Vertical Head Difference Targets

Vertical head difference targets were developed using the same dataset as the head targets described previously. Vertical head difference targets for the NCDM were computed as the difference in heads at observation wells in different hydrogeologic units in the same general geographic location. The well pairs that define a given vertical head difference target were selected from locations within the NCDM domain that had a cluster (nest) of wells open to different hydrogeologic units. These targets were developed to provide information about the head losses that occur as water flows from one hydrogeologic unit to another. Eight vertical head difference targets were developed for the NCDM calibration, and their locations are shown in Figure 5-3 (target dhv_3 is not shown in the figure but is co-located with targets dhv_1 and dhv_2) and component observation wells and corresponding levels shown in Table 5-7.

Table 5-7. Vertical head difference targets and associated observation wells

Target Name	Well 1			Well 2		
	District ID	Hydrogeologic Unit	Head	District ID	Hydrogeologic Unit	Head
dhv_1	2624	Upper Floridan aquifer	70.20	2625	Upper Confining unit	70.00
dhv_2	2625	Upper Confining unit	69.88	2626	Surficial aquifer system	75.90
dhv_3	2624	Upper Floridan aquifer	70.07	2626	Surficial aquifer system	75.90
dhv_4	9809	Upper Floridan aquifer	89.42	9811	Surficial aquifer system	123.49
dhv_5	12336	Upper Floridan aquifer	92.00	12337	Surficial aquifer system	96.49
dhv_6	12768	Upper Floridan aquifer	77.28	12769	Lower Floridan aquifer	77.01
dhv_7	12797	Upper Floridan aquifer	98.85	12798	Surficial aquifer system	119.12
dhv_8	12852	Lower Floridan aquifer	110.53	12854	Lower Floridan aquifer	126.35

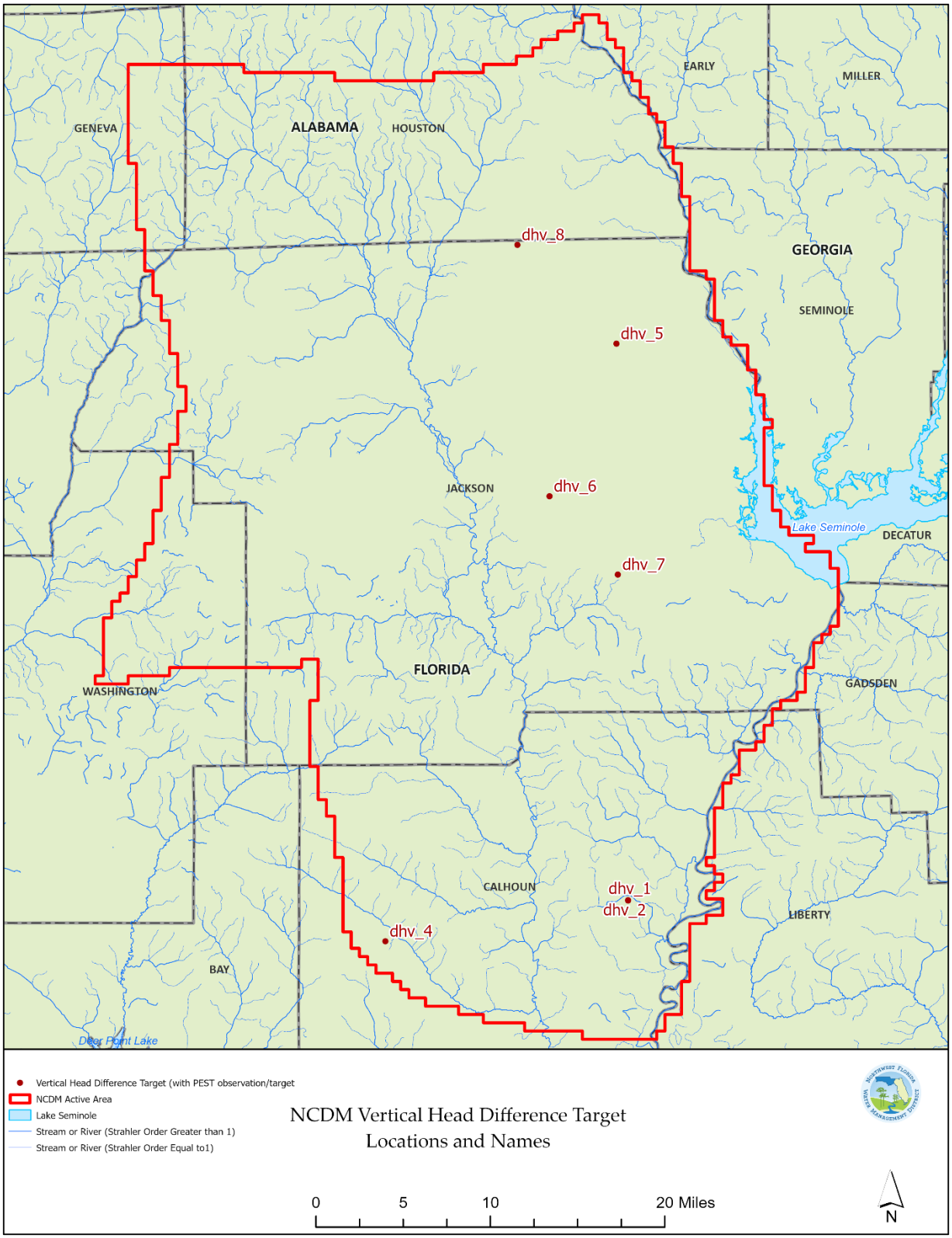

Figure 5-3. Locations and names of NCDM vertical head difference calibration targets.

5-1-2-4. Baseflow Targets

A set of five baseflow target values were used in the NCDM model calibration. Three of the targets are associated with the reaches that are gaged by two U.S. Geological Survey streamflow stations: 02358789 Chipola River at Marianna, Florida and 02359000 Chipola River near Altha, Florida (Figure 5-4). Two targets represent the cumulative groundwater discharge to the two reaches of the Chipola (and associated tributary streams) corresponding to these two gages. The third target represents groundwater discharge to the reach of the Chipola (and associated tributary streams) draining the area between these two gages and is computed as the difference between the estimated cumulative groundwater discharge to these two gages. The remaining two baseflow targets correspond to Merritts Mill Pond and Spring Creek.

The low-pass filter method of baseflow separation method described by Perry (1995) was used to estimate baseflow at the two Chipola River gages. The method is also known as the 'USF method' and consists of two steps. In the first step, the user specifies a time duration in days (time-window) and moving-minimum value of streamflow is computed from a daily streamflow time series, with the minimum value assigned to the day at the center of the time window (or a day that includes the time at the center of the window). In the second step, a time-series of moving-average values is computed using the moving-minimum time-series generated during the first step (and also using the same length time window). The time-series of moving-average values that results from the second step constitutes the time-series of baseflow-separated values, and baseflow targets based on the two Chipola River gages were computed by averaging values from the part of this baseflow flow time series that coincides with the January 1, 2017, to December 31, 2019, NCDM calibration period.

A variety of window lengths were evaluated (7-, 14-, 30-, 45-, and 60-days) when applying this baseflow separation method. A 14-day window length was chosen for both gages. Selection of this window was aided by an analysis of the relation between field measurements of specific conductance and discharge at the Chipola River near Altha stream gage. Specific conductance can serve as a proxy for a natural, conservative, chemical tracer, and when combined with concurrent discharge data, used to estimate the fraction of streamflow derived from groundwater discharge using a simple, two-end member mixing model of specific conductance for each discrete measurement. Streamflow composed entirely of direct runoff was assumed to occur at or below the minimum measured specific conductance value (48 μS/cm) and streamflow composed of entirely groundwater assumed to occur at or above a specific conductance value of 180 μS/cm. The results from the chemical mixing model analysis were most consistent with the results obtained with the USF method of baseflow separation using a 14-day time window. The results of the above

baseflow analyses of data from the Chipola River at Marianna and near Altha gages are shown in Table 5-8.

The two other targets correspond to two spring-fed stream reaches were used in the NCDM calibration: Merritts Mill Pond and Spring Creek. The baseflow target for the outflow from Merritts Mill Pond was computed by averaging the differences between daily concurrent flows from Jackson Blue Spring and the downstream outlet for Merritts Mill Pond during the NCDM calibration period and then adding this value to the Jackson Blue Spring flow target. The baseflow target for Spring Creek was estimated by evaluating the difference between measured flows at the mouth of Spring Creek with concurrent (same day) mean daily outflows from Merritts Mill Pond. There were nine days where flow measurements at the mouth of Spring Creek and mean daily flow Merritts Mill Pond were available. The difference between the flow measured at the mouth of Spring Creek and the daily mean flow from Merritts Mill Pond (Spring Creek flow minus Merritts Mill Pond outflow) on these days ranged from -41 to 36 cfs. These data provided no indication that groundwater inflow to Spring Creek was significantly different than zero because the mean (-7 cfs) and median (-6 cfs) of the change in flow along the reach were well within an interquartile range (-41 to 20 cfs) that included zero. Accordingly, the baseflow target for Spring Creek was set to zero.

Note that there are some stream and river reaches without baseflow targets in the NCDM domain. These reaches include the Chipola River and its tributaries downstream from the Altha gage, and the upper reaches of Econfina, Holmes, or Wrights Creek. All of these reaches are ungaged within the NCDM domain. Although stream gages do exist for the lower Chattahoochee and Apalachicola Rivers, baseflow targets weren't developed for these gages because of the difficulty in estimating groundwater discharge to these large river reaches and because the NCDM domain only includes the western parts of their respective groundwater contributing areas. Despite this, the PEST calibration framework was set up so that simulated values of baseflow are generated during postprocessing for these reaches that lack baseflow targets so that they were available for evaluation. Also note that simulated values are referred to as "model-generated observations" or simply as "observations" in the PEST software documentation, and the names used to identify these simulated values are listed in Table 5-8, under the heading "Baseflow Observation Name".

Table 5-8. Names and descriptions of NCDM baseflow observation reaches, including calibration target reaches

Baseflow Observation Name	Baseflow Data Available (Calibration Target)?	Stream Reach Description	Calibration Target Value, in ft^3/s
q_2358789 (observation zone 1)	Yes	Reaches contributing to flow to the Chipola River at Marianna gage (02358789)	551
q_2359000 (observation zone 2)	Yes	Reaches contributing flow to the Chipola River near Altha gage (02359000) but downstream from the Chipola River at Marianna gage (02358789)	609
qsum_2359000 (observation zones 1 and 2)	Yes	Reaches contributing flow to the Chipola River near Altha gage (02359000)	1160
q_zone03 (observation 3)	No	Reaches contributing flow to the Chipola River downstream of the Altha gage (02359000)	--
q_zone04 (observation 4)	No	Reaches contributing flow to the Apalachicola River, but downstream of the confluence of the Chattahoochee, Flint, and Apalachicola Rivers	--
q_zone05 (observation 5)	No	Reaches contributing flow to the Apalachicola River, at and upstream of the confluence of the Chattahoochee, Flint, and Apalachicola Rivers	--
q_zone06 (observation 6)	No	Reaches contributing to Holmes Creek	--
q_zone07 (observation 7)	No	Reaches contributing to Econfina Creek	--
q_zone08 (observation zone 8)	Yes	Merritts Mill Pond, including contributions from Jackson Blue Spring	239
q_zone09 (observation zone 9)	Yes	Spring Creek	0

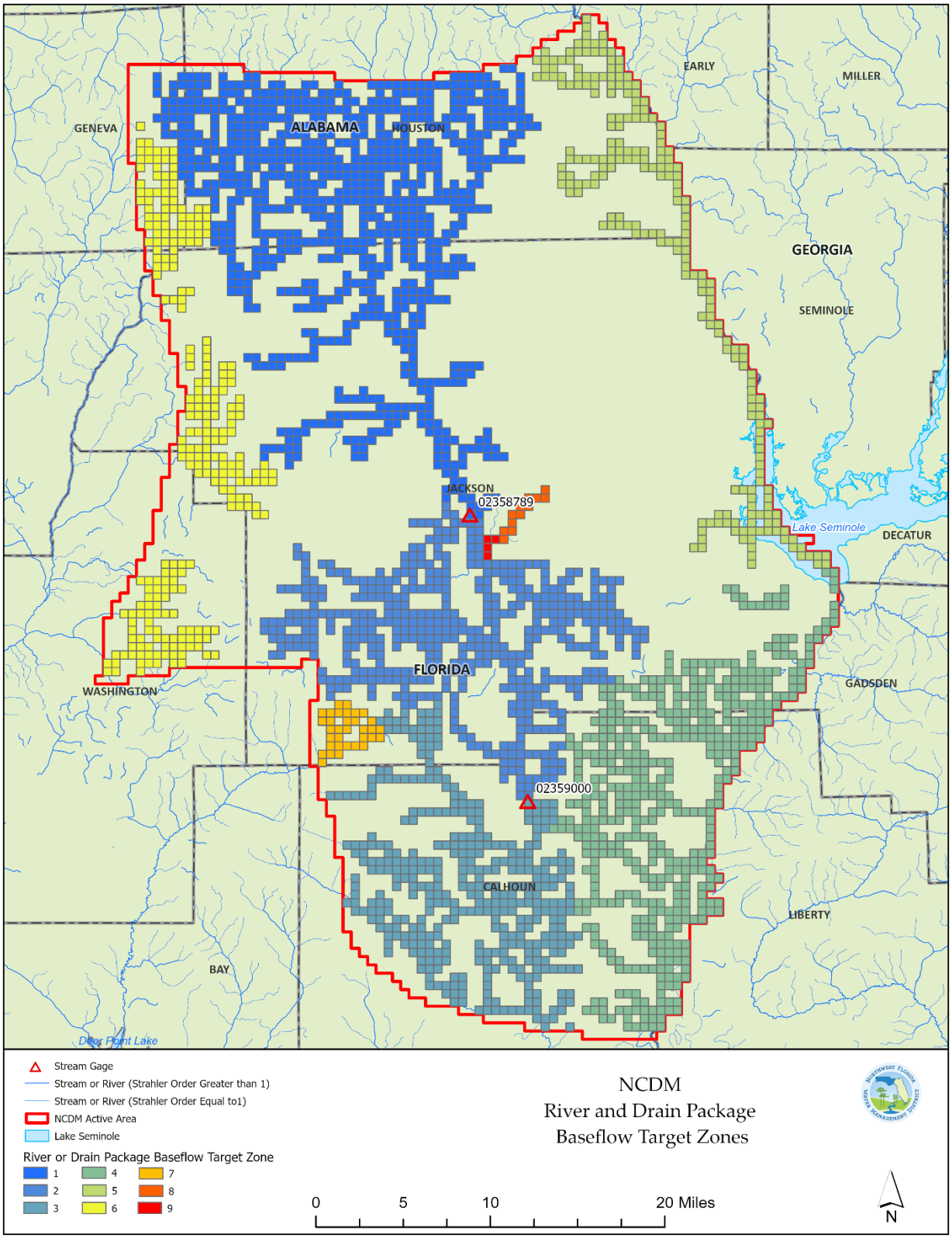

Figure 5-4. Locations of NCDM baseflow calibration target zones.

5-1-2-5. Springflow Targets

There were 39 springs in the NCDM domain that were used a spring flow calibration targets. These targets were created whenever a spring had at least one measurement either at the spring or at a location that measures the collective flow of that spring and other nearby springs that together constitute a 'spring group.' The District identifiers and names of these springs are list in Table 5-9 along with their corresponding calibration target name (PEST observation name) and values. The locations of these spring flow targets are shown in Figure 5-5. Only six of these 39 springs had more than one flow measurement available from the historical record. Jackson Blue Spring was the exception, having 124 measurements available when the spring flow targets were computed, 22 of which were made during the calibration period. Jackson Blue Spring was also the only spring in the NCDM domain with more than six historical measurements. The extensive record of historical measurements at Jackson Blue Spring is the basis for a historical daily flow time series for the spring that began in December 2004 and (as of the date this was written) extends to the present. The target for Jackson Blue Spring was calculated as the arithmetic average of these daily Jackson Blue Spring daily values from during the calibration period.

Table 5-9. NCDM spring flow calibration target names, values and associated spring names and site identifiers

District Identifier	Spring Name	PEST Observation (Calibration Target) Name	Calibration Target Value, in ft^3/s
008628	Hamilton Spring	qspr_008628	1.45
008794	Window Spring	qspr_008794	3.37
008787	Mcrae Spring #1	qspr_008787	0.83
008788	Mcrae Spring #2	qspr_008788	0.83
008789	Mcrae Spring #3	qspr_008789	0.83
008790	Mcrae Spring #5	qspr_008790	0.83
008791	Mcrae Spring #4	qspr_008791	0.83
008629	Sally Spring	qspr_008629	3.10
008631	Grotto Spring	qspr_008631	2.24
008896	Spelman Spring	qspr_008896	5.67
009633	Circle Spring	qspr_009633	2.14
008892	Rocky Creek Spring	qspr_008892	29.13
008719	Rooks Spring #1	qspr_008719	1.59
008720	Rooks Spring #2	qspr_008720	1.60
007946	Black Spring	qspr_007946	65.19
007956	Gadsen Spring	qspr_007956	15.40
007958	Mill Pond Spring	qspr_007958	30.06
007955	Double Spring	qspr_007955	37.50
007960	Springboard Spring	qspr_007960	17.40
008713	Maund Spring	qspr_008713	8.24
009445	Hole-In-The-Wall Spring	qspr_009445	1.28
008666	Twin Caves Spring	qspr_008666	1.60
007959	Sandbag Spring	qspr_007959	1.61
008665	Shangri La Spring	qspr_008665	3.87
005042	Jackson Blue Spring	qspr_005042	99.87
007953	Blue Hole Spring	qspr_007953	10.50
008654	Baltzell Spring #2	qspr_008654	4.66
007954	Baltzell Spring #3	qspr_007954	33.26
008653	Baltzell Spring #1	qspr_008653	1.70
008680	Hays Spring #3	qspr_008680	9.66
008679	Hays Spring #2	qspr_008679	9.66
008678	Hays Spring #1	qspr_008678	9.66
008676	Daniel Spring #7	qspr_008676	1.91
008675	Daniel Spring #6	qspr_008675	1.91
008674	Daniel Spring #5	qspr_008674	1.91
008673	Daniel Spring #4	qspr_008673	1.91
008670	Daniel Spring #1	qspr_008670	1.91
008672	Daniel Spring #3	qspr_008672	1.91
008671	Daniel Spring #2	qspr_008671	1.91

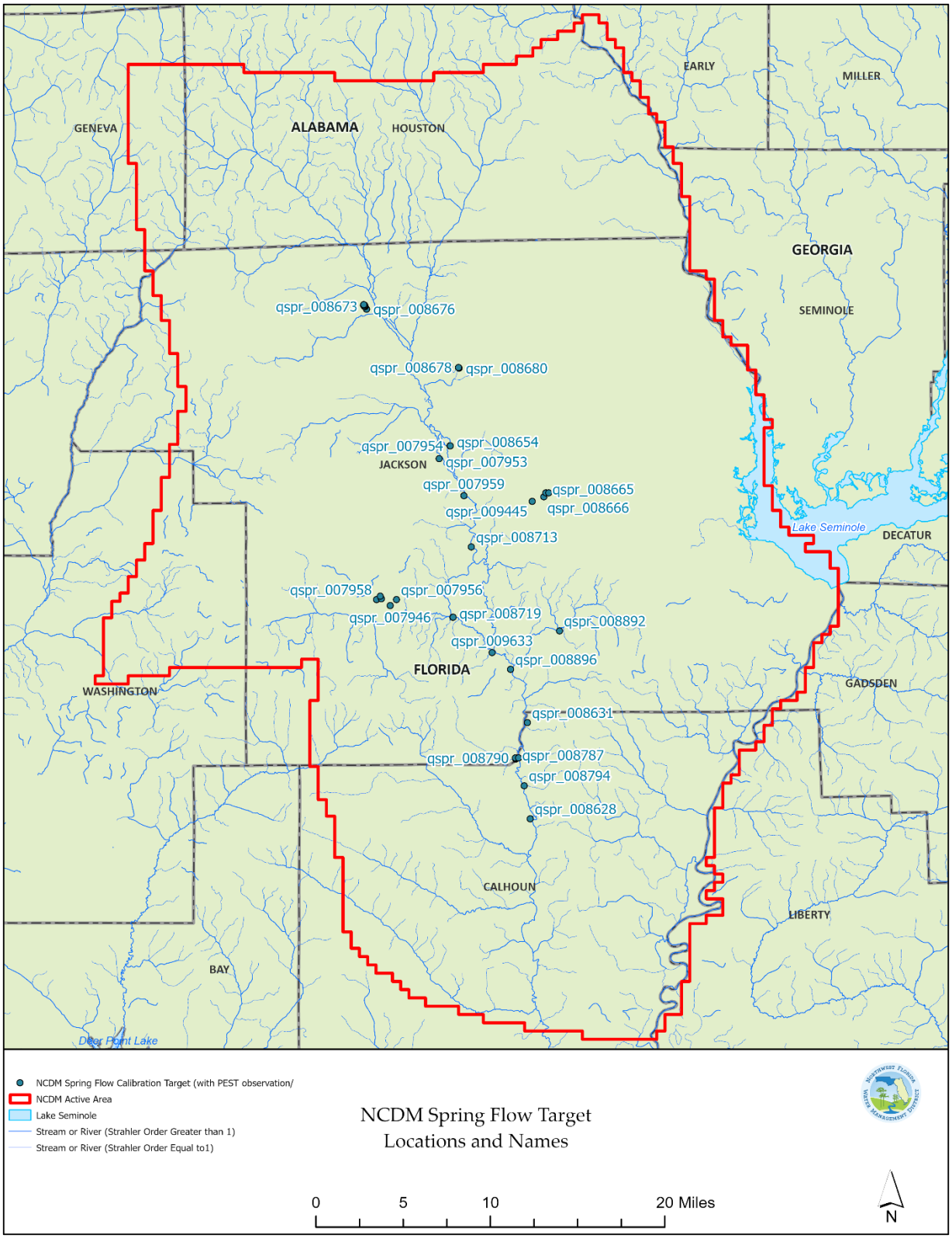

Figure 5-5. Locations of NCDM spring-flow calibration targets.

Spring flow target values for most of the remaining springs were calculated using several methods. If one or more measurements were available at an individual spring, target values for a given spring were calculated as the median of all available historical flow measurements at the spring. The median was chosen because of its resistance to outliers, and therefore more robust estimation of central tendency for small sample sizes (Helsel and others, 2020). Note that many of the springs only had one measurement from the historical record, so the median value for these springs was just equal to the value of the flow. A second method was employed if one or more measurements were not available at an individual spring but were available for a location at which the aggregate flow from group of springs containing that spring were measured. In all but one of these cases, the spring flow target values were calculated as the median of the available historical flow measurements for the spring group divided by the number of springs in the group, thereby distributing the total flow from the spring group in equal parts to each member of the group.

A variation of the second method described above was used in one case (Baltzell Spring). A recent (June 2024) composite measurement was available for the Baltzelll Spring group, and each of the three springs that constitute the group also had one individual measurement made on either the first or second of October 2003. In this case, the fractional contribution of each spring to the collective flow from the group was computed by dividing each spring's measured flow on either the first or second of October 2003 by the sum of the measured flows from the springs on these dates. The June 2024 composite measurement was then multiplied by the fractional contribution each spring to the group's aggregate flow in October 2003 to provide target values for the individual springs that better reflect their individual contributions to the spring group and also better reflect more recent conditions.

5-1-2-6. Flooding Penalty Function Targets

A set of flooding penalty-function targets were developed to mitigate against simulated heads that exceeded land surface to an unreasonable degree. A target value of zero was assigned to each cell in the uppermost active model layer. During the calibration of the NCDM simulated-equivalents of these target values were assigned a value of zero if the simulated head was below land surface (thereby matching the corresponding calibration target and resulting in no increase in the objective function); otherwise, the simulated target value was assigned a value equal to the difference between the simulated head and land surface.

5-1-3. Calibration Target Weighting

As noted previously, calibration of the NCDM sought to minimize an objective function consisting of two parts: (1) a measurement component, which was the sum of the squared, weighted differences between calibration target values and their model-simulated

equivalents, and (2) a regularization component, consisting of the sum of the squared, weighted differences between some article of prior information and the corresponding representation in the model. To implement the first part, it was necessary to assign weights to each calibration target value.

The calibration targets are organized into the following target groups: groundwater levels (heads), horizontal head differences, vertical head differences, baseflow and baseflow difference targets, spring flow targets, and flooding penalty functions. Calculation of target weights generally occurred in two steps and was a function of these groupings. In the first step, initial weight values were calculated within each calibration-target group, establishing the relative weight values within each group. In the second step, these initial, within-group weight values were scaled by factors (one scaling factor per group) so that each target group contributed to the objective function in the desired amount at the outset of a given calibration run.

5-1-3-1. Within-Group Weighting

At the outset of the calibration effort, weight values for the (non-differenced) head targets were all set to 1, with two exceptions. The target associated with observation well 012769 Jackson Blue #2 – Floridan was set to 100, reflecting the fact that it is about 1,100 feet from Jackson Blue Spring and one cell to the southeast of the model grid cell containing Jackson Blue Spring. A 'soft' head calibration target (calibration target name sh_jbs) was also created for the cell associated with Jackson Blue Spring, and assigned head target value that was 0.25 feet higher than that assigned to the Jackson Blue Spring pool elevation (reflecting the expectation of very little head difference between pool elevation and the simulated aquifer head) and a weight of 100. In both cases, the higher weights at these two locations were a reflection of their proximity to Jackson Blue Spring and the objective of producing a model for predicting changes in flows from this spring. These within-group weight values (values prior to adjusting intergroup weighting) assigned earlier in the calibration process were subsequently modified during the calibration effort so that all but one head target had within-group weight values of 1 (35 of the 46 head targets) or 2 (10 of the 46 targets). The remaining head target was located at well 004912 William Fisher and its within-group weight value was reduced to 1/60 because of its close proximity to the western boundary of the model.

Within-group weighting for the horizontal and vertical head difference targets were very similar to that ultimately used for the head targets. Three of five the non-zero weighted horizontal head difference targets had within-group weight values of 1, and the remaining two targets had within-group weights of 2. Among the eight vertical head difference targets, all but one had a within-group weight of 1, with the remaining target having a value of 2.

Within-group weights for the NCDM baseflow targets were calculated using an approach intended to mitigate against targets with smaller value receiving insufficient weight in the calibration, by increasing the weights of smaller-valued baseflow targets (relative to those of larger-valued baseflow targets). The three baseflow targets associated with the Chipola River (targets q_2358789, q_2359000, and qsum_2359000) had within-group weights that, when multiplied by their respective target values, were individually equal to about 28 percent of the sum of the weighted baseflow target values. The baseflow target associated with Merritts Mill Pond was assigned a within group weight that, when multiplied by its corresponding target value, was equal to about 16 percent of the sum of the weighted baseflow target values. The one remaining target, associated with Spring Creek, had a zero-valued target and it was assigned a within group weight that was about 10 times higher than the weight associated with the baseflow target with the next lowest weight (Merritts Mill Pond).

Within-group weights for the NCDM spring flow targets were also calculated using an approach that mitigates against targets with smaller value receiving insufficient weight in the calibration, although the approach was different because much less data was generally available for the spring flow targets. For spring flow targets, the within-group weights were generally calculated as the inverse of an estimate of the time sampling uncertainty (standard deviation of the target estimation error) of the target. This sampling uncertainty was estimated based on the number of spring flow measurements that were available at a given spring. For springs with only one measurement in the historical record, the sampling uncertainty was estimated as being equal to 0.6 times the target value. For springs with two to three measurements, the target sampling uncertainty was estimated as 0.4 times the target value. For springs with more than three measurements (not including Jackson Blue Spring), the target sampling uncertainty was estimated as 0.3 times the target value. Note that the above values used to scale target values to estimate target uncertainties were based on results from a resampling experiment that indicated that the ratio of the standard deviation of the sampling error (estimated as the median of a small, random sample of Jackson Blue Spring measurements minus the calibration period mean of measured discharge values at Jackson Blue Spring) and the Jackson Blue Spring measured discharge decreased from about 0.55 to 0.3 for sample sizes ranging from one to five, respectively.

For springs that were part of a spring group, the target sampling uncertainty was estimated as the product of 0.6, the number of springs in the group, the target value, and 0.9. This approach is similar to that described for springs with one measurement, but accounts for the fact that target flow values of individual springs in a spring group are based on dividing the measured flow from the spring group by the number of springs. The 0.9 scalar multiplier is an expression of an estimate that any one spring might account for up to 90 percent of the total flow from the group.

For Jackson Blue Spring the sampling uncertainty was estimated as the root-mean square error of the rating in effect during the calibration period (standard deviation of residuals from the Baxter well rating) divided by the square root of the number of days in the calibration period. The resulting weight, computed as the inverse of this sampling uncertainty was subsequently increased by a factor of 10, reflecting the fact that simulating changes in flow at Jackson Blue Spring was the primary objective of the NCDM.

Flooding penalty function target weights were assigned values that decreased as topographic relief increased. Therefore, simulated flooding in cells with a relatively flat topography caused the objective function to increase to a greater degree than flooding in cells with greater topographic relief. A detailed description of the calculation of within-group weight values of the flooding penalty function targets are provided in Tetra Tech (2024).

5-1-3-2. Intergroup Weighting

Once the within-groups were defined, the weights used during a given calibration run were generally calculated by multiplying each within-group target weight by a scaling factor associated with that target's group. The scaling factor values were calculated by first defining the desired relative contributions of each target group to the objective function at the outset of a given calibration run. The scaling factor values for each group were then calculated by determining the values that would result in the desired contributions after computing the sum of the squared product of each target residual, the corresponding weight for that residual, and the scaling factor for the corresponding target group. The desired relative contributions used in the final stages of the NCDM calibration effort are shown for each target group in Table 5-10.

Table 5-10. Relative contributions of calibration target groups during the final stages of the NCDM calibration.

Target Group[1]	Relative Contribution to Initial Objective Function Value
Head Targets (h_obs)	0.300
Horizontal Head Difference Targets (dhh_obs)	0.105
Vertical Head Difference Targets (dhv_obs)	0.105
Baseflow Targets (qstream_obs)	0.140
Spring Flow Targets (qspring_obs)	0.300
Flooding Penalty Function Targets (pen_fxns)	0.050

[1] *PEST target group names are shown in parentheses.*

5-1-4. Postprocessing of Model Outputs

Following the completion of each execution of the model, model-simulated equivalents (PEST observations) of calibration targets are obtained by postprocessing model outputs. Postprocessing occurs in a series of steps in which programs from the PEST Utility (Doherty,

April 2023), PEST Groundwater Utilities (Doherty, August 2021; Doherty, May 2023) and custom-built Python scripts for the NCDM calibration are executed, producing output files that are read by the PEST-HP software (Doherty, February 2020) and used to calculate the objective function associated with the parameter values used to construct a given candidate version of the NCDM.

The first postprocessing step is the interpolation of simulated head values at hydraulic head calibration target locations. This was accomplished using the MOD2SMP PEST Groundwater Utility (Doherty, May 2023), which interpolates the simulated head value at the horizontal location (defined by 'easting and westing' coordinates) of a hydraulic-head calibration target. The simulated value is obtained through bilinear interpolation of simulated heads from the four closest grid-cell centers that surround the target location and that are within the layer containing the target.

The simulated head values at hydraulic head targets obtained in the previous step are subsequently used to calculate simulated horizontal and vertical head difference values from well pairs that define NCDM horizontal and vertical head difference calibration targets. These head difference calculations are performed by the OBS2OBS PEST Utility program (Doherty, April 2023).

Flooding penalty function values are then calculated for each grid cell in the uppermost active layer of the NCDM using an NCDM-specific Python script (penalty_function.py). This program reads the MODFLOW unformatted heads file and computes the difference between the mean land surface of a cell and the simulated head in the uppermost active layer of that cell. If the simulated head is greater than land surface, a penalty function value equal to the simulated head minus the land surface elevation is assigned to the flooding penalty function target assigned to that cell. A penalty function value of zero is assigned if the simulated head in the cell is less than or equal to the mean land surface of the cell, or if the cell is dry or inactive.

Simulated flow to the river and stream reaches defined in Table 5-3 is then calculated by the NCDM-specific Python script "compute_riv_and_drn_fluxes.py." This program reads information in the MODFLOW-NWT River, Drain, and Time-Varying Specified Heads (CHD) Package input files, and the unformatted heads file. It then computes the flux from each River and Drain Package feature and then computes the net simulated groundwater flow to each of the baseflow calibration targets defined in Table 5-3. Simulated flows computed by this Python script for the reaches contributing flow to the 02358789 Chipola River at Marianna gage (River and Drain Package parameter and calibration target zone 1) and the reaches contributing flow to the 02359000 Chipola River near Altha gage but downstream from the 02358789 Chipola River at Marianna gage (River and Drain Package parameter and

calibration target zone 2) are then summed using the OBS2OBS PEST Utility program (Doherty, April 2023).

The final step in the postprocessing sequence is the calculation of simulated flows at the 39 NCDM spring flow targets. This was accomplished using the NCDM-specific Python script compute_spring_fluxes.py. This program computes the flux from each of the MODFLOW-NWT Drain Package features that represent the springs in the NCDM, using the same methods as MODFLOW-NWT and that are described in Harbaugh (2005).

5-1-5. Tikhonov Regularization

Large numbers of adjustable parameters are needed to represent real-world groundwater flow systems, given the inherent complexity of these systems. Unfortunately, relevant data such as groundwater heads, baseflows, and spring flows are rarely available in sufficient quantity or accuracy to capture this complexity. Therefore, calibrating (history matching) groundwater flow models is almost always an 'ill-posed problem' - that is one with more parameters than available observations. Tikhonov regularization (often combined with singular value decomposition) is a common means for solving such problems (Doherty, 2015) and has been applied in a wide range of applications including geophysics (groundwater flow and transport problems, and petroleum reservoir analysis), medical imaging (Vogel, 2002), and signal processing/telecommunications (Mallat, 2009).

Tikhonov regularization was used throughout the NCDM calibration effort. In the earlier stages of this effort, regularization was implemented a 'preferred value' approach, wherein the preferred values that were based on values equal to those described in the conceptual model section of this report and all of the preferred values were assigned equal weights. These preferred values were updated later as the calibration effort progressed, reflecting information gained through the initial calibration effort and the limitations associated with using aquifer performance results to estimate K_h parameter variations at the scale of the NCDM.

During the final stages of the calibration effort, a 'preferred homogeneity' approach was adopted for regularization. This approach has the distinct advantage of not requiring prior estimates of preferred values. In this approach, the preferred condition is that parameter fields (such as K_h or recharge) be as uniform as possible unless information in the calibration dataset indicates that introducing additional spatial heterogeneity warranted. This approach was implemented by using PEST prior information records (Doherty, January 2023) with equations indicating that there should be no difference between the value of a parameter from a given parameter group (for example a K_h or recharge multiplier values) at a given pilot point location and the value of a parameter from that same parameter group at an adjacent pilot point location. Preferred-homogeneity prior-information equations were defined for all

possible combinations of neighboring pilot points for each pilot-point based parameter group, and all of these equations were assigned equal weights.

5-2. Calibration Results

The bulk of the NCDM calibration effort occurred as a set of about 40 individual calibration runs. The results of each run were evaluated by assessing statistical summaries and plots of residual values (simulated value minus its corresponding calibration target value) of head, horizontal head difference, vertical head difference, baseflow, and stream flows from the calibration target dataset, as well as the occurrence of simulated heads higher than land surface (simulated flooding). Maps of these residuals, hydraulic properties, and the simulated flooding were also evaluated during these assessments. Evaluation of the results of a given calibration run resulted in refinements or corrections to the parameterization or preprocessing of model inputs, parameter initial values or bounds, model boundary conditions, postprocessing of model outputs, calibration target values or associated weights, or regularization constraints. Near the conclusion of this process, a set of additional model runs were initiated to test incremental changes to selected K_h, anisotropy, and recharge pilot point values to see if the heterogeneity of their respective fields could be reduced in some areas without adversely affecting the model fit, and the results of successful test runs were incorporated into a final calibration run that resulted in the final version of the NCDM. Those results are shown in the text, tables, and figures in this section of the report.

5-2-1. Model Fit

Summary statistics of differences between calibration target values and their simulated equivalents (target residuals or residuals) are shown in Table 5-11, and tables of calibration targets and corresponding simulated and residual values for the various calibration target groups are shown in Table 5-12 through Table 5-16. Scatterplots of calibration target and corresponding simulated values and maps of target residuals are shown in Figure 5-6 through Figure 5-14. The mean and median residuals (Table 5-11) indicated a relatively unbiased, well-fit model, particularly for the head and spring flow targets, which were treated as higher-priority targets during the NCDM development. Median and mean residuals for the head targets were less than 1 foot. Measures of the variability of the head targets residuals were also quite low: the standard deviation (root-mean square error) and mean absolute value (mean absolute error) residual statistics were both less than 2.5 feet. The mean absolute value of the residual was about 0.7 feet lower than the residual standard deviation because of one larger than typical residual of 9.2 feet associated with the 004912 William Fisher calibration head target. It's important to note that the parameters that the Jackson Blue Spring is most sensitive to are unlikely to be those that the William Fisher head

target is sensitive to because of the distance between the two targets and the fact that the Chipola River lies between them and is incised into the Upper Florida aquifer, further limiting the potential for these two targets to have conflicting parameter sensitivities.

Table 5-11. Statistical summary of calibration target residuals of the NCDM.

Calibration Target Group Name	Count	Minimum	25th Percentile	Mean	Median	Standard Deviation	Mean Absolute Value	75th Percentile	Maximum
dhh_obs	5	-1.4	-0.7	-0.6	-0.4	0.5	0.6	-0.3	-0.2
dhv_obs	8	-1.9	-0.1	1.0	0.9	1.9	1.7	2.4	3.7
h_obs	46	-3.9	-0.5	0.4	0.4	2.1	1.4	1.2	9.2
pen_fxns	7205	0.0	0.0	0.0	0.0	0.7	0.0	0.0	31.6
qspring_obs	39	-24.8	-1.8	-1.1	0.0	5.1	2.6	0.6	8.7
qstream_obs	5	-6.3	7.7	55.0	21.7	66.0	57.6	115.2	136.9

Table 5-12. Values of head calibration targets, simulated equivalents of targets, and target residuals

District Identifier	Well Name	Target Name	Target Value, in feet	Simulated Value, in feet	Residual Value, in feet
002145	OKALOOSA ASPHALT	h_002145	94.23	92.46	-1.77
002624	NWFWMD-BLOUNTSTOWN FLORIDAN	h_002624	70.18	69.34	-0.84
002625	NWFWMD-BLOUNTSTOWN INTERMEDIATE	h_002625	70.00	71.09	1.09
002626	NWFWMD-BLOUNTSTOWN SURFICIAL	h_002626	75.63	75.49	-0.14
003775	ALTHA EAST #2	h_003775	54.12	54.57	0.45
004681	USGS #39/HOMER HIRT	h_004681	73.98	73.85	-0.13
004795	INTERNATIONAL PAPER @ CYPRESS	h_004795	92.46	91.36	-1.10
004912	WILLIAM FISHER	h_004912	64.32	73.51	9.19
005062	COTTONDALE #3	h_005062	110.37	109.66	-0.71
005147	W.R. BUCKHALTER	h_005147	78.70	78.58	-0.12
005151	FRANCIS RETTIG 4-INCH	h_005151	75.46	75.75	0.29
005226	NWFWMD-BAXTER SAND PIT VISA	h_005226	79.67	81.30	1.63
005266	NWFWMD-PITTMAN VISA/S661	h_005266	84.58	85.36	0.78
005408	NWFWMD-2 EGG AMBIENT #3	h_005408	94.96	92.76	-2.20
005603	GRACEVILLE #3	h_005603	126.27	125.73	-0.54
005654	NORTH AMER FARMS #9	h_005654	111.93	111.75	-0.18
005655	NORTH AMER FARMS #7	h_005655	103.68	106.32	2.64
005671	NWFWMD-HWY 71 NORTH OF MALONE	h_005671	119.73	117.07	-2.66
005697	DITTY JC-3 (JK-30)	h_005697	112.23	114.11	1.88
005718	DITTY JC-1 (JK-28)	h_005718	114.26	115.55	1.29
006665	AQUACULTURE FARM #3	h_006665	44.29	48.74	4.45
007471	NORTH AMER FARMS #2	h_007471	103.43	103.86	0.43
007925	NORTH AMER FARMS #16	h_007925	96.15	98.42	2.27
008226	NORTH AMER FARMS #17	h_008226	102.14	98.23	-3.91
009809	WOERNER - MO #1	h_009809	89.42	91.36	1.94
009810	WOERNER - MO #2	h_009810	94.40	91.38	-3.02
009811	WOERNER - MO #4	h_009811	123.49	123.19	-0.30
010053	SUNLAND MONITOR/S730	h_010053	79.04	79.81	0.77
012066	SC MON #1	h_012066	80.02	80.05	0.03
012068	SC MON #3	h_012068	103.49	104.22	0.73
012069	SC MON #4	h_012069	89.07	89.58	0.51
012336	STURGEON AQUAFARM - MO #1	h_012336	92.49	95.40	2.91
012337	STURGEON AQUAFARM - MO #2	h_012337	96.66	95.86	-0.80
012359	ICE RIVER SPRINGS- HAYS WELL # 2 - BU #5	h_012359	82.29	81.58	-0.71
012360	ICE RIVER SPRINGS - HAYS WELL # 1 - BU #4	h_012360	80.79	81.58	0.79
012544	STURGEON AQUAFARM - MO #3	h_012544	94.69	96.77	2.08
012768	JACKSON BLUE #1 - CLAIBORNE	h_012768	77.30	77.95	0.65
012769	JACKSON BLUE #2 - FLORIDAN	h_012769	77.05	77.54	0.49
012797	CYPRESS PARK #1 - FLORIDAN	h_012797	97.01	98.25	1.24
012798	CYPRESS PARK #2 - SURFICIAL	h_012798	118.50	119.07	0.57
012844	GRAND RIDGE #4	h_012844	92.40	94.72	2.32
012847	CHIPOLA WMA #1	h_012847	93.26	93.27	0.01
012852	NWFWMD-MALONE APT CAS-M1	h_012852	110.56	111.23	0.67
012854	NWFWMD-MALONE APT FAS-M2	h_012854	125.72	123.49	-2.23
012067	SC MON #2	h_012067	91.92	91.80	-0.12
--	--	sh_jbs	76.97	76.74	-0.23

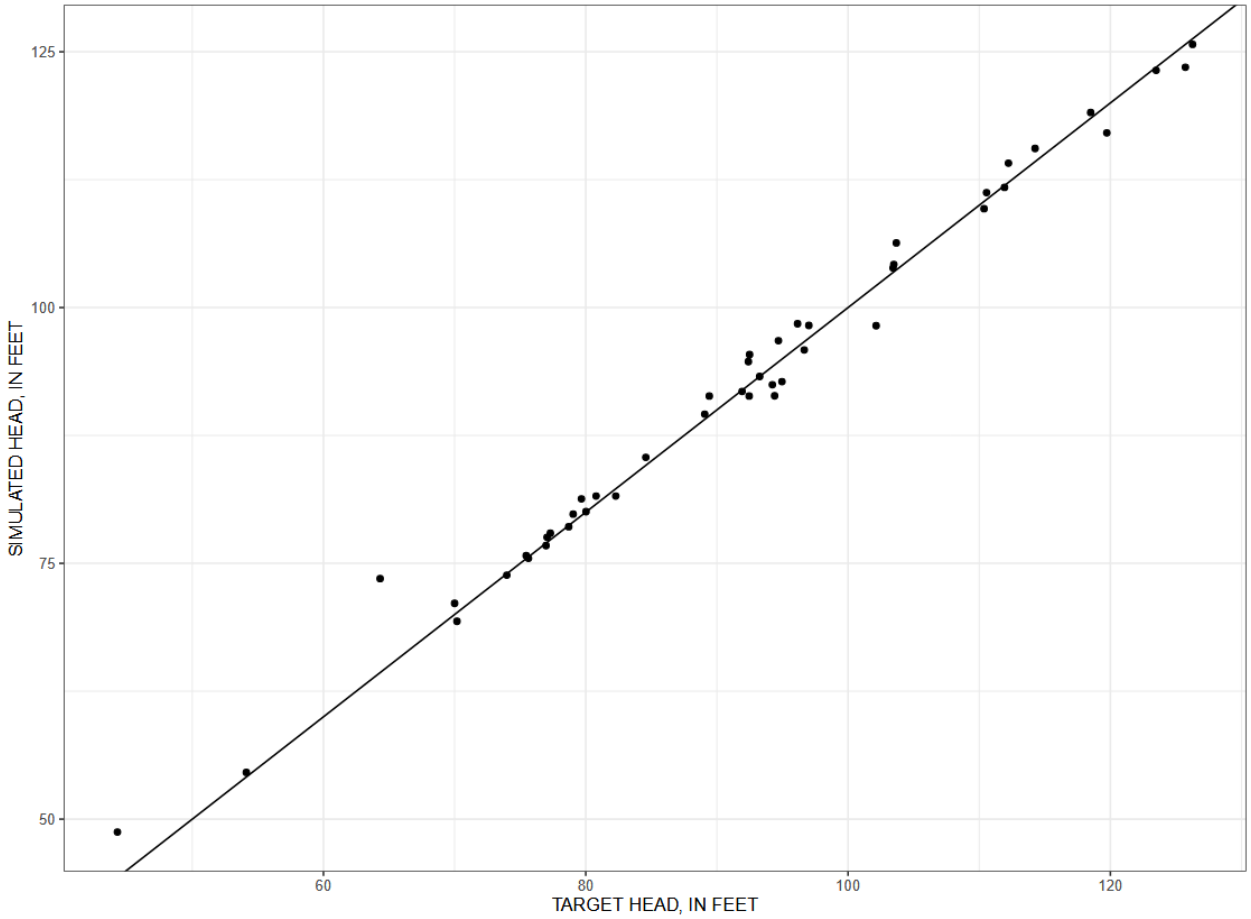

Figure 5-6. Plot of simulated versus calibration target values of hydraulic head.

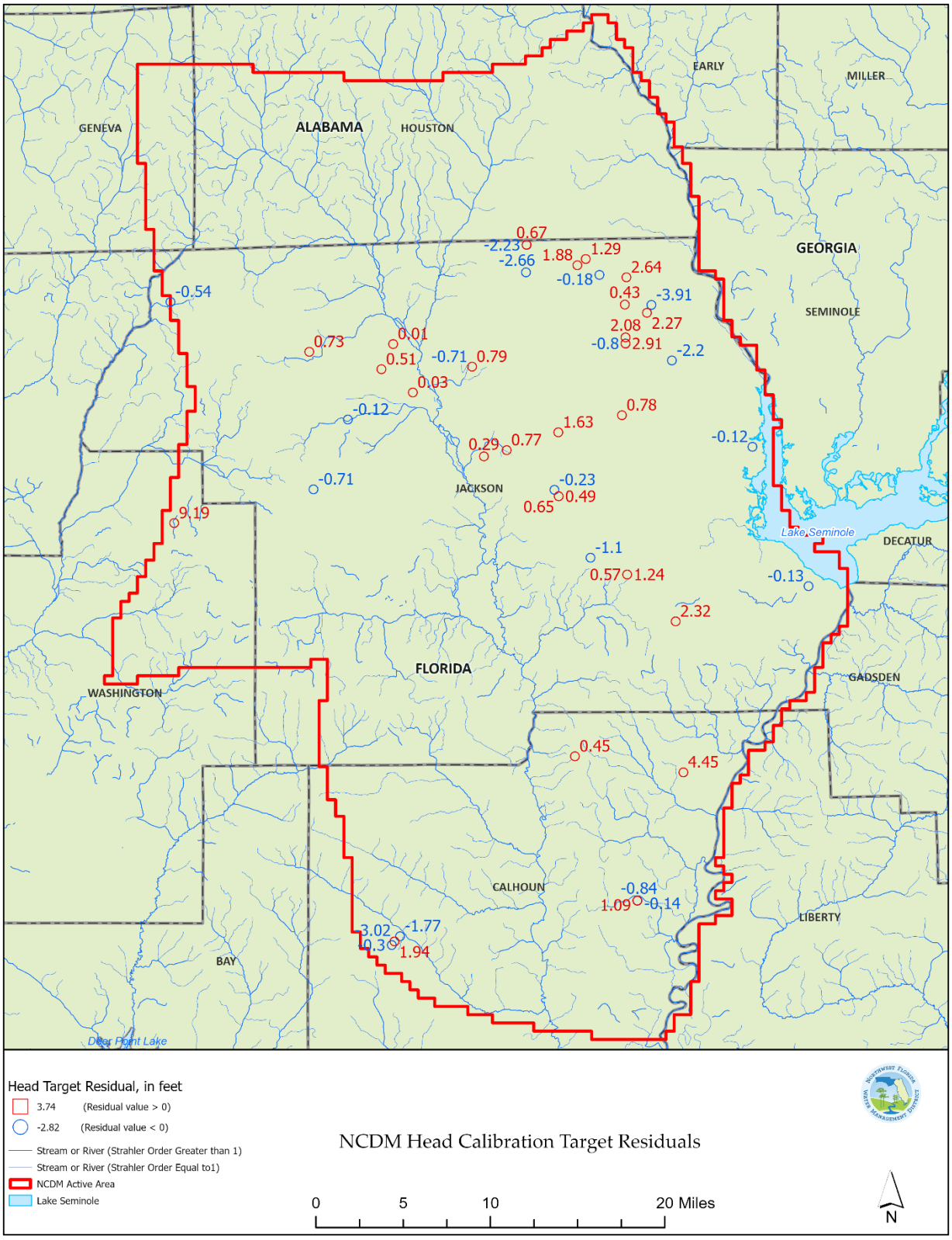

Figure 5-7. Map of head calibration target residuals.

The spring flow targets are considered to be generally well fit, especially relative to the uncertainty of the target values. As noted previously, nearly all (33 of the 39) of the spring flow targets were based on only one historical measurement, and only one spring (Jackson Blue Spring) had one or more measurements that were made during the 2017-2019 calibration period. Thus, with the exception of Jackson Blue Spring, the uncertainty of the spring flow target values was high because of sample size limitations. The residual for the Jackson Blue Spring target was within 1 percent of the target value, indicating a very good fit at this target. The standard deviation and mean absolute value of a given spring target's residual relative to its corresponding target value were 0.57 and 0.38, respectively, which is consistent with the expected uncertainties in the target values. The median of the ratio of a given spring target's residual to its corresponding target value was 0.02, respectively, indicating a lack of bias in the model fit to the spring flow targets. The poorest fit among the spring flow targets occurred at 007954 Baltzell Spring #3, which had a target value of residual of about -25 cfs.

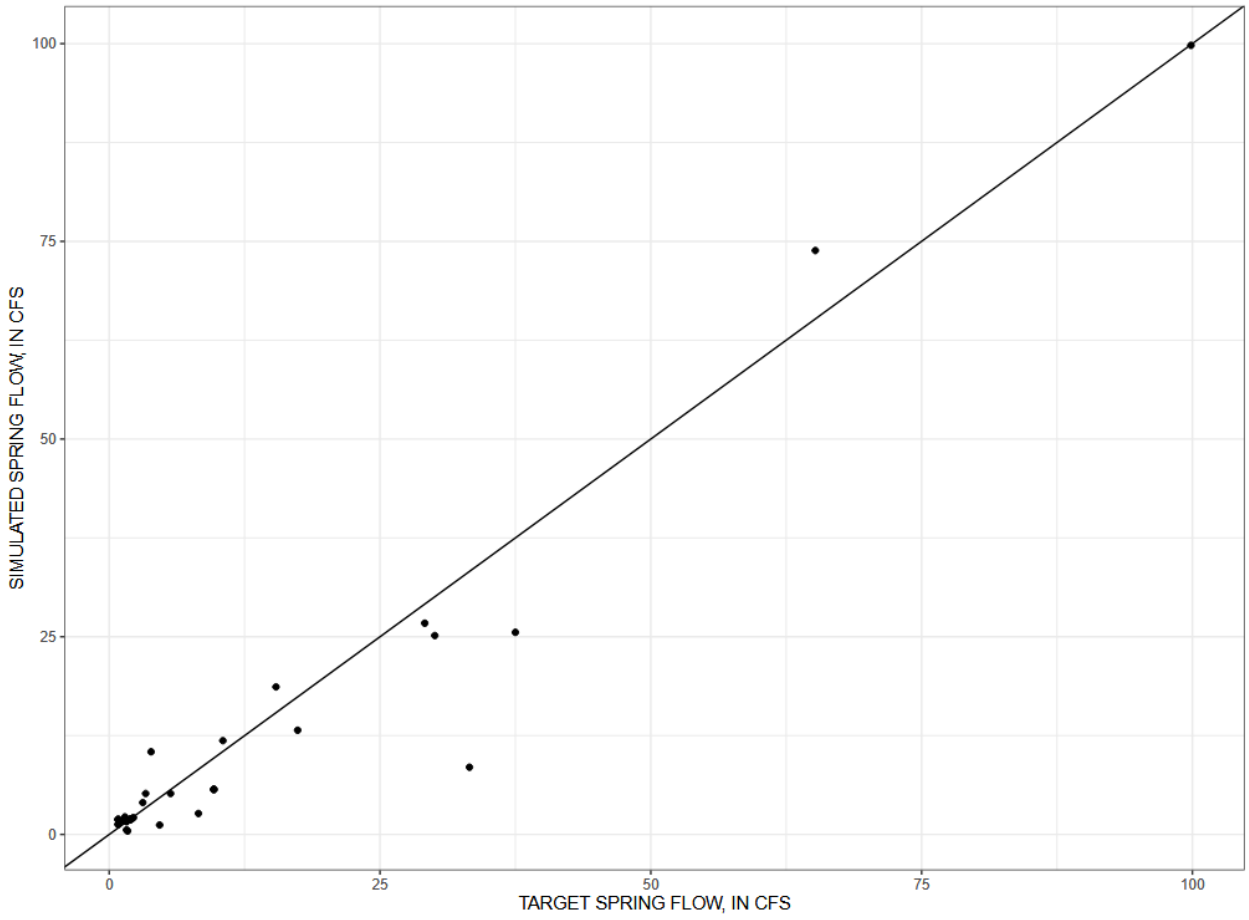

Figure 5-8. Plot of simulated versus calibration target values of spring flows

Table 5-13. Values of spring flow calibration targets, simulated equivalents of targets, and target residuals.

District Identifier	Spring Name	Target Name	Target Value, in cfs	Simulated Value, in cfs	Residual, in cfs
008628	Hamilton Spring	qspr_008628	1.45	2.22	0.77
008794	Window Spring	qspr_008794	3.37	5.18	1.81
008787	Mcrae Spring #1	qspr_008787	0.83	1.89	1.06
008788	Mcrae Spring #2	qspr_008788	0.83	1.89	1.06
008789	Mcrae Spring #3	qspr_008789	0.83	1.89	1.06
008790	Mcrae Spring #5	qspr_008790	0.83	1.27	0.44
008791	Mcrae Spring #4	qspr_008791	0.83	1.27	0.44
008629	Sally Spring	qspr_008629	3.10	4.03	0.93
008631	Grotto Spring	qspr_008631	2.24	2.13	-0.11
008896	Spelman Spring	qspr_008896	5.67	5.18	-0.49
009633	Circle Spring	qspr_009633	2.14	2.02	-0.12
008892	Rocky Creek Spring	qspr_008892	29.13	26.71	-2.42
008719	Rooks Spring #1	qspr_008719	1.59	1.68	0.09
008720	Rooks Spring #2	qspr_008720	1.60	1.69	0.09
007946	Black Spring	qspr_007946	65.19	73.84	8.65
007956	Gadsen Spring	qspr_007956	15.40	18.66	3.26
007958	Mill Pond Spring	qspr_007958	30.06	25.15	-4.91
007955	Double Spring	qspr_007955	37.50	25.56	-11.94
007960	Springboard Spring	qspr_007960	17.40	13.17	-4.23
008713	Maund Spring	qspr_008713	8.24	2.65	-5.59
009445	Hole-In-The-Wall Spring	qspr_009445	1.28	1.74	0.46
008666	Twin Caves Spring	qspr_008666	1.60	0.58	-1.02
007959	Sandbag Spring	qspr_007959	1.61	1.61	0.00
008665	Shangri La Spring	qspr_008665	3.87	10.45	6.58
005042	Jackson Blue Spring	qspr_005042	99.87	99.79	-0.08
007953	Blue Hole Spring	qspr_007953	10.50	11.86	1.36
008654	Baltzell Spring #2	qspr_008654	4.66	1.19	-3.47
007954	Baltzell Spring #3	qspr_007954	33.26	8.50	-24.76
008653	Baltzell Spring #1	qspr_008653	1.70	0.43	-1.27
008680	Hays Spring #3	qspr_008680	9.66	5.69	-3.97
008679	Hays Spring #2	qspr_008679	9.66	5.69	-3.97
008678	Hays Spring #1	qspr_008678	9.66	5.69	-3.97
008676	Daniel Spring #7	qspr_008676	1.91	1.86	-0.05
008675	Daniel Spring #6	qspr_008675	1.91	1.86	-0.05
008674	Daniel Spring #5	qspr_008674	1.91	1.86	-0.05
008673	Daniel Spring #4	qspr_008673	1.91	1.86	-0.05
008670	Daniel Spring #1	qspr_008670	1.91	1.86	-0.05
008672	Daniel Spring #3	qspr_008672	1.91	1.86	-0.05
008671	Daniel Spring #2	qspr_008671	1.91	1.86	-0.05

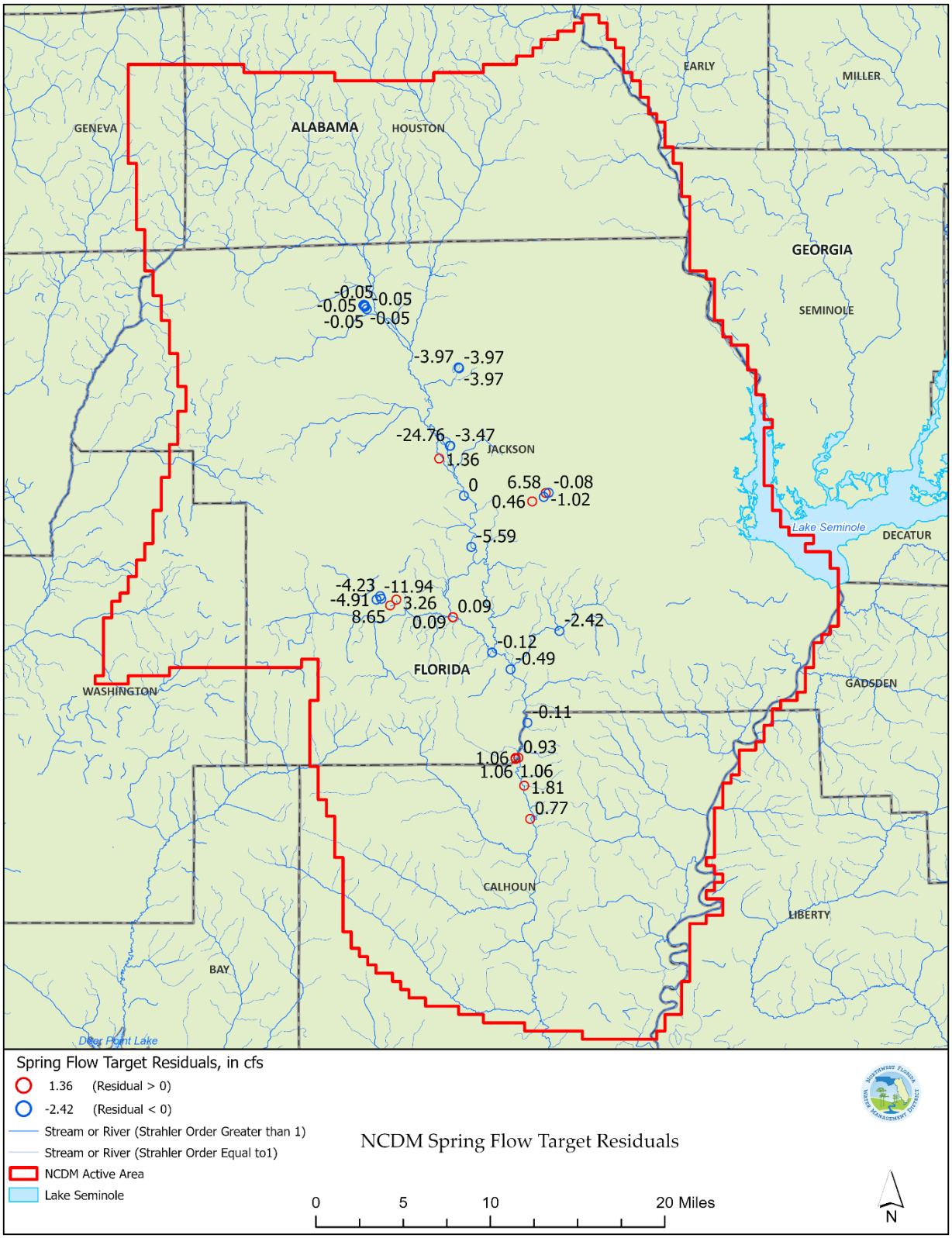

Figure 5-9. Map of spring-flow calibration target residuals

The horizontal head difference targets were very well fit. There was some under-simulation tendency, based on the fact that simulated values of all targets were less than their corresponding target values (Figure 5-10). However, the magnitude of the residuals was small in absolute value and in comparison to the magnitude of the target value, indicating a good fit to this target group. In particular, the model fits were very good at the two horizontal head difference targets (dhh_1 and dhh_3) that are the most relevant to the intended use of the model because they both include the Upper Floridan aquifer well near Jackson Blue Spring as one of the wells in the well pairs that define the targets.

Table 5-14. Values of horizontal head difference calibration targets, simulated equivalents of targets, and target residuals

Target Name	Target value, in feet	Simulated value, in feet	Residual Value, in feet
dhh_1	-19.96	-20.71	-0.75
dhh_2	-23.03	-24.40	-1.37
dhh_3	-7.53	-7.82	-0.29
dhh_4	-5.99	-6.41	-0.42
dhh_6	-14.42	-14.64	-0.22

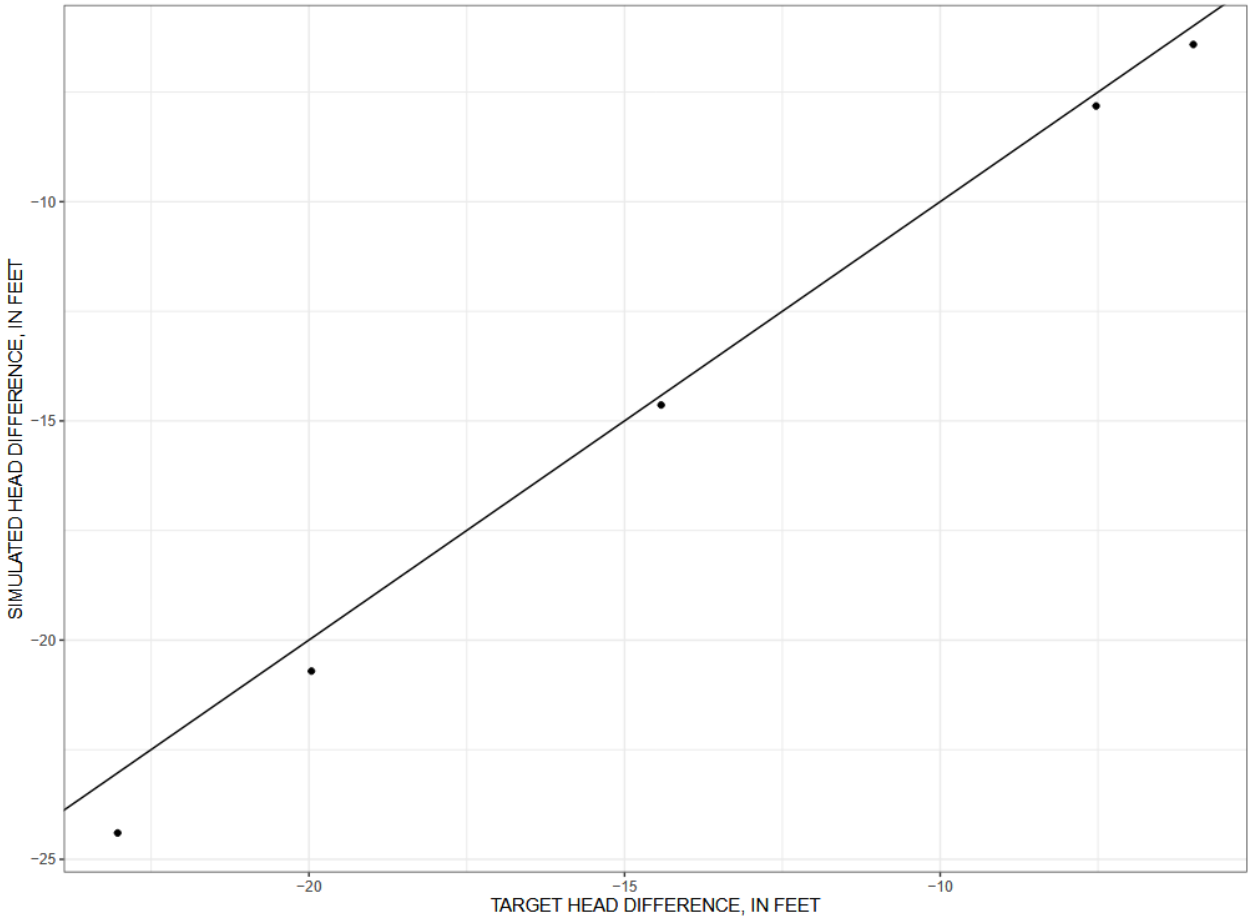

Figure 5-10. Plot of simulated versus calibration target values of horizontal head differences

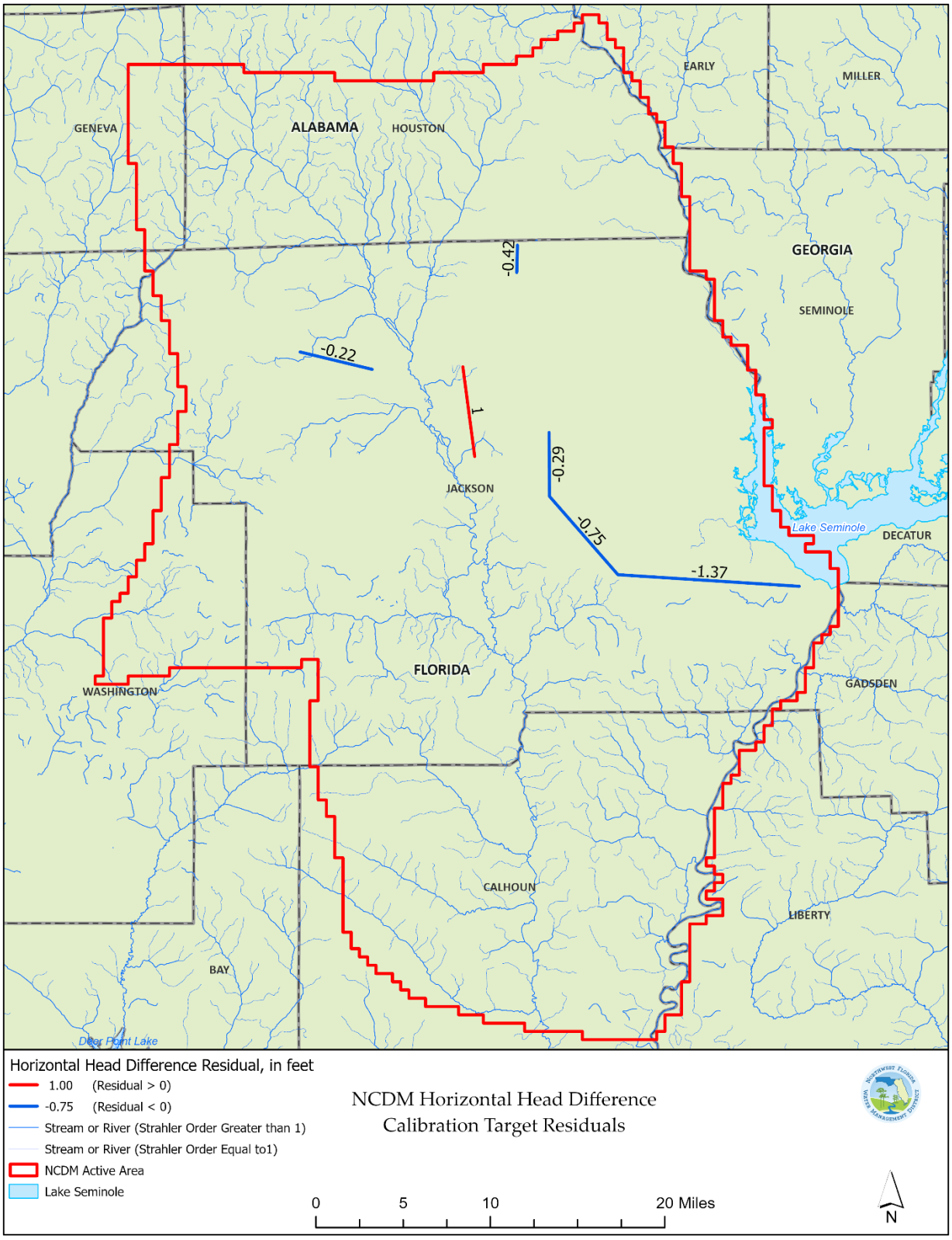

Figure 5-11. Map of simulated versus calibration target values of horizontal head differences

Among the eight available vertical head difference targets, the targets dhv_6 and dhv_7 are closest to Jackson Blue Spring (Figure 5-3). Target dhv_6 is only about 0.25 mile south-southeast of Jackson Blue Spring and represents the head difference between the Claiborne and Upper Floridan aquifers. Target dhv_7 is located about 6.2 miles southeast of Jackson Blue Spring and represents the head difference between the Upper Floridan aquifer and the surficial aquifer system. The model fit at both of these sites was excellent.

Target dhv_5 is located about 9.4 miles north-northeast of Jackson Blue Spring and represents the head difference between the Upper Floridan aquifer and surficial aquifer system. The simulated value of target dhv_5 likely underpredicts the actual head difference between the Upper Floridan aquifer and the surficial aquifer system at this site to some degree. However, this is difficult to assess because all of the five available calibration period vertical head difference measurements were made during the latter part of 2019 (these vertical head difference values ranged between about -3 and -6 feet). The simulated value of the northernmost vertical head difference target (dhv_8) had a value of about -12 feet, which was well within the range of measured values (approximately -10 to -27 feet) of this difference between Claiborne and Upper Floridan aquifer heads during the calibration period.

The remaining vertical head difference targets were located further south. Targets dhv_1, dhv_2, and dhv_3 are all located near Blountstown, Florida, near the southeastern corner of the boundary of the active model domain. A good fit was achieved at target dhv_3, which represented the difference between surficial aquifer system and Upper Floridan aquifer heads at this location. Targets dhv_1 and dhv_2 represent head differences between the upper confining unit and the underlying Upper Floridan aquifer and overlying surficial aquifer system, respectively. Head gradients within the upper confining unit are typically steeper, making head measurements in this unit more sensitive to vertical position of an observation well's open or screened interval within the unit or to local variations in lithology within the confining unit. These types of targets are therefore often more challenging to fit because they depend in part on head measurements in the upper confining unit. Measured values of the vertical head difference associated with target dhv_1 ranged between about -0.2 to about 1 foot during the calibration period, which (when compared to the simulated value of -1.8 feet) suggests some degree of overestimation of the head difference between the upper confining unit and Upper Floridan aquifer at this location. Target dhv_4 is located in the southwestern corner of the active model domain and was considered to be well fit because the simulated value (-31.83) was well within the approximately -45 to – 28 feet range of vertical head difference values that were measured during the calibration period.

Table 5-15. Values of vertical head difference calibration targets, simulated equivalents of targets, and target residuals

Target Name	Target value, in feet	Simulated value, in feet	Residual Value, in feet	Description
dhv_1	0.18	-1.75	-1.93	Upper Floridan aquifer minus upper confining unit
dhv_2	-5.63	-4.40	1.23	Upper confining unit minus surficial aquifer system
dhv_3	-5.45	-6.16	-0.71	Upper Floridan aquifer minus surficial aquifer system
dhv_4	-34.07	-31.83	2.24	Upper Floridan aquifer minus surficial aquifer system
dhv_5	-4.17	-0.46	3.71	Upper Floridan aquifer minus surficial aquifer system
dhv_6	0.25	0.40	0.15	Clairborne aquifer minus Upper Floridan aquifer
dhv_7	-21.49	-20.82	0.67	Upper Floridan aquifer minus surficial aquifer system
dhv_8	-15.16	-12.25	2.91	Clairborne aquifer minus Upper Floridan aquifer

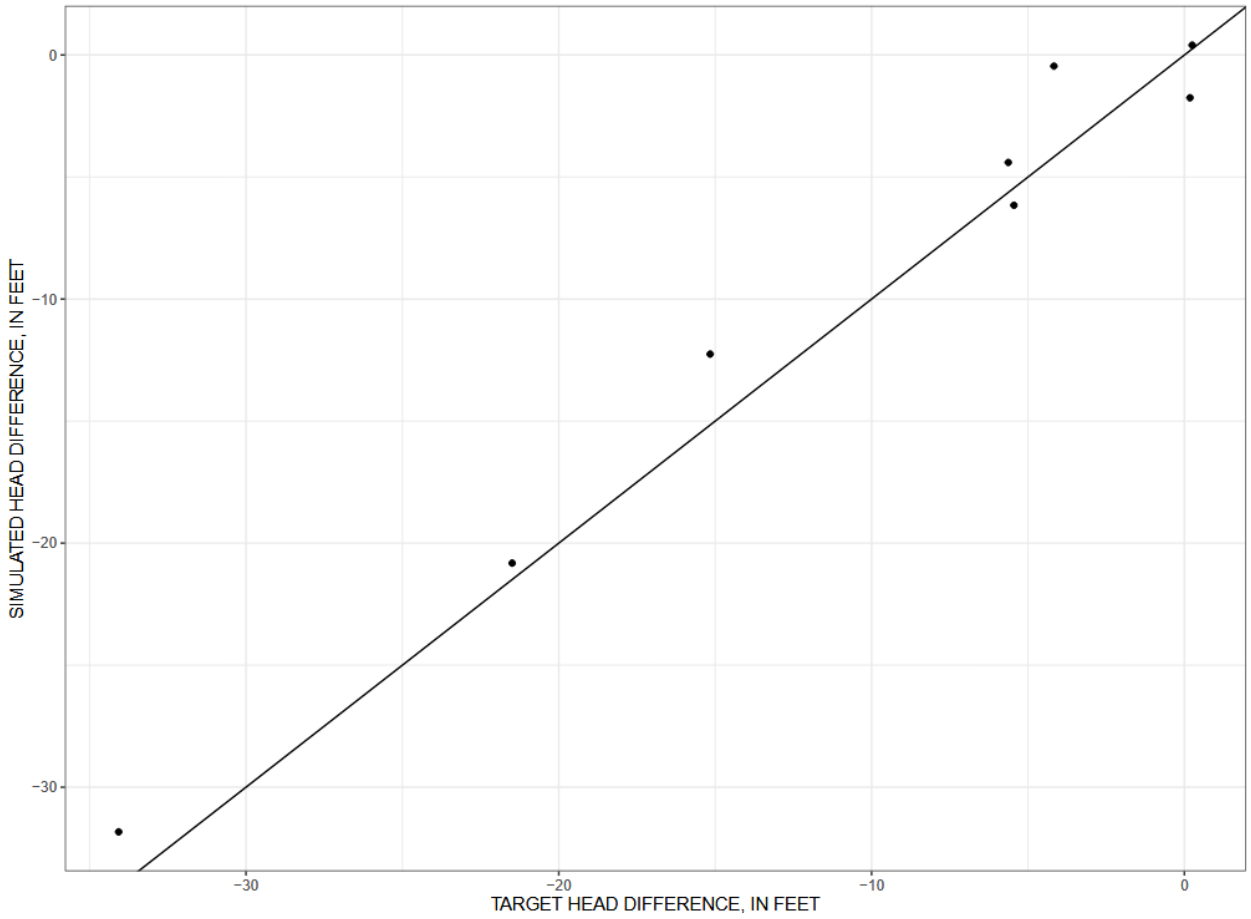

Figure 5-12. Plot of simulated versus calibration target values of vertical head differences

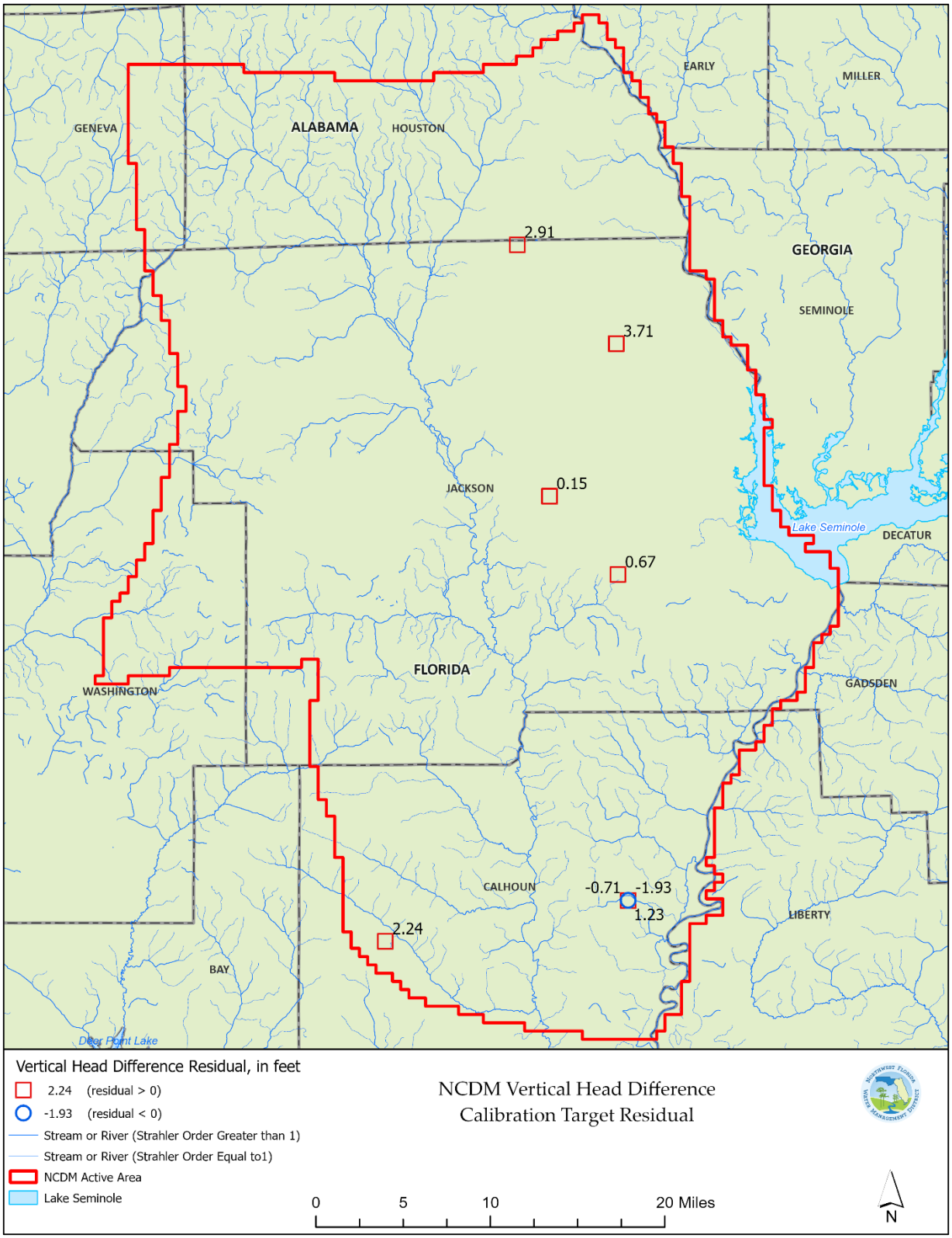

Figure 5-13. Map of vertical head difference residuals.

The simulated values of baseflows were very similar to their corresponding target values (Table 5-16 and Figure 5-14). Baseflow residuals ranged from about 3 to 19 percent of their corresponding target values, which are within plausible levels of uncertainty in these target values. The target for Spring Creek (q_zone09) was very uncertain and the zero-valued target reflects the fact that concurrent measurements at the upstream and downstream limits of the reach (that define this target) indicated no consistent pattern of net inflow to or leakage from the reach. The simulated value of 7.7 cfs is considered to be a reasonable value for this reach, because the simulated value was well within the range of measured values (-41 to 36 cfs).

Table 5-16. Values of baseflow calibration targets, simulated equivalents of targets, and target residuals

Target Name	Target Value, in cfs	Simulated Value, in cfs	Residual Value, in cfs
q_2358789	551	572.7	21.7
q_2359000	609	724.2	115.22
qsum_2359000	1160	1296.9	136.9
q_zone00	--	0.0	--
q_zone01	551	572.7	21.7
q_zone02	--	483.8	--
q_zone03	--	187.1	--
q_zone04	--	155.1	--
q_zone05	--	209.5	--
q_zone06	--	-177.0	--
q_zone07	--	-18.6	--
q_zone08	239	232.7	-6.3
q_zone09	0	7.7	7.7

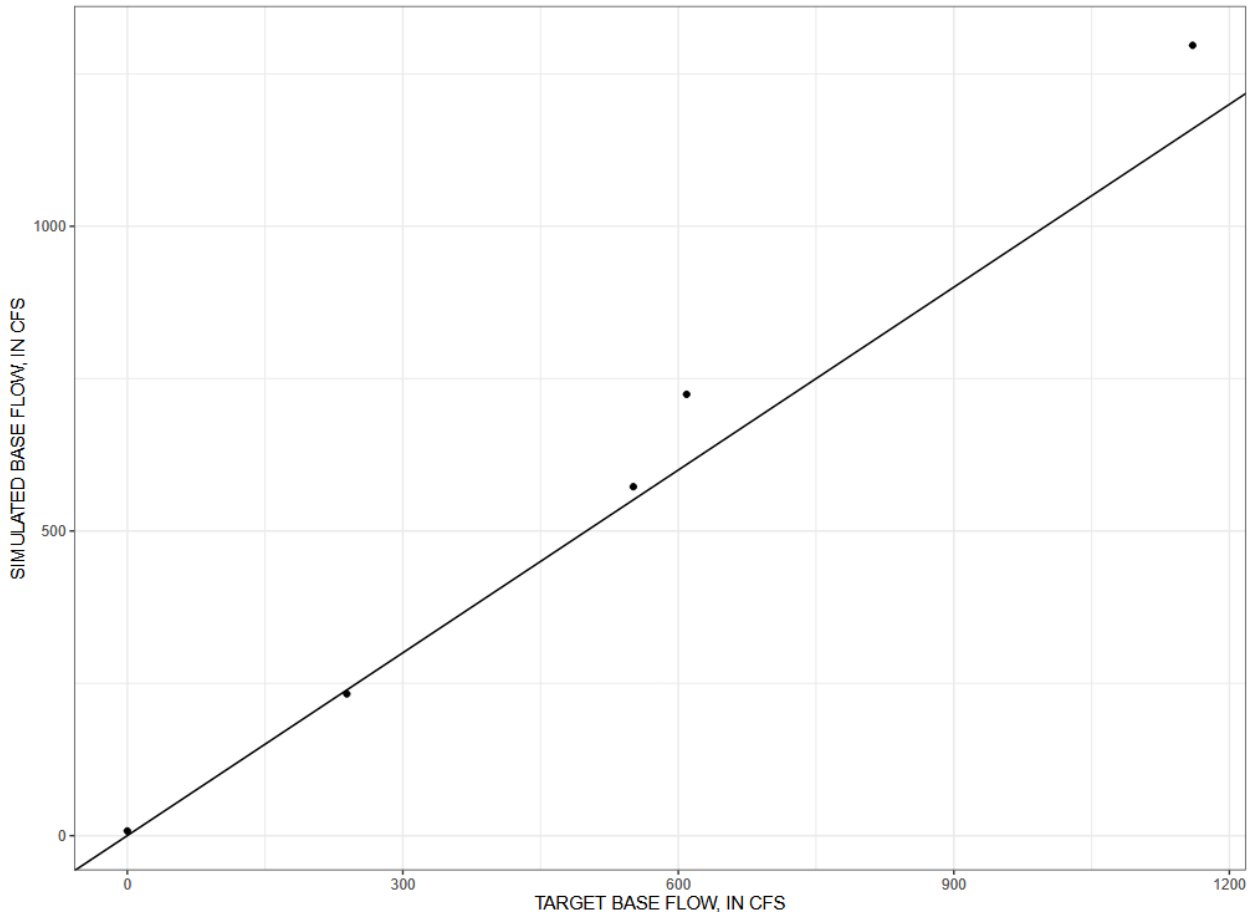

Figure 5-14. Plot of simulated versus calibration target values of baseflows

5-2-2. Simulated Groundwater Heads

Very little simulated groundwater flooding (heads in the uppermost active model layer exceeding land surface) was evident in the NCDM results (Figure 5-15), and where it did occur was generally less than 5 feet. Simulated heads exceeded land surface to the greatest degree near the southwestern boundary of the model, where the simulated heads in seven model grid cells were 10 to 32 feet higher than land surface. This lack of excessive simulated flooding is consistent with precalibration expectations.

Simulated groundwater heads were consistent with head patterns seen in historical potentiometric surface maps and expected patterns based on physical characteristics. For example, simulated groundwater heads in shallower model layers were generally higher in topographically high areas, and lower in areas near streams and other topographically-low areas. Spatial patterns of simulated heads in layer 3 were also similar to those observed in historical potentiometric maps. For example, simulated head gradients were steeper in the northern part of the domain where the Floridan Aquifer system is thinner, and flatter in the eastern central area surrounding Jackson Blue Spring. Past potentiometric surface maps of

the Upper Floridan aquifer have exhibited higher groundwater levels east and west of the lower Chipola River and a pattern of east-to-west outflowing groundwater (towards Holmes Creek) across the area traversed by the central part of the western NCDM boundary, and these patterns were also evident in the simulated heads in NCDM layer 3. As expected, the spatial patterns in the simulated heads in layers 4 and 5 were similar to, but smoother than, those of layer 3, reflecting the reduced influence of groundwater-surface water interactions on deeper parts of the groundwater flow system.

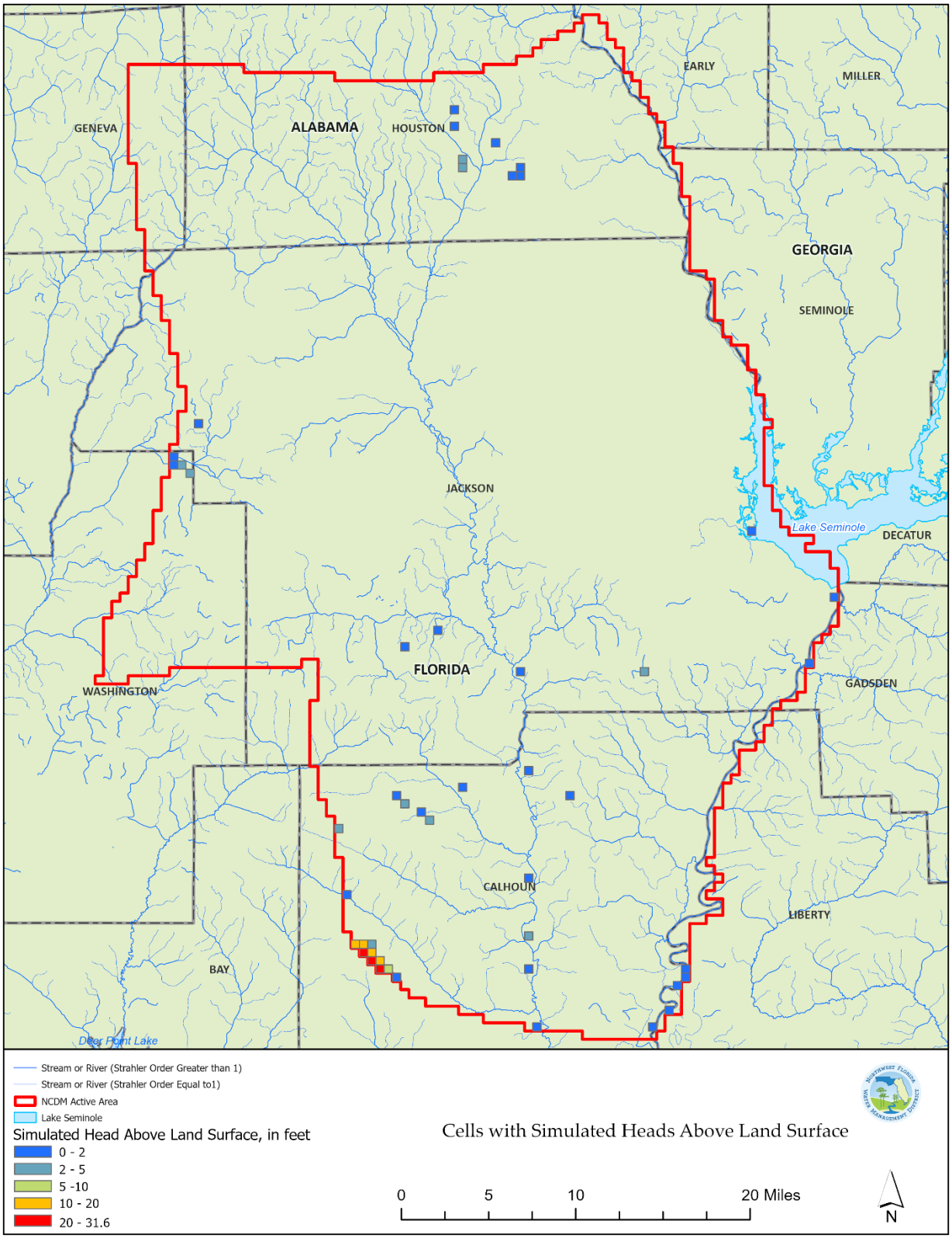

Figure 5-15. Map of NCDM grid cells with simulated heads above land surface

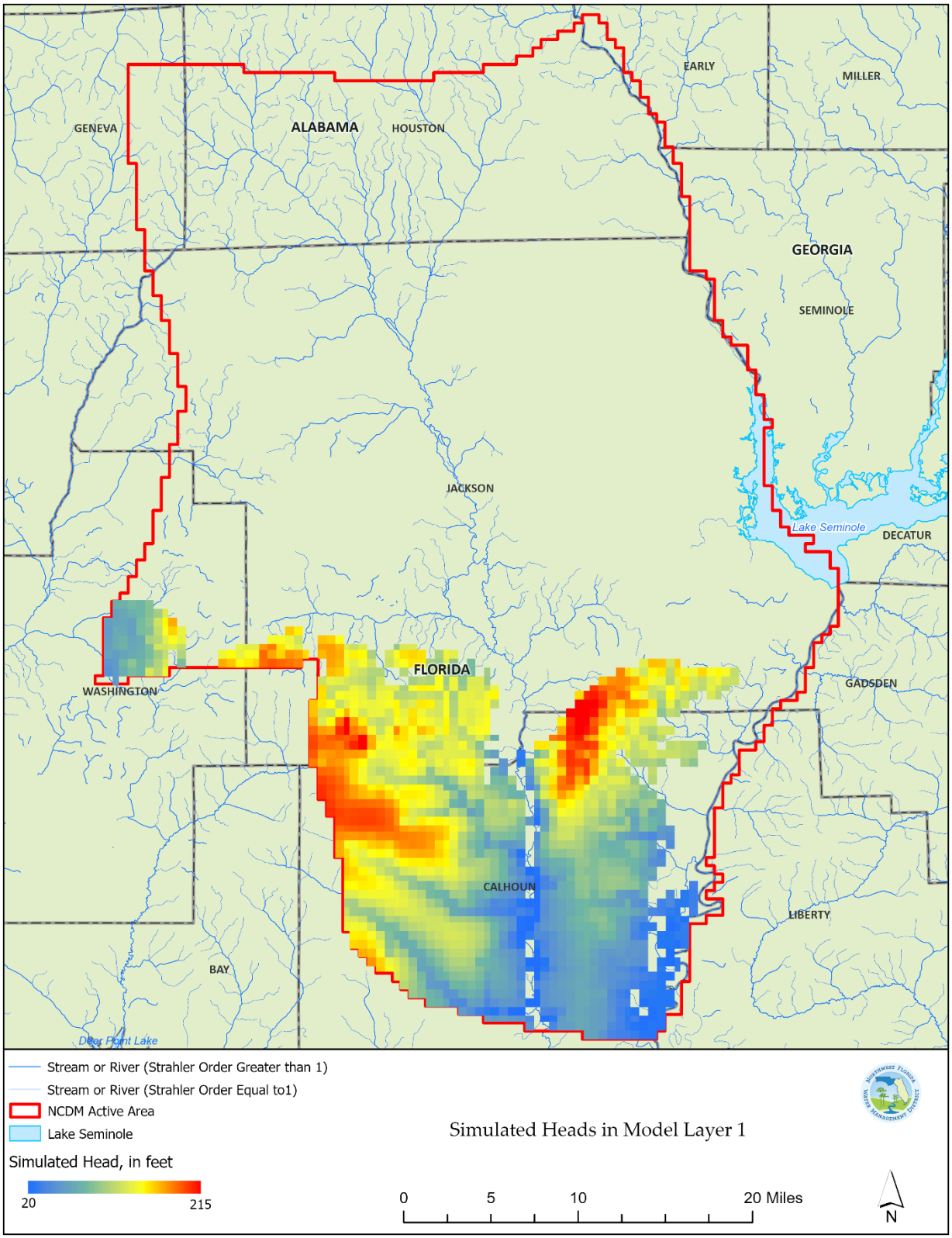

Figure 5-16. Simulated head values from model layer 1

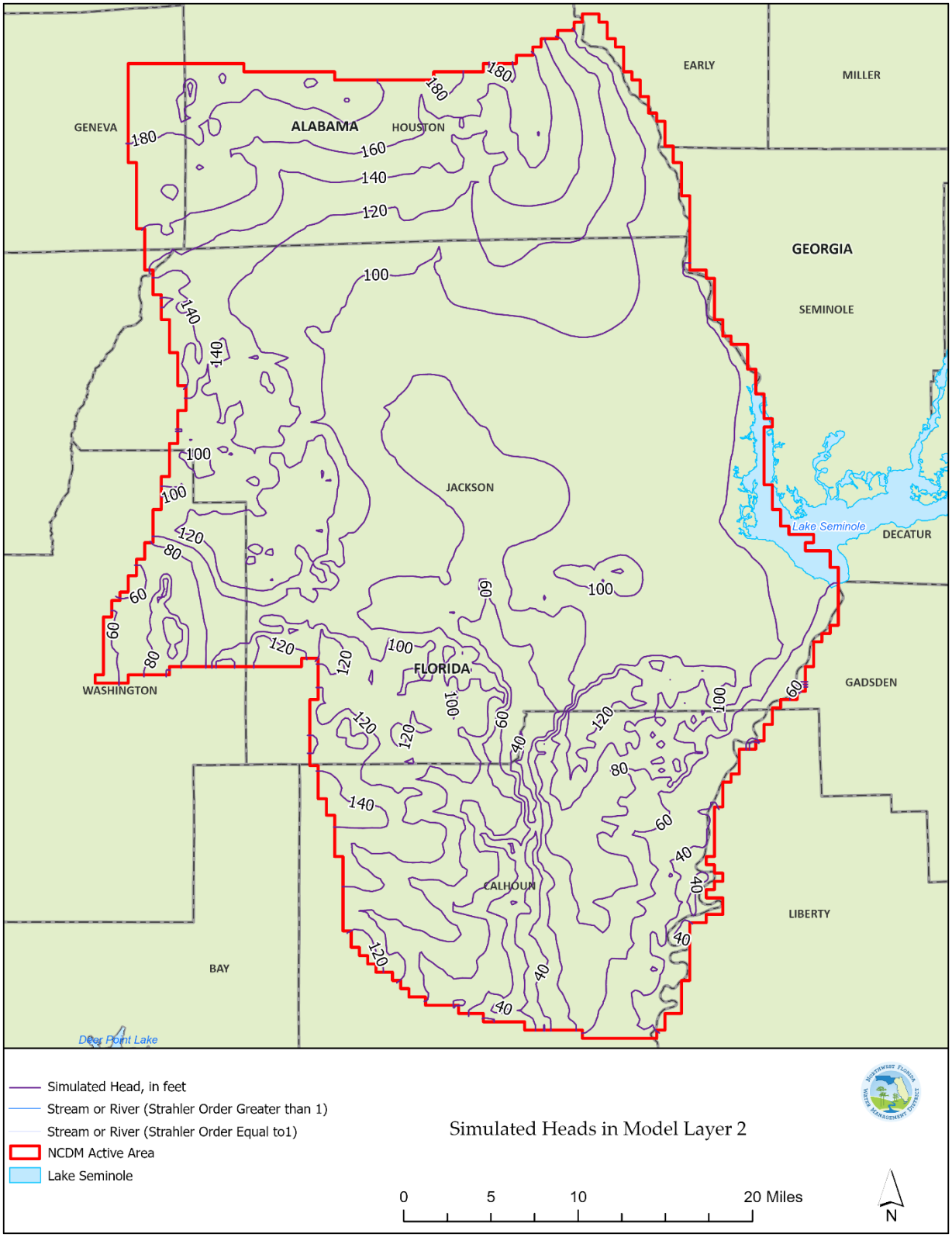

Figure 5-17. Simulated head contours from model layer 2

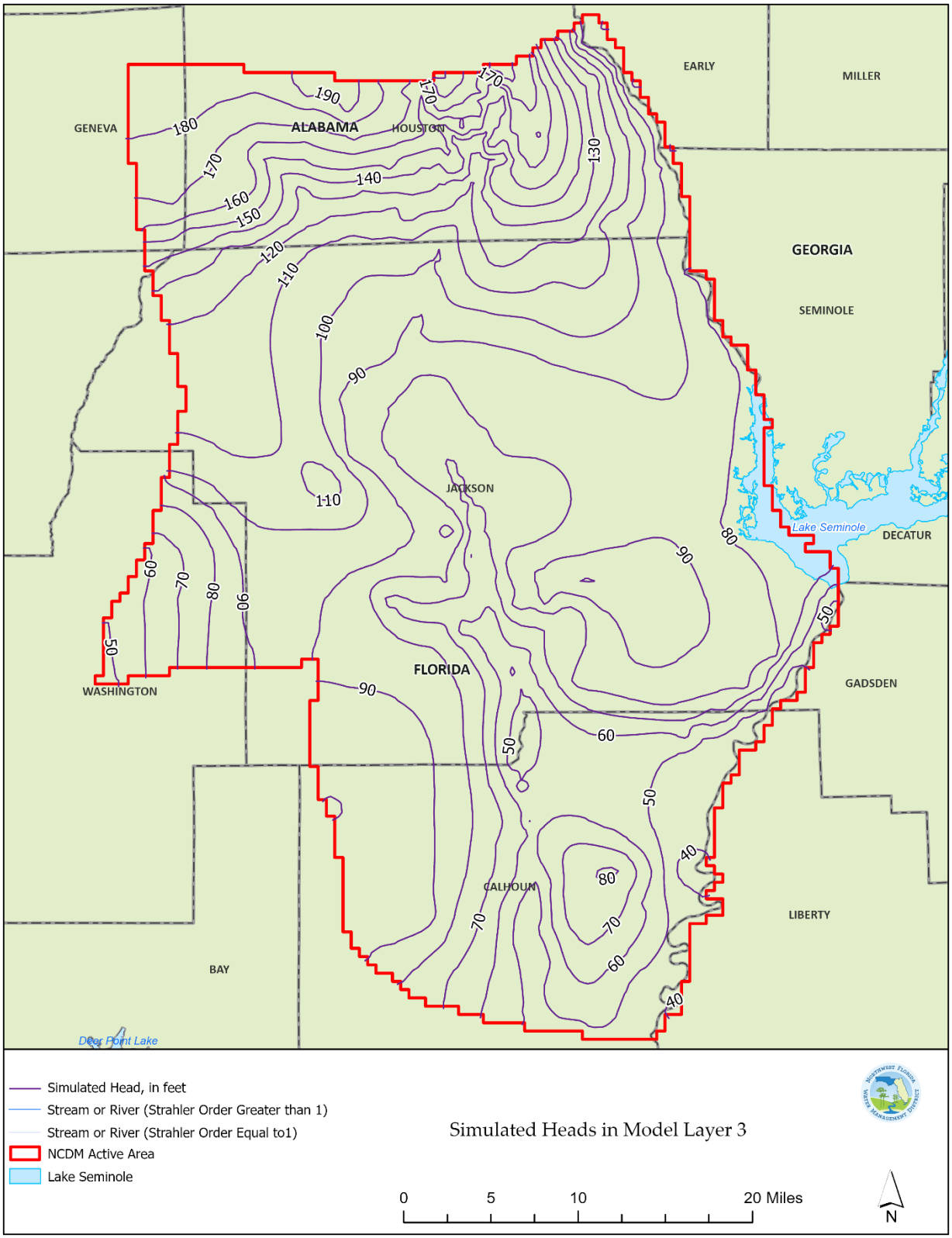

Figure 5-18. Simulated head contours from model layer 3

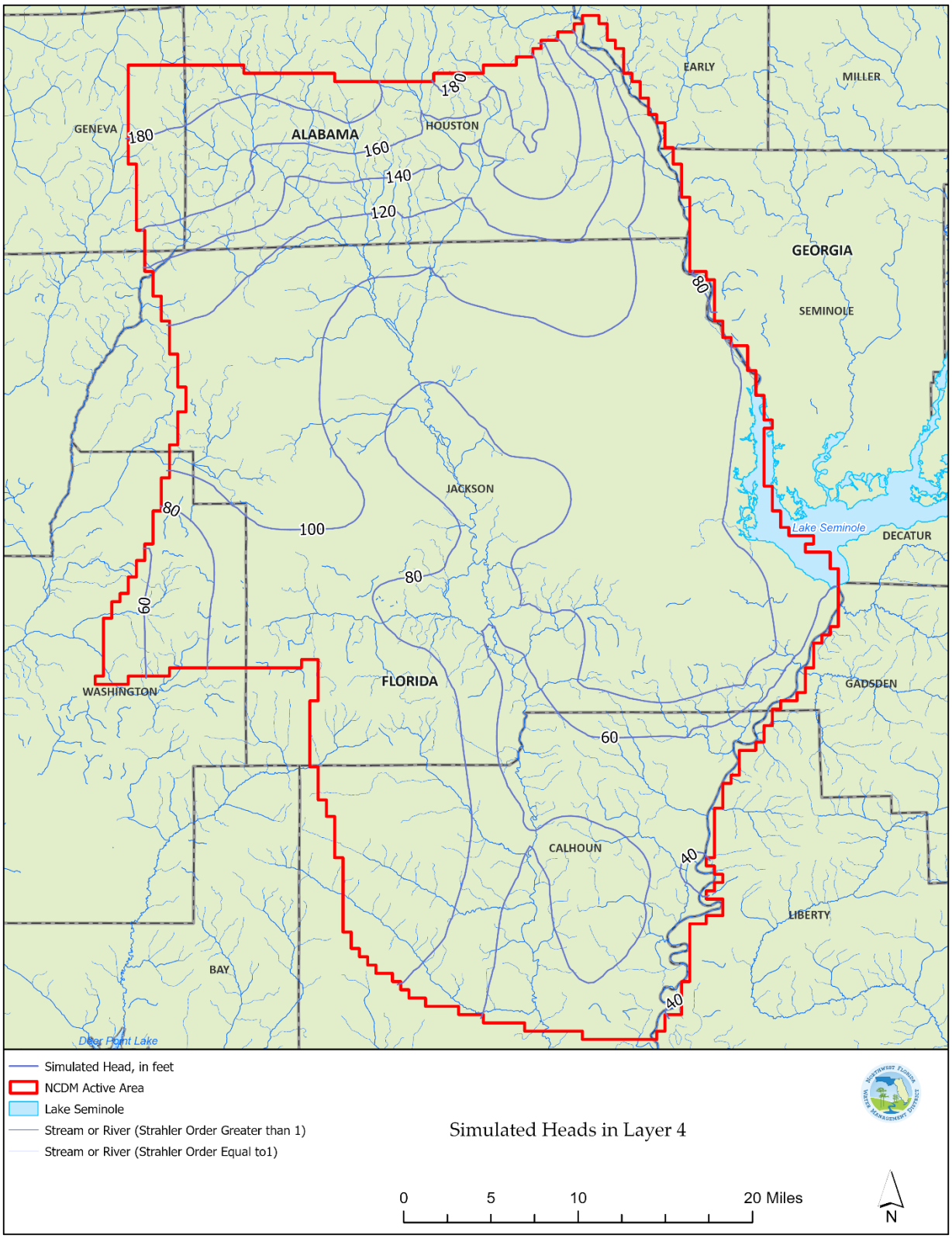

Figure 5-19. Simulated head contours from NCDM layer 4

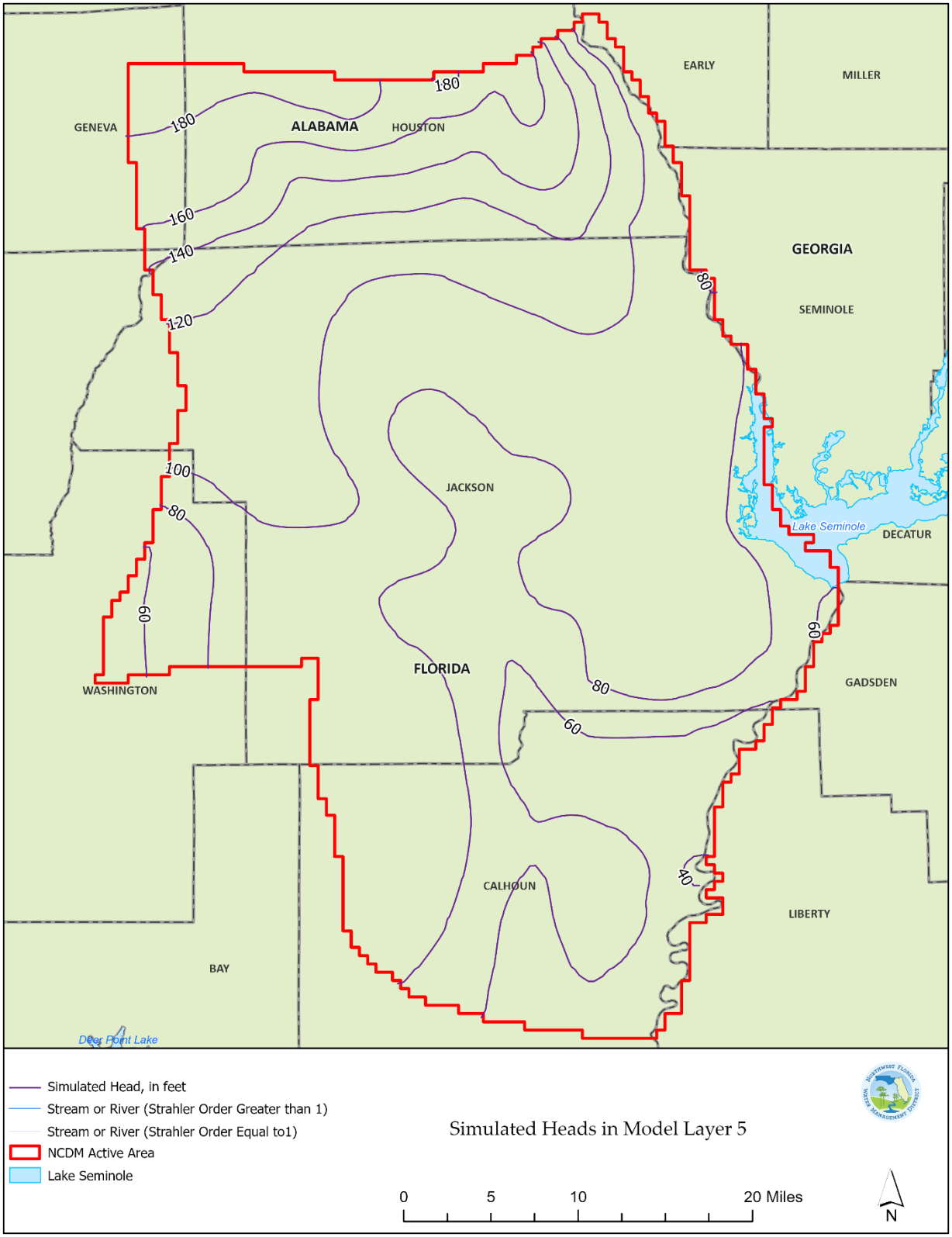

Figure 5-20. Simulated head contours from model layer 5

5-2-3. Hydraulic Conductivity, Recharge, and Evapotranspiration from Groundwater

Calibrated values of hydraulic conductivity (*K*) were consistent with expected ranges for the NCDM domain and similar karst regions in Florida. NCDM horizontal hydraulic conductivity (K_h) values for the surficial aquifer system generally ranged from about 1 to 50 feet per day (Figure 5-21). The lowest values occur in the western part of the active model domain near the boundaries between Jackson and northeastern Washington counties, coinciding with an area with less permeable lithologies. Upper confining unit K_h values generally ranged between 0.003 to 0.04 feet/day (Figure 5-22). Higher upper confining unit K_h values occur near the constant head boundaries along the central part of the western boundary and near the southeastern limits of the active NCDM domain; however, fewer calibration data are available in these areas and the upper confining unit *Kh* values therefore less certain in these areas.

NCDM horizontal hydraulic conductivity (K_h) values for the Upper Floridan aquifer generally range between 10 and 1,000 feet per day (Figure 5-23), which is consistent with values in similar areas of Florida. As expected, the highest values are near Jackson Blue Spring. Relatively high values also occur in areas near and west of the northernmost group of springs in the NCDM and near a cluster of springs in the western central part of the active NCDM domain. Middle confining unit K_h values in the NCDM are between about 0.1 and 10 feet per day, and generally within a range about 0.2 and 2.5 feet per day (Figure 5-24), which is consistent with a limited degree (lower permeability relative to the UFA and LFA, but still leaky) of confinement of this hydrogeologic unit. Lower Floridan aquifer K_h values in the NCDM are generally between 7 and 100 feet per day (Figure 5-25). An area of higher values between 200 and 700 feet per day occurs in an area just east of the Chipola River, although the significance of these geographic differences in K_h within the Lower Florida aquifer is limited by the lack of head targets within this unit.

Spatial patterns of NCDM vertical hydraulic conductivity (K_v) values were generally very similar to corresponding spatial patterns of NCDM (K_h) values. K_v values at a given location were typically about one tenth the corresponding K_h value, which is consistent with the pre-calibration estimate of the ratio K_h/K_v. Differences between K_h and K_v spatial patterns values were greatest for the upper confining unit, although these patterns were still quite similar.

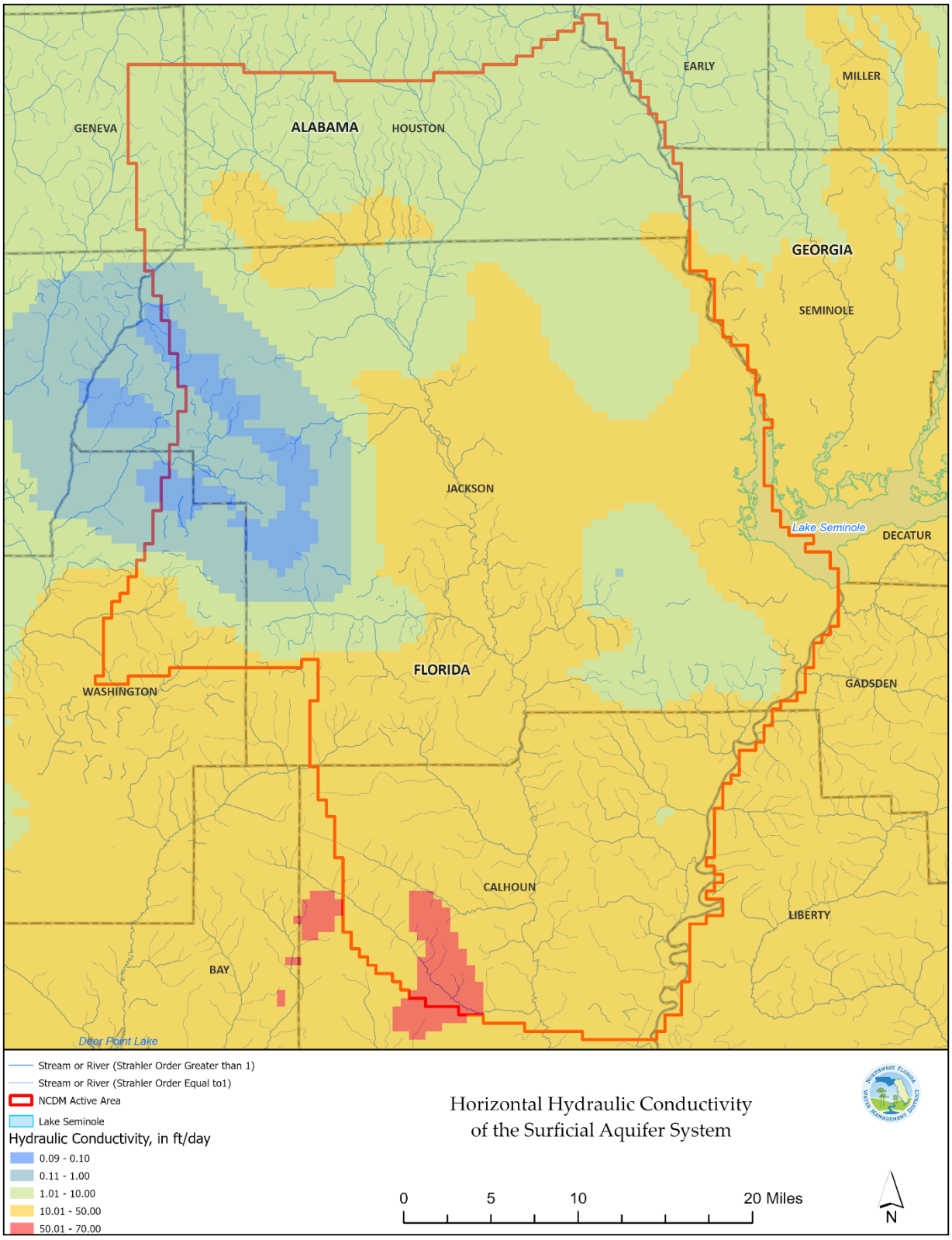

Figure 5-21. Calibrated values of the surficial aquifer system horizontal hydraulic conductivity

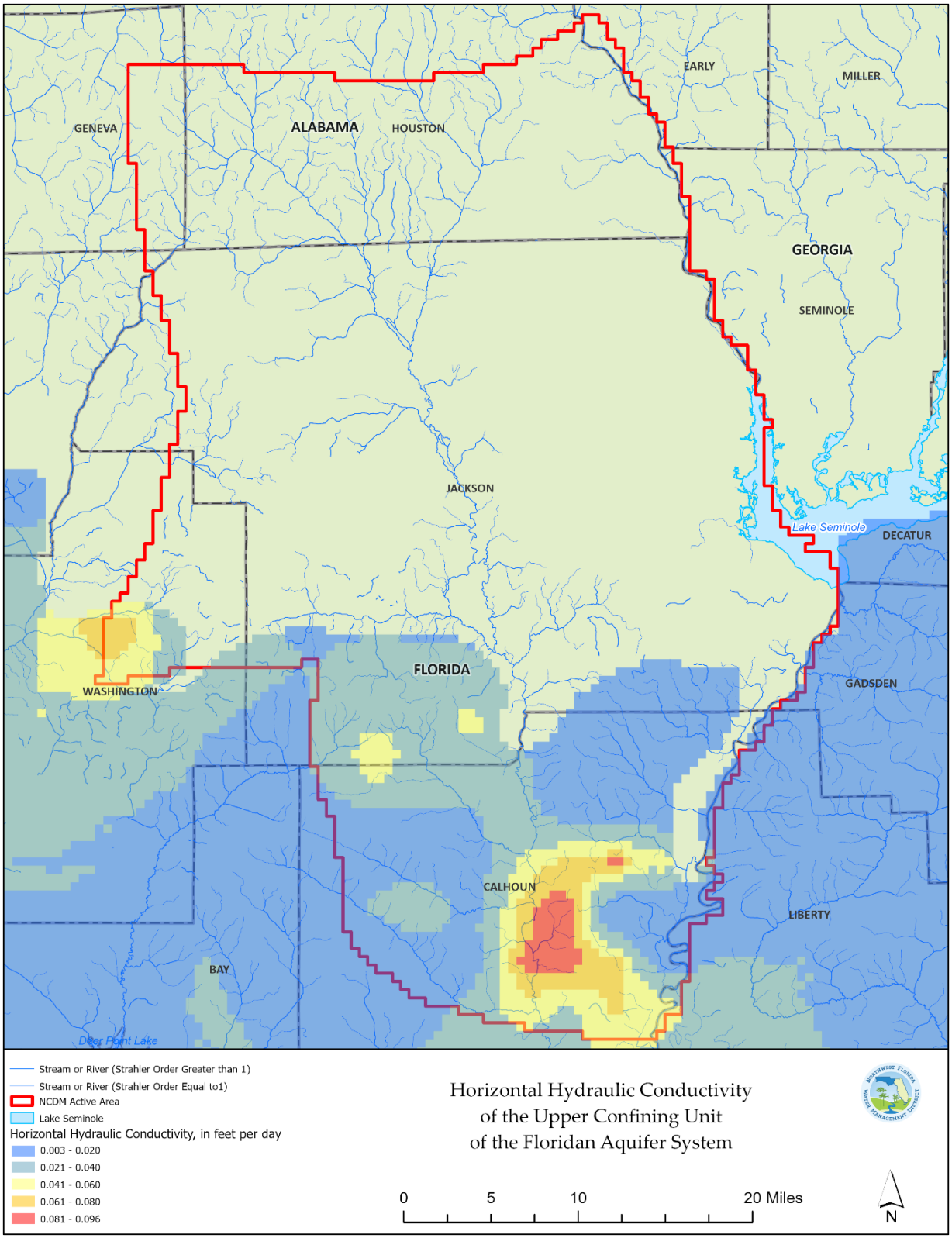

Figure 5-22. Calibrated values of the horizontal hydraulic conductivity of the upper confining unit of the Upper Floridan aquifer

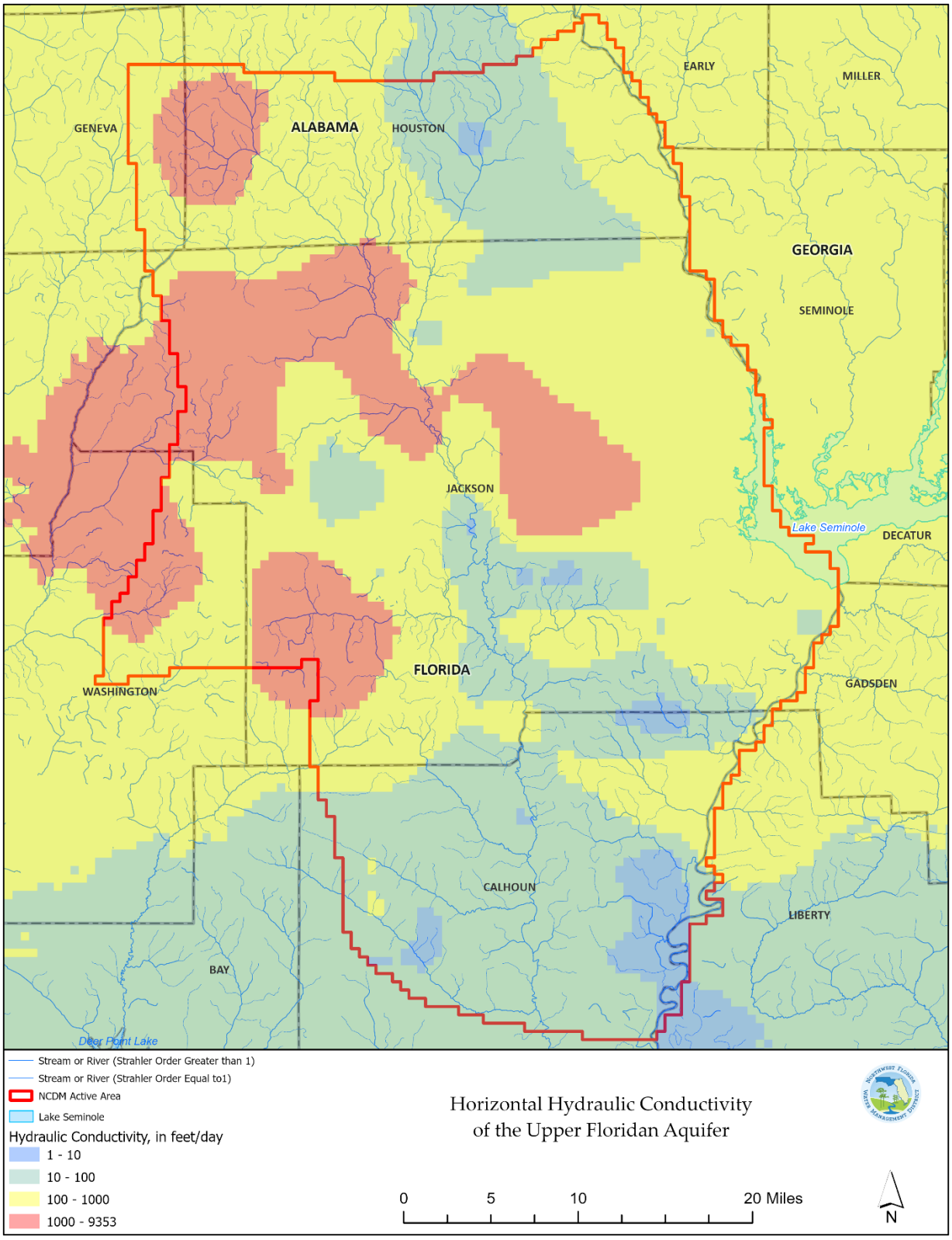

Figure 5-23. Calibrated values of Upper Floridan aquifer horizontal hydraulic conductivity

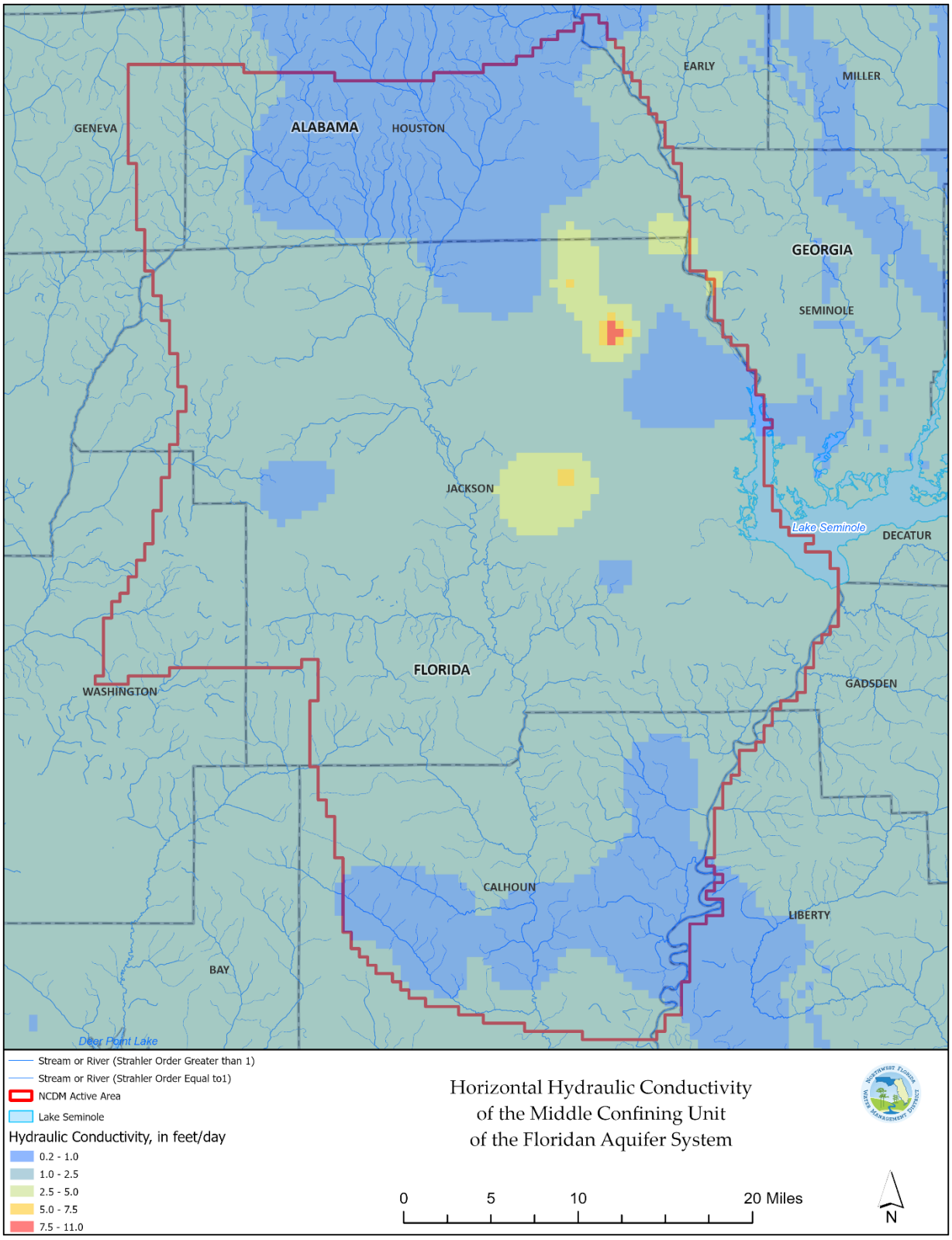

Figure 5-24. Calibrated values of middle confining unit horizontal hydraulic conductivity

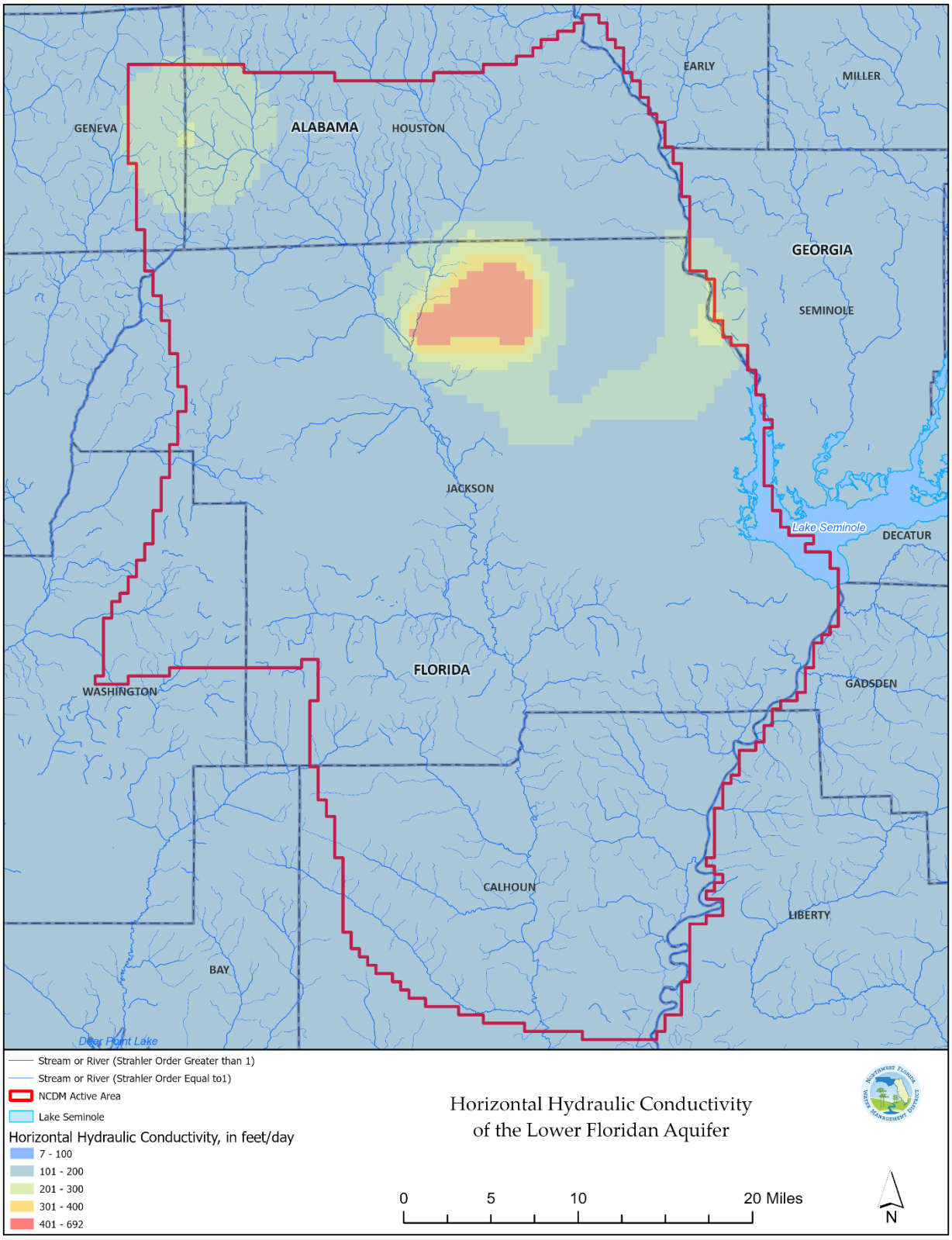

Figure 5-25. Calibrated values of Lower Floridan aquifer horizontal hydraulic conductivity

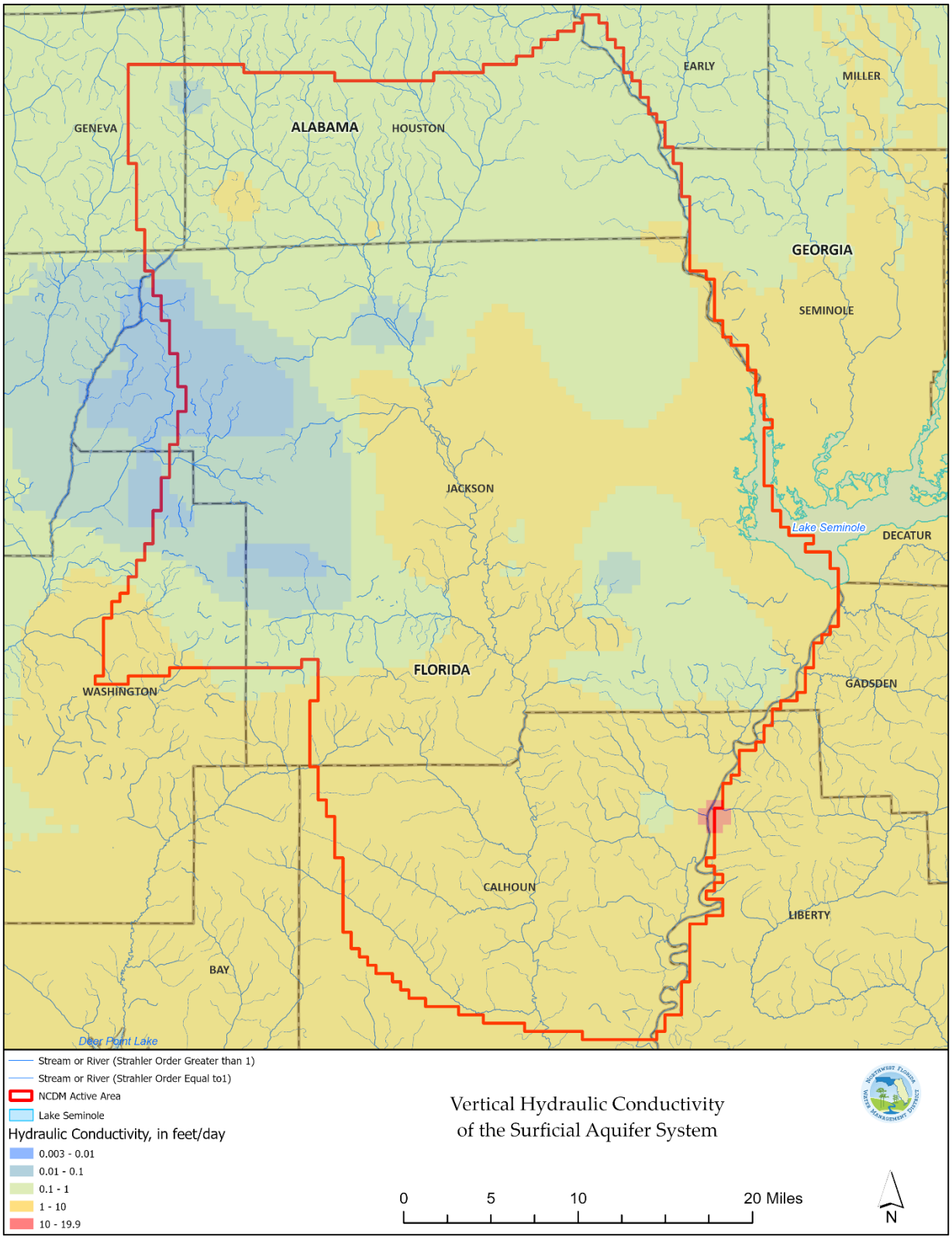

Figure 5-26. Calibrated values of surficial aquifer system vertical hydraulic conductivity

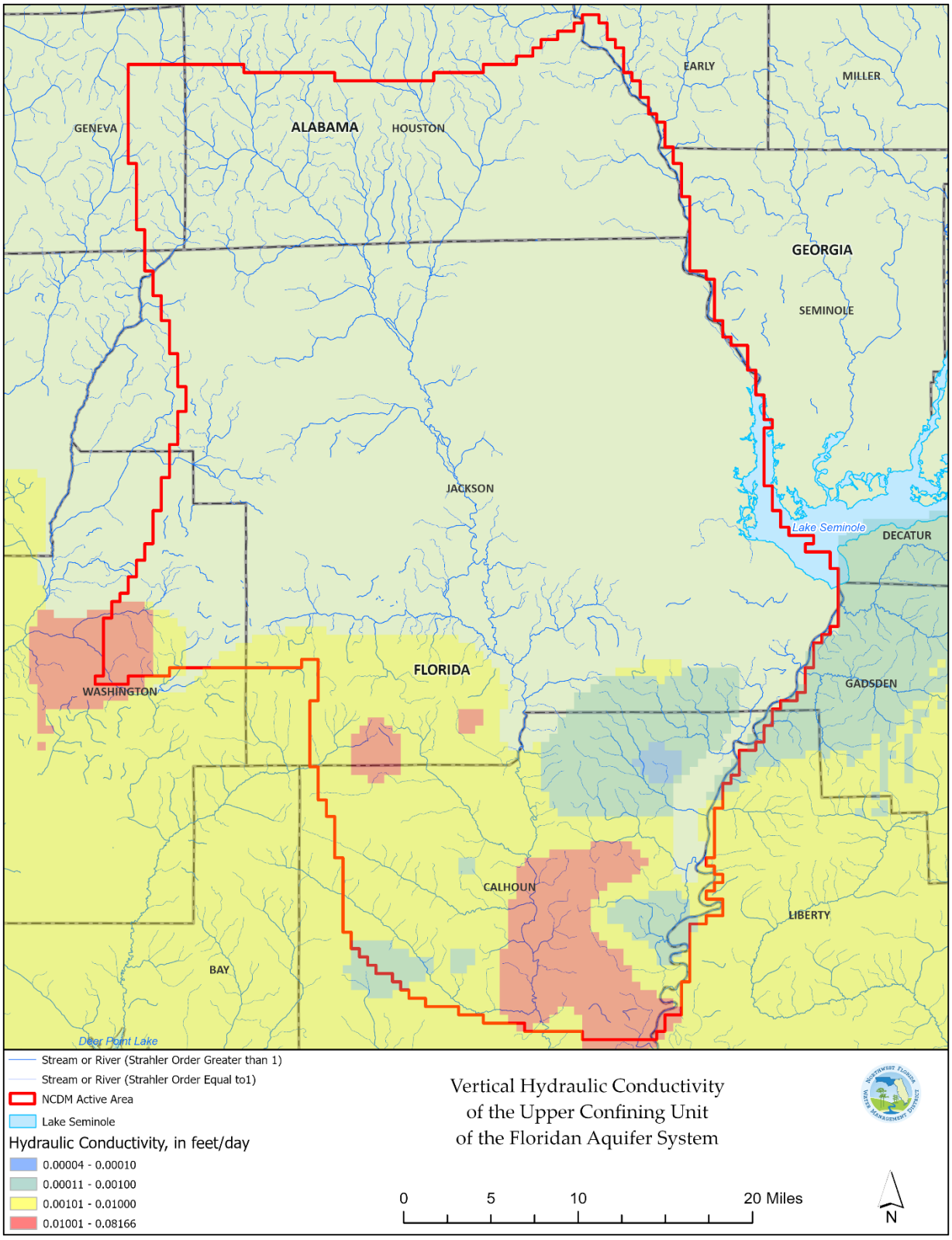

Figure 5-27. Calibrated values of upper confining unit vertical hydraulic conductivity

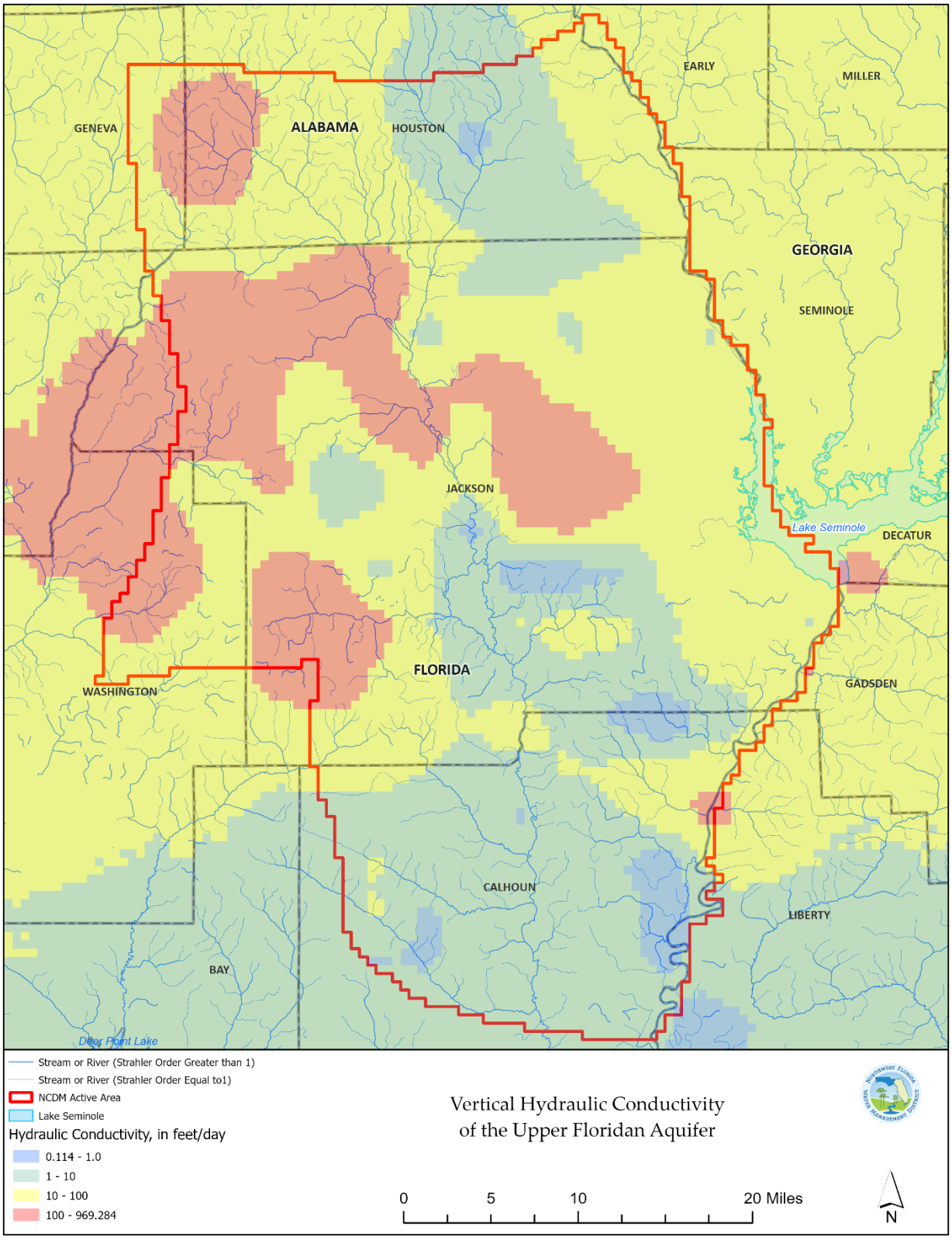

Figure 5-28. Calibrated values of Upper Floridan aquifer vertical hydraulic conductivity

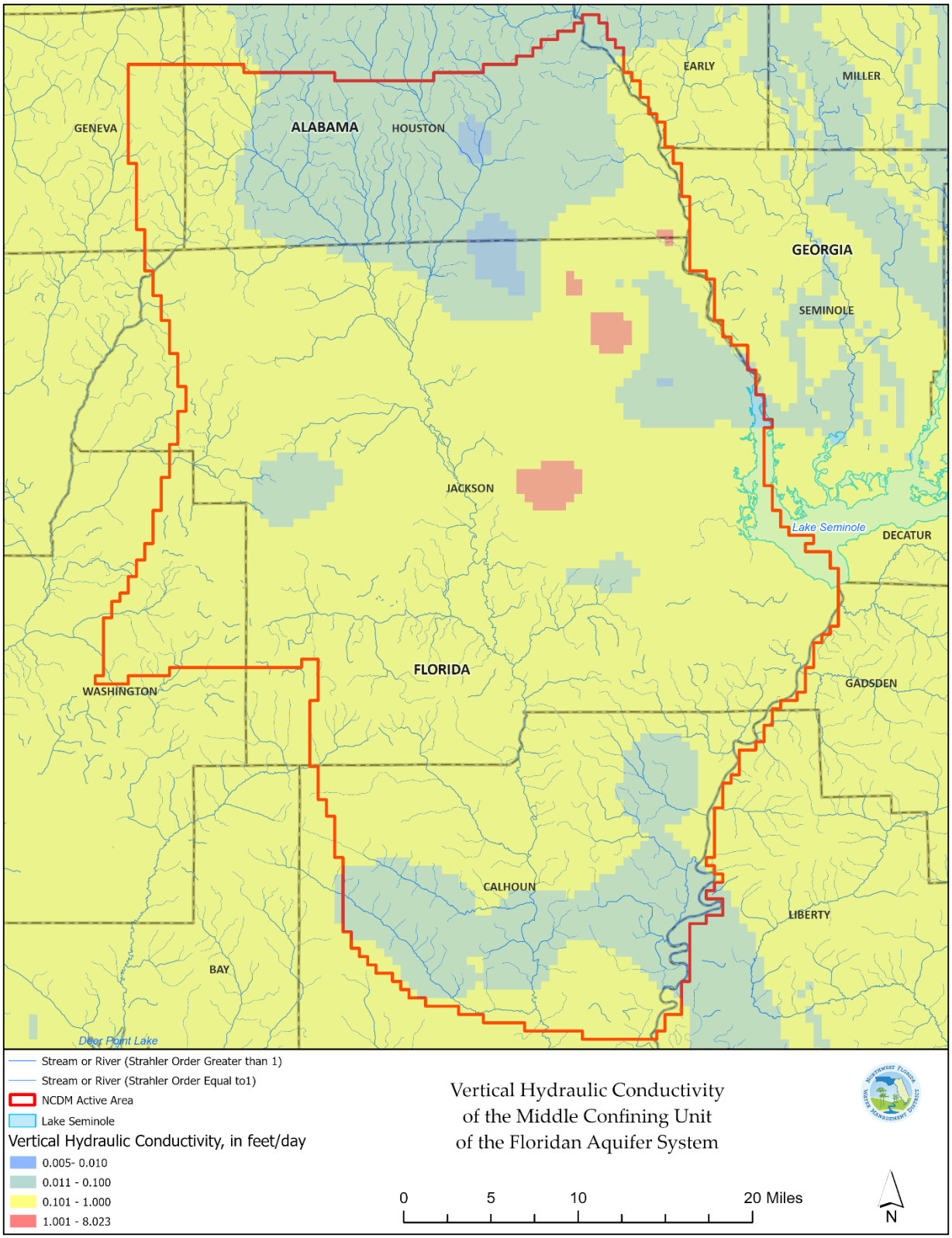

Figure 5-29. Calibrated values of middle confining unit vertical hydraulic conductivity

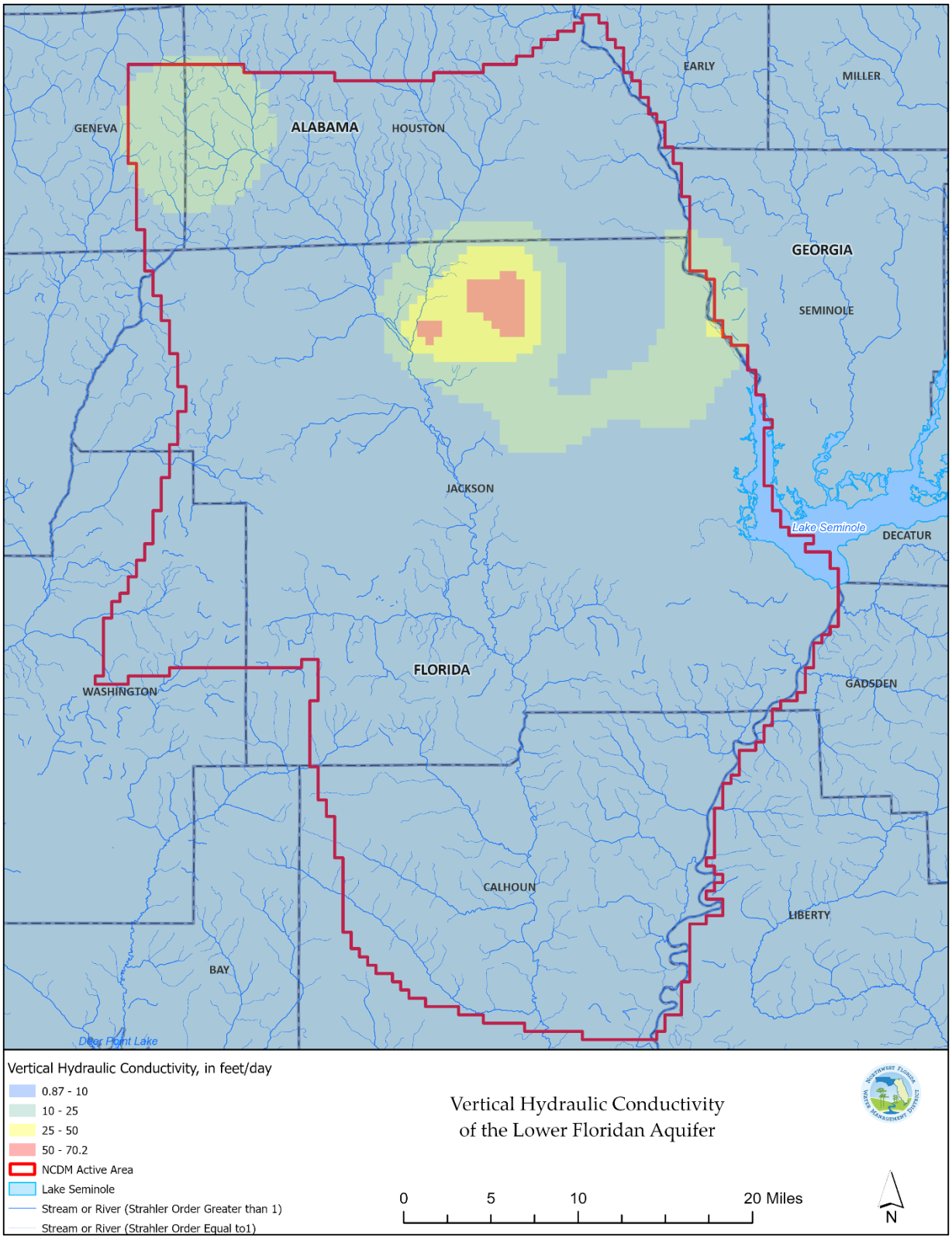

Figure 5-30. Calibrated values of Lower Floridan aquifer vertical hydraulic conductivity

Spatial patterns of NCDM recharge and simulated evaporation from groundwater (ET_{gw}) are shown in Figure 5-31 and Figure 5-32, respectively. Calibrated recharge values in much of the domain are within a range of about 10 to 30 inches per year. The lowest values generally occur near stream and river features, where direct runoff is expected to be concentrated. The highest values (between about 30 and 50 inches per year) generally occur in the central part of the domain, although values in this range also occur elsewhere in the active NCDM domain. NCDM ET_{gw} values are generally less than 5 inches per year and are equal to zero in about 60 percent of the model domain because non-zero values will only occur in areas where the simulated water table nearer the land surface, such as wetlands and floodplains. Accordingly, the highest simulated ET_{gw} values occurred near such features, including areas near the Chattahoochee, Apalachicola, and Chipola Rivers and in wetland areas just east of Chipley, Florida.

5-2-4. Simulated Domain Water Budget

Simulated values of components of the NCDM water budget are shown in Table 5-17. Individual component values are consistent with conceptual model estimates. As expected, groundwater discharge to streams, rivers, and springs is the largest outflow term in the simulated water budget, representing about two thirds of total simulated outflows. Nearly all of the remaining simulated outflows are accounted for by evapotranspiration from the water table and net groundwater flow out of the NCDM domain, and nearly all of the latter was accounted for by net groundwater flow across the western boundary of the NCDM towards the spring-fed reach of Holmes Creek. Groundwater withdrawals from wells represent a relatively small part of the water budget.

Table 5-17. Simulated water budget for the NCDM domain

Budget Term	Simulated Value, inches per year
Recharge	22
Evapotranspiration from the water table	4
Groundwater withdrawal from wells	0.5
Net groundwater discharge to streams, rivers, and springs	14
Net groundwater flow out of the NCDM domain	3

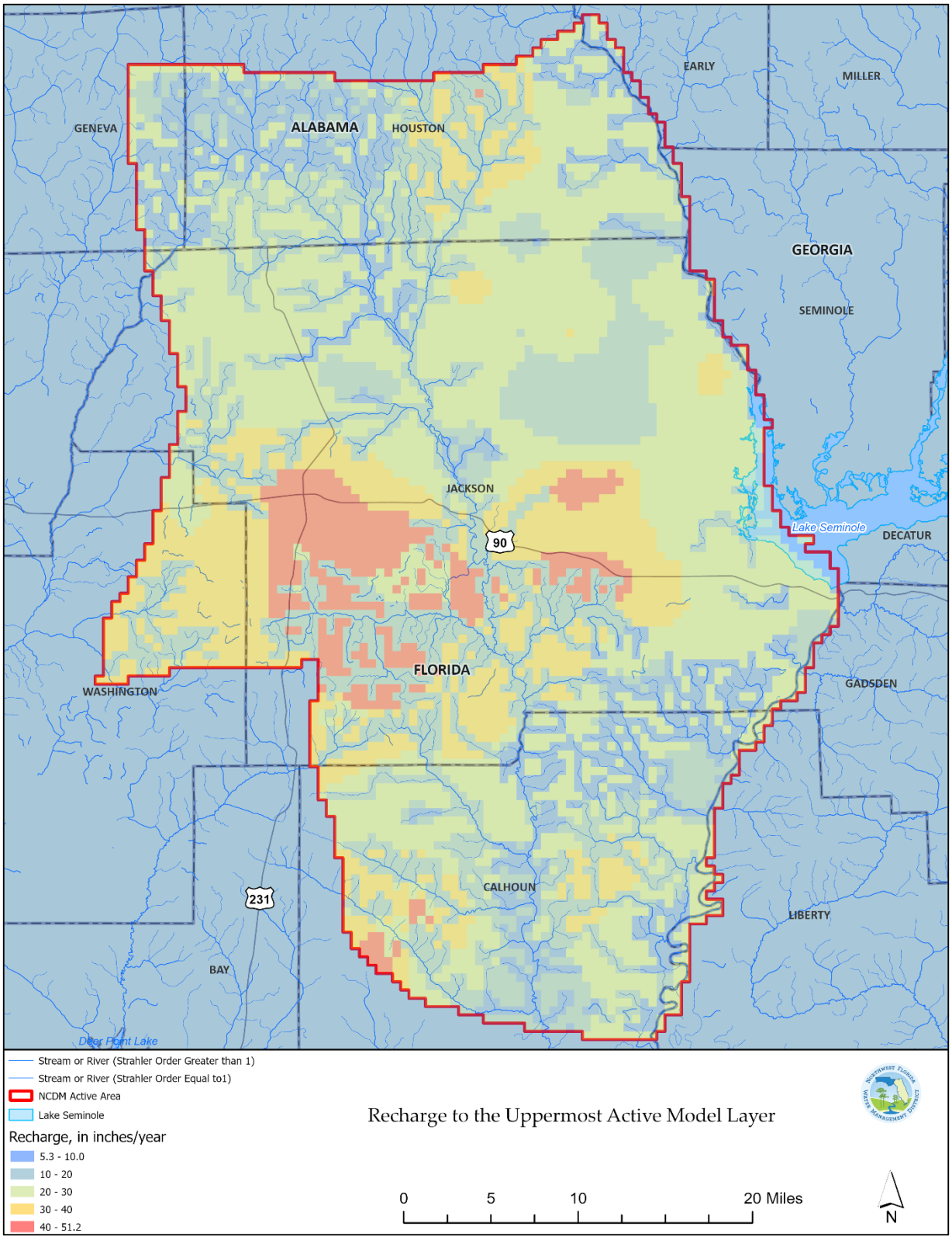

Figure 5-31. Calibrated values of recharge

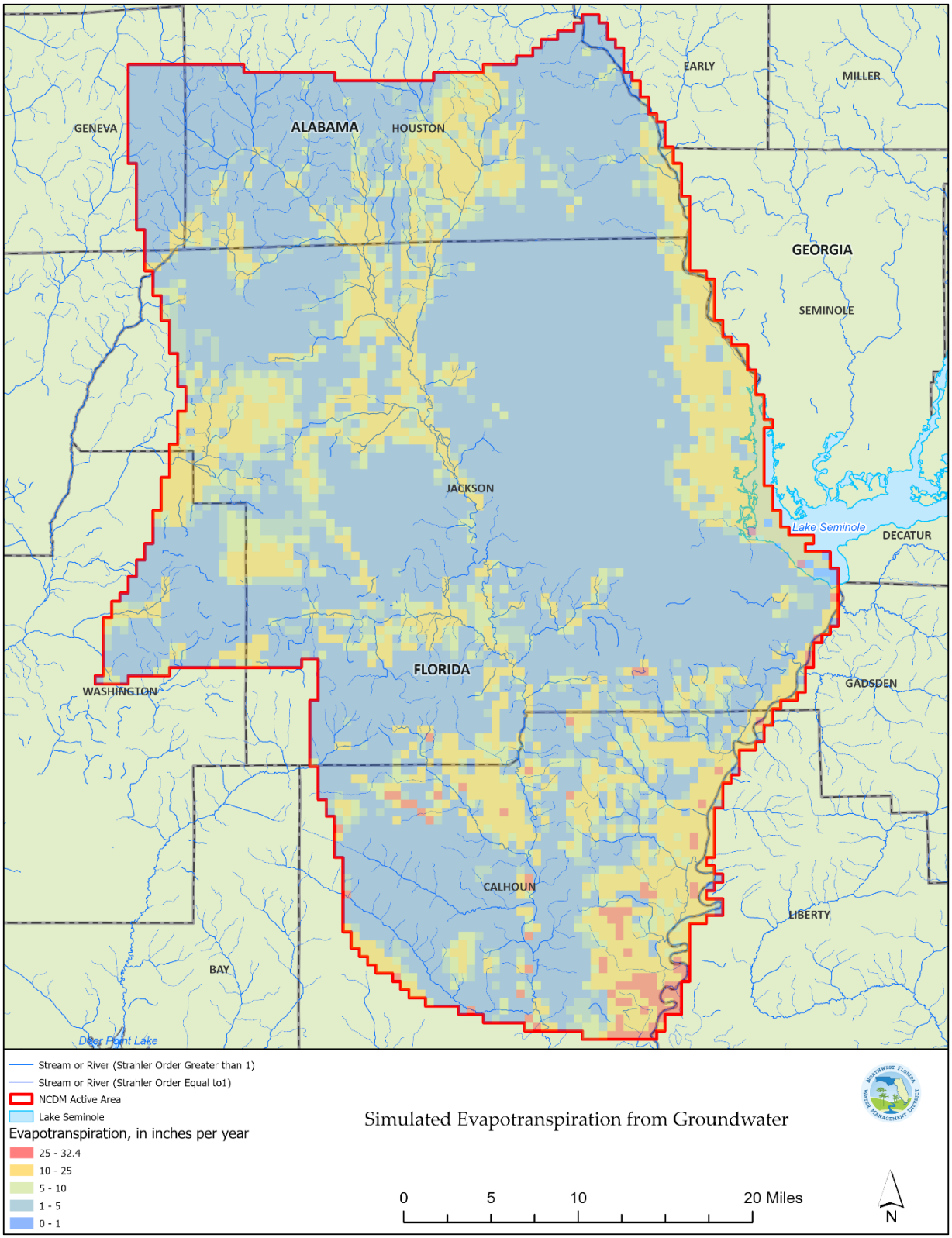

Figure 5-32. Simulated groundwater evapotranspiration

5-2-5. Sensitivity Analysis

The sensitivity of model outputs to model parameters was assessed by computing composite-scaled sensitivities (Hill and Tiedeman, 2007) for each model parameter group. The composite-scaled sensitivities are computed by first computing the derivative ('sensitivity') of each calibration target with respect to each model parameter, and then computed the weighted sum of these sensitivities across sets of calibration targets as follows:

$$css_i = \sum_{j=1}^{N} \left| \frac{\partial h_j}{\partial k_i} \right| k_i w_j$$

where:

css_i is the composite-scaled sensitivity for parameter k_i

N is the number of calibration targets of calibration targets used in the computation

$\frac{\partial h_j}{\partial k_i}$ is the sensitivity of calibration target y_j with respect to parameter k_i

w_j is the weight assigned to calibration target y_j.

These composite-scaled sensitivities can be aggregated across all members of a parameter group or, alternatively, computed based on any combination of parameters and calibration targets. Composite-scaled sensitivities are particularly suited to modern model-development approaches that use large numbers of parameters. Examples of this type of sensitivity analysis can be found in Durden and others (2019) and Sepulveda and others (2012).

Composite-scaled sensitivities were aggregated for each parameter group in the NCDM as follows:

- Composite-scaled sensitivities for groundwater head calibration targets
- Composite-scaled sensitivities for horizontal head-difference calibration targets
- Composite-scaled sensitivities for vertical head-difference calibration targets
- Composite-scaled sensitivities for spring flow calibration targets
- Composite-scaled sensitivities for baseflow calibration targets

Note that the sensitivity ($\frac{\partial h_j}{\partial k_i}$) value for a given combination of parameter and calibration target is computed by first increasing the value of a given NCDM parameter by an incremental amount while leaving other parameter values unchanged and then executing

the model with this adjusted parameter value. The derivative ('sensitivity') of each calibration target with respect to each model parameter is then calculated by dividing the change the calibration target value by the incremental change in the parameter value. Note that sensitivities for log-transformed parameters ($\frac{\partial h_j}{\partial log_{10}(k_i)}$) were untransformed to values of $\frac{\partial h_j}{\partial k_i}$ prior to calculating composite-scaled sensitivity values.

Composite scaled sensitivity (CSS) values were consistent with sensitivity analysis results seen with many groundwater models, including those that include regions containing the Floridan aquifer system. The head calibration target group was most sensitive to pilot point parameters representing (in decreasing order of sensitivity) recharge multipliers, and the horizontal hydraulic conductivity of the Upper and Lower Floridan aquifers (Figure 5-33; note that descriptions of parameter abbreviations shown in this figure are described in Table 5-1). CSS values for the horizontal head difference group exhibited a similar pattern (Figure 5-34). Vertical head difference targets were most sensitive to recharge parameters (Figure 5-35), although these targets were more sensitive to a larger variety of parameter groups, with much of the remaining collective CSS for the vertical head difference target group accounted for by the horizontal hydraulic conductivity parameters for the Upper Floridan aquifer, upper confining unit, and surficial aquifer system, as well as anisotropy parameters for the upper confining unit. This is not unexpected, because the vertical head difference targets are based on heads from the multiple aquifers.

Spring flow targets were most sensitive to recharge and the horizontal hydraulic conductivity of the Upper Florida aquifer, and to a lesser extent by spring and river conductance parameters (Figure 5-36). This result is consistent with the fact that flow to these springs is concentrated discharge from the Upper Florida aquifer, and that the spatial distribution of horizontal hydraulic conductivity within the Upper Florida aquifer and the conductance values of perennial river and spring features govern the fraction of groundwater discharge from the Upper Floridan aquifer that flows to springs and spring-dominated river reaches. Stream flow targets were most sensitive to recharge multiplier and Upper Floridan aquifer horizontal hydraulic conductivity parameters (Figure 5-37). This result is consistent with the fact that recharge ultimately determines the amount of water available to stream and river features, that the stream and river reaches represented by the baseflow targets derive much of their flow from groundwater discharge from the Upper Floridan aquifer, and that the spatial distribution of Upper Floridan aquifer horizontal hydraulic conductivity affects the spatial distribution of groundwater discharge from the aquifer (which is ultimately derived from recharge). Flooding penalty functions were most sensitive to recharge and evapotranspiration multiplier parameters (Figure 5-38). This result is consistent with the

expected sensitivity of shallow groundwater levels to recharge and direct evapotranspiration from the water table.

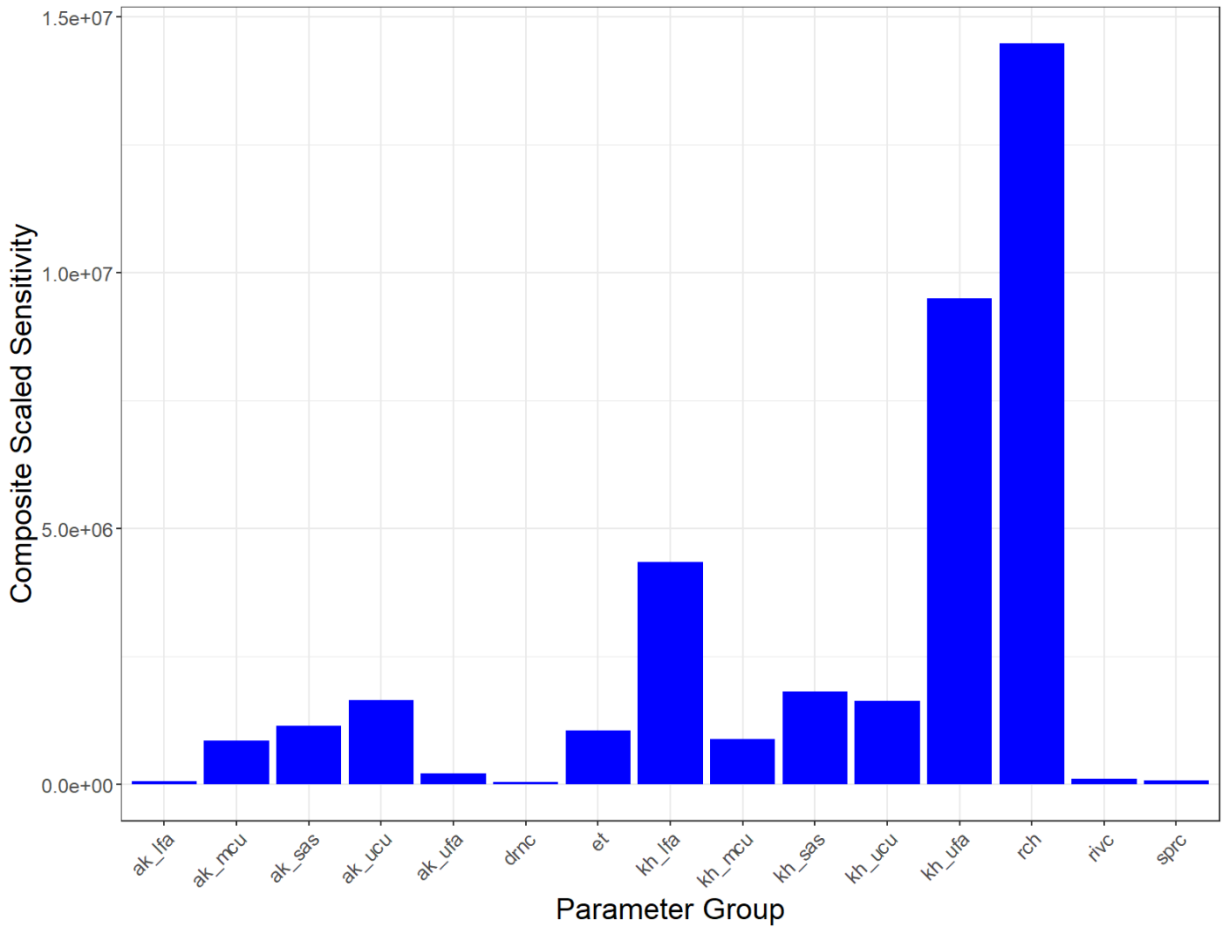

Figure 5-33. Composite scaled sensitivity values for the head calibration target group

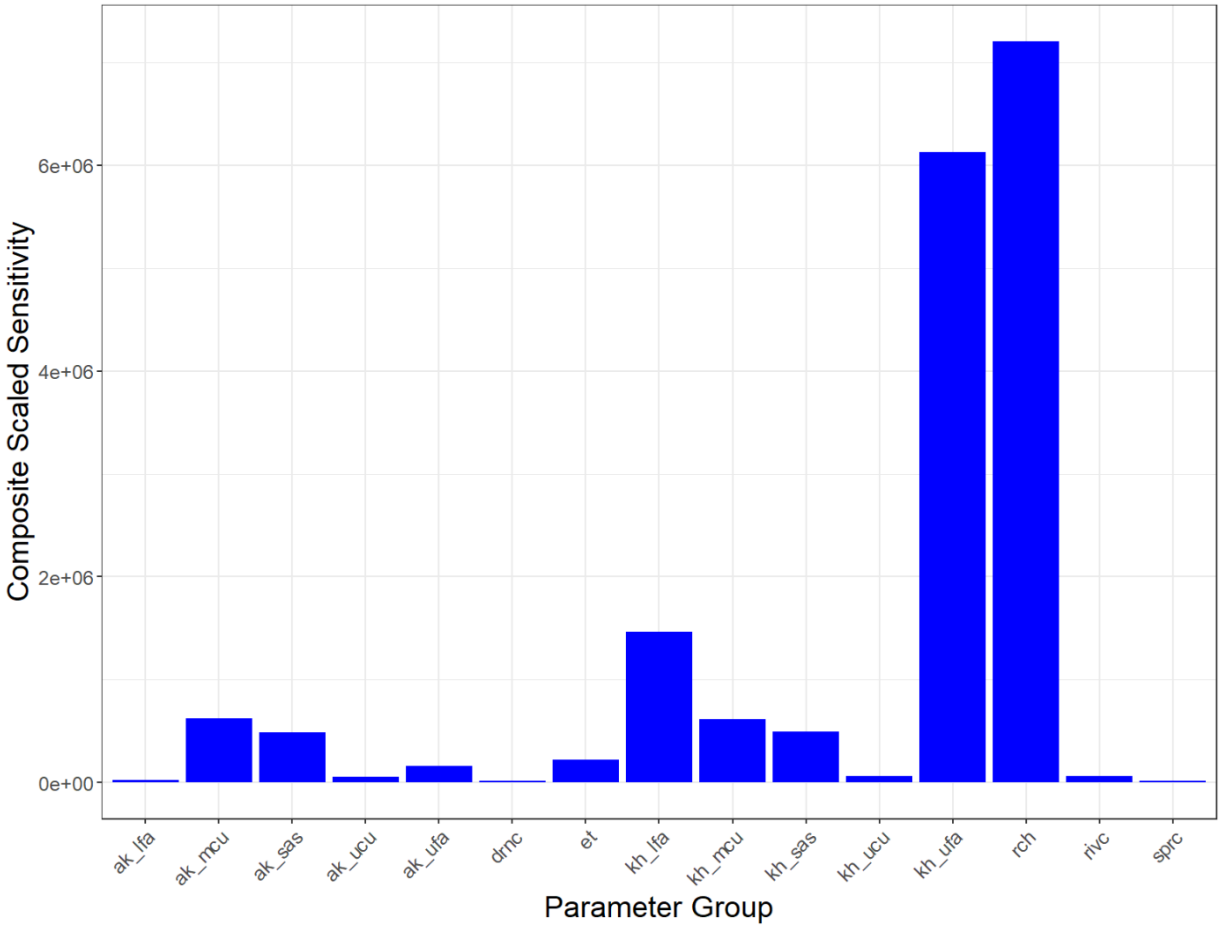

Figure 5-34. Composite scaled sensitivity values for the horizontal head-difference calibration target group

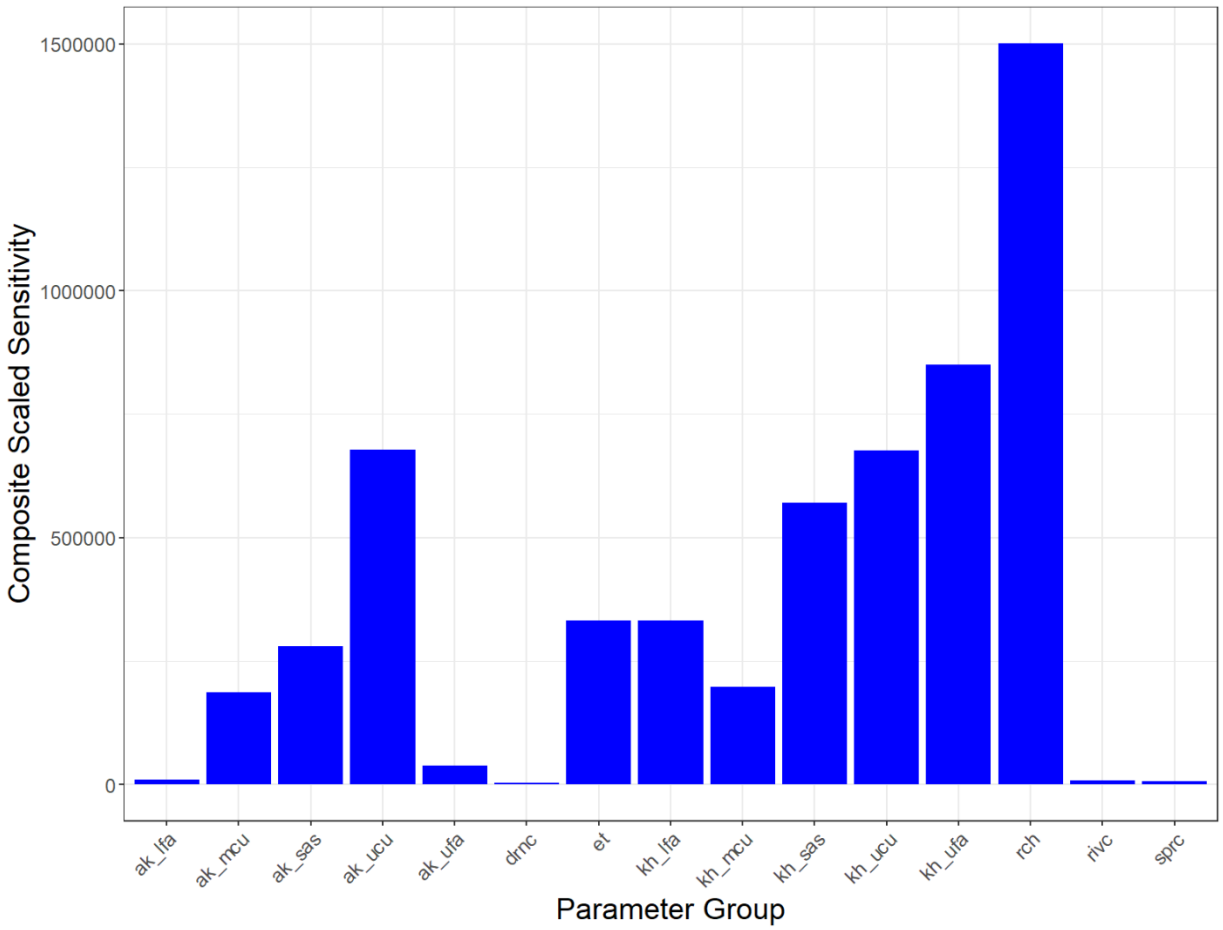

Figure 5-35. Composite scaled sensitivity values for the vertical head difference calibration target group

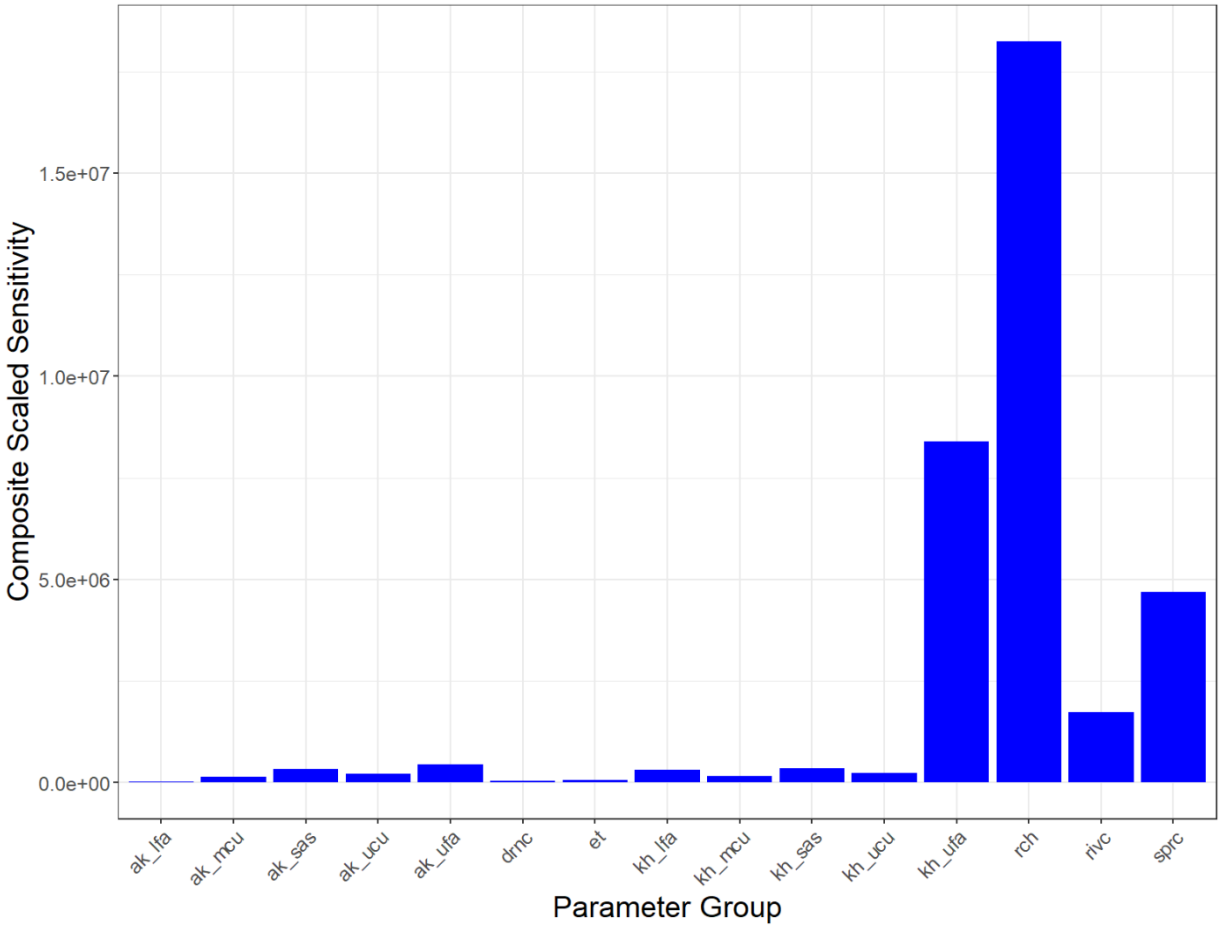

Figure 5-36. Composite scaled sensitivity values for the spring flow calibration target group

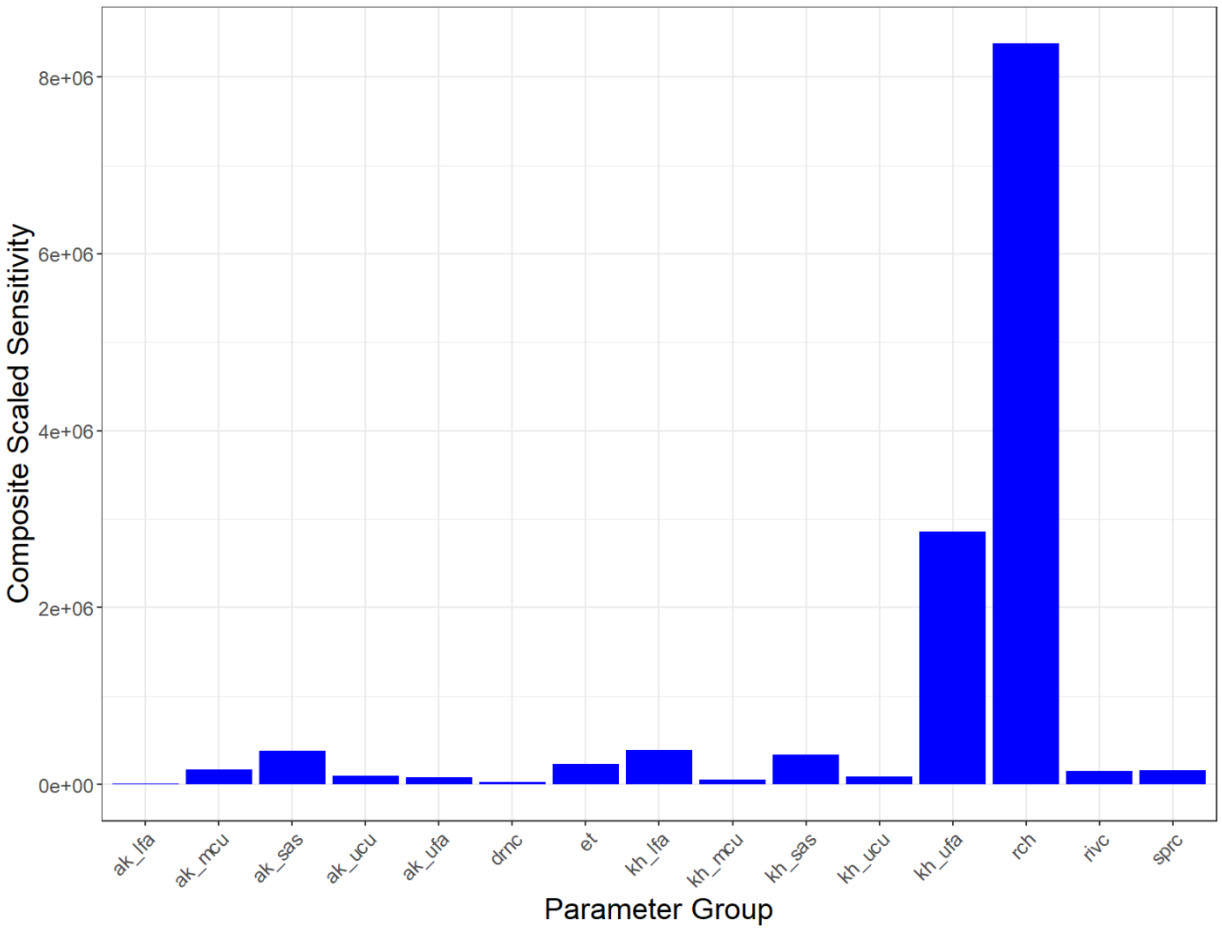

Figure 5-37. Composite scaled sensitivity values for the baseflow calibration target group

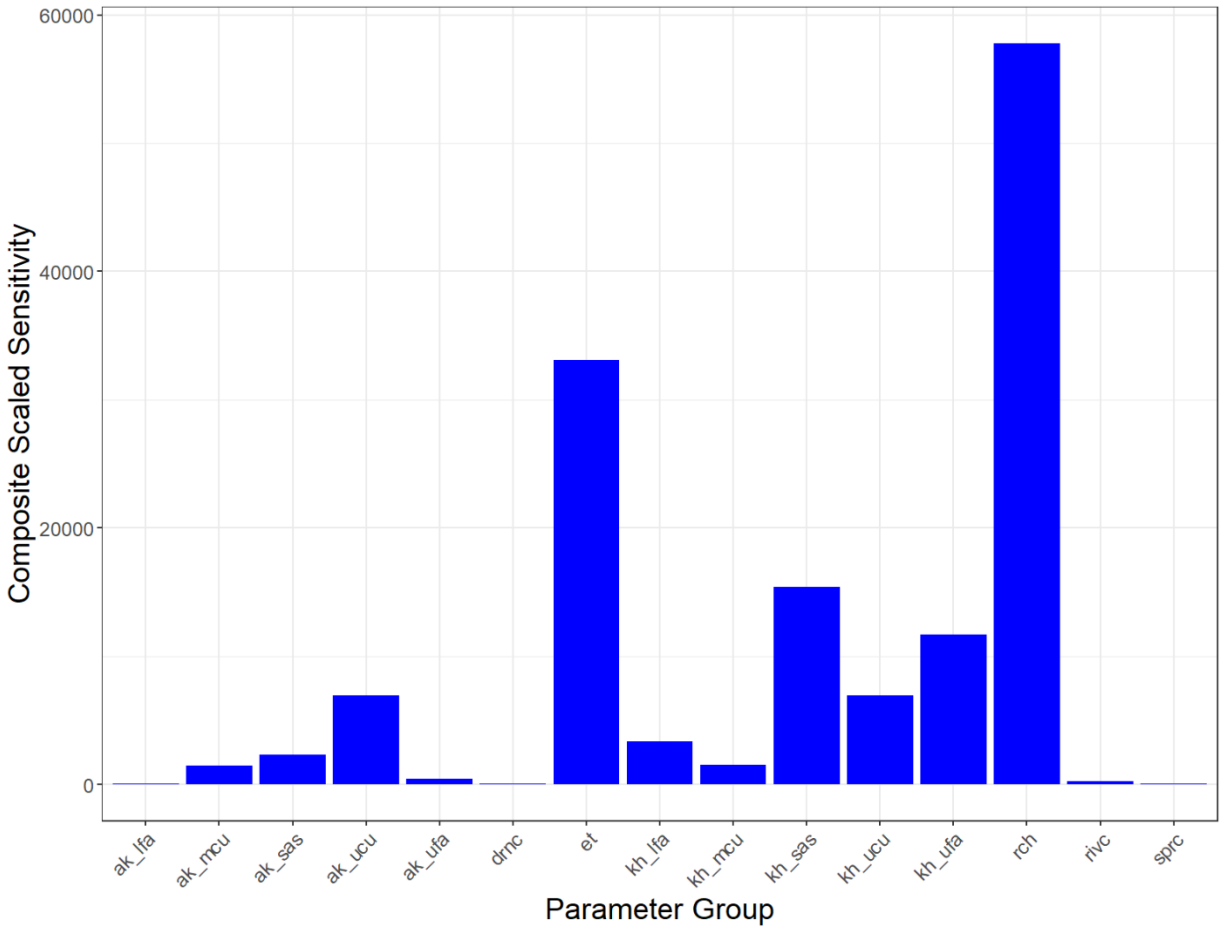

Figure 5-38. Composite scaled sensitivity values for the flooding penalty function calibration target group

6. Simulation of Pumping Impacts on Groundwater Flow to Jackson Blue Spring and Merritts Mill Pond

An initial application of the NCDM was to estimate historical and projected impacts of pumping on groundwater flow to Jackson Blue Spring and Merritts Mill Pond. Continuous estimates of the mean daily flow from Jackson Blue Spring are available for the period from December 21, 2004, until December 31, 2024. Estimates of the impact of pumping during this period were computed from a set of five NCDM steady-state simulations, representing pumping for calendar years 2000, 2005, 2010, 2015, and 2020 and a no-pumping simulation. An estimate of the impact of projected pumping on groundwater flow to Jackson Blue Spring and Merritts Mill Pond in 2045 was also computed from a steady-state NCDM simulation using projected withdrawal rates for 2045. It should be noted that these simulations are not intended to simulate groundwater flows and heads during the years represented by these scenarios. As stated above, these simulations are intended to estimate pumping effects. This was accomplished by changing the locations and rates of pumping for each simulation, while keeping all other aspects of the model constant. The sections that follow describe the development of the MODFLOW Well Package input files for these NCDM simulations, execution and postprocessing of those simulations, and the results of those simulations.

6-1. Development of Well Package Input Files

To implement the historical pumping simulations, it was necessary to create a set of MODFLOW Well Package input files representing the spatial distribution of withdrawals in years 2000, 2005, 2010, 2015, 2020 and 2045. The first step in this process was to estimate historical pumping in each of these years of interest. This information was then used to create a MODFLOW Well Package input file for each year.

6-1-1. Estimation of Historical Pumping

Estimates of the location and rates of historical pumping within the active NCDM domain were computed for each of the years of interest (2000, 2005, 2010, 2015, 2020 and 2045), and the estimation methods for various water use categories, years of interest, and regions varied depending on data availability. Best available data was utilized for all historical water use estimates. The District contracted with the Balmoral Group to estimate historical pumping rates and locations for these years of interest. The methods they employed are described in a report by The Balmoral Group (2024) and are also briefly summarized here. The estimated groundwater withdrawals in the NCDM for each category of water use are shown in Table 6-1.

Table 6-1. Estimated annual groundwater withdrawals in the NCDM for years 2000, 2005, 2010, 2015, 2020, and 2045

Use Type	Annual Groundwater Withdrawal, in MGD					
	2000	**2005**	**2010**	**2015**	**2020**	**2045**
Agricultural Irrigation	20.01	20.29	32.55	30.23	29.97	42.18
Livestock or Aquaculture	0.64	0.81	0.97	2.69	2.69	2.69
Public Supply	3.45	3.68	5.59	4.37	4.98	5.26
Domestic Self Supply	4.24	3.88	3.77	4.36	3.34	3.70
Commercial-Industrial-Institutional	0.17	0.00	0.00	0.01	0.00	0.00
Recreational Irrigation	0.03	0.00	0.03	0.06	0.02	0.02
Power Generation	0.00	0.26	0.28	0.23	0.13	0.14
Total	**28.54**	**28.92**	**43.19**	**41.95**	**41.13**	**53.99**

Locations and rates of withdrawals for Public Supply and Commercial-Industrial-Institutional uses in Alabama were obtained from the Alabama Office of Water Resources. This dataset did not include any Commercial-Industrial-Institutional, Power Generation, or Recreational Irrigation water users in the NCDM region (Balmoral Group, 2024). Projected Public Supply water use in 2045 was based on estimates of the average rate of increase in Public Supply water use from 2010 to 2040 in the three Hydrologic Unit Code 8 (HUC8) basins underlying the NCDM (Balmoral Group, 2024; Atkins and others, 2017). Comparison of the top and bottom elevations of the open intervals of public-supply wells in the Alabama portion of the NCDM domain with hydrogeologic unit top and bottom elevations indicated that the Upper Floridan aquifer intersected about 71 percent of the open intervals of these wells, with the Lower Floridan aquifer accounting for the remaining 29 percent.

Withdrawals for Domestic Self-supplied (DSS) uses in the Alabama portion of the NCDM domain in years 2000, 2005, 2015, and 2020 were estimated based on the percentage of the population using self-supplied groundwater and the per-capita DSS groundwater use (Balmoral, 2024; Harper and others, 2015). Projected DSS use in 2045 was estimated by increasing the 2020 DSS estimates by the projected rate of increase in Public Supply use in the Alabama portion of the NCDM for the period from 2020 to 2045. All Alabama DSS use estimates were distributed to withdrawal points located at the centroids of U.S. Census Blocks. These DSS estimates were further distributed vertically based on the open-interval exposure of Alabama Public Supply wells in the NCDM domain, with 71 percent of the

withdrawals assigned to the Upper Floridan aquifer, and the remaining 29 percent of withdrawals assigned to the Lower Floridan aquifer.

Withdrawals for agricultural irrigation in Alabama were estimated by first identifying irrigated areas in 2015 and 2020 based on the USGS field verification of irrigated areas by Marella and Dixon (2015) and an analysis of aerial imagery (Balmoral, 2024). Irrigated acreage totals in 2010, 2005, and 2000 were then estimated based on the rate of change in county-wide irrigated acreage totals from 2000 to 2015. Irrigated areas for years 2010, 2005, and 2000 (working backward in time) were then estimated by deleting areas in the 2015 irrigated-area dataset so that the total irrigated acreage in 2010, 2005, and 2000 were approximately equal to the county-wide irrigated-acreage totals estimated for these years. Remotely-sensed estimates of the frequency of irrigation were used in this process to prioritize areas for deletion, with less-frequently irrigated areas removed first. Once the irrigated areas were defined in years 2000, 2005, 2010, 2015, and 2020, irrigation rates for these areas were estimated based on crop type and associated irrigation requirements, and crop moisture index values from May through August, which are the peak irrigation months in each year for the dominant crop types in the NCDM domain (Balmoral Group, 2024). Irrigation withdrawals in 2045 were based on projections from the Alabama Office of Water Resources projections (Balmoral, 2024). Livestock groundwater uses in Alabama were based on county-wide U.S. Geological Survey estimates of these uses and were spatially distributed to pasture areas delineated in the 2020 U.S. Department of Agriculture Crop Sequence Boundary dataset (U.S. Department of Agriculture, 2023). Total livestock water use was assumed to be constant for all the years of interest, based on USGS water usage (USGS 2023) and USDA animal inventory data (U.S. Department of Agriculture, 2023). No aquaculture water use was identified in the Alabama portion of the NCDM. Further details of the process used to estimate agricultural withdrawals in Alabama are described in Balmoral (2024).

The locations and rates of groundwater withdrawals for Public Supply, Commercial/Industrial/Institutional, Power Generation, and Recreational Irrigation use types for the Florida portion of the NCDM area in years 2000, 2005, 2010, 2015, and 2020 were based on District's well-construction database and annual water-use reported to the District through consumptive use permitting requirements. The estimated withdrawals in 2045 were based on the projections from the District's 2023 Water Supply Assessment Update (Northwest Florida Water Management District, December 2023).

DSS water use estimates in Florida were based on USGS water use estimates of county-wide DSS use for years 2000, 2005, 2010, and 2015, and on the Districtwide per capita rate of 85 gallons per day for years 2020 and 2045 (Balmoral, 2024; Northwest Florida Water Management District, December 2023). These estimates were distributed spatially to U.S.

Census blocks in proportion to the estimated fraction of a given county's DSS users that resided in a given census block. The estimated use within each block was then distributed to the locations within the block that corresponded to DSS wells in the District's well-construction database, equally dividing the total estimated use within a given census block among active DSS wells within that block. Further details of this process are described in Balmoral (2024).

Groundwater withdrawal rates for agricultural irrigation in the Florida portion of the domain for years 2000, 2005, 2010, 2015, and 2020 were obtained from the District's water use permitting database and spatially distributed to wells in the District's well-construction database that are associated with agricultural withdrawal permits. These rates were checked by computing irrigation demands from crop irrigation requirement and crop moisture index values and were replaced with these irrigation demand estimates when permittee-reported values exceed the 10^{th} or 90^{th} percentile of District irrigation intensity. Groundwater withdrawals for the year 2045 were based projected withdrawals for agricultural irrigation from FSAID version 10 (Florida Department of Agriculture and Consumer Services, 2023).

Groundwater withdrawal rates for livestock use in the Florida portion of the NCDM domain were obtained from the Florida Statewide Agricultural Irrigation Demand dataset (FSAID9: Florida Department of Agriculture and Consumer Services, 2022), which is a GIS layer of polygons representing areas of livestock groundwater use. Where possible, these groundwater withdrawals for livestock were linked to locations of wells in District databases by joining these data sources using consumptive use permit numbers. Unmatched FSAID livestock groundwater withdrawals were assigned to the centroid of FSAID livestock polygon features. Groundwater withdrawals for aquaculture in years 2015 and 2020 were based on data from the FSAID9 dataset (Florida Department of Agriculture and Consumer Services, 2022), and aquaculture use data sourced from District consumptive-use reports. Locations of these aquaculture withdrawals were determined using the same approach as that used for locating livestock groundwater withdrawals. Groundwater withdrawals for livestock and aquaculture uses in 2045 were assumed to be equal to those in 2020 (Florida Department of Agriculture and Consumer Services, 2022).

6-1-2. Generation of Well Package Input Files

Translation of the groundwater withdrawal estimates in the years 2000, 2005, 2010, 2015, 2020, and 2045 to MODFLOW Well Package input files was accomplished using an approach similar to that used for creating the Well Package input file for the 2017-2019 calibration period that was described previously. The primary difference between the processes used for the calibration period and historical datasets was that a method for efficiently processing

multiple years of withdrawal data was required. This process essentially consisted of a two-step process: (1) a preprocessing step in which the historical datasets generated by Balmoral (2024) were translated into metadata and withdrawal rate datasets that had a consistent format, and (2) generation of the Well Package input files for each of the years of interest by using these metadata and withdrawal-rate datasets as inputs to a Python programming language script that joined these inputs with model layer elevation and hydraulic conductivity data to distribute the groundwater withdrawals to appropriate model layers and then output these results as MODFLOW Well Package input files. These preprocessing and Well Package input file generation steps are briefly described in the sections that follow.

6-1-2-1. Preprocessing of Historical Pumping Estimates

There was limited information regarding historical withdrawal locations and amounts for the Alabama portion of the NCDM domain. In order to assign withdrawals to individual layers in the NCDM, casing depth and total depth for wells within the Alabama portion of the model domain were estimated. The available well construction information from 33 production wells in Alabama were compared with NCDM layer elevations (cell top and cell bottom) to determine the fraction of the screened or open interval that is open to each hydrogeologic unit. An average value for the fractions associated with each hydrogeologic unit was then calculated from the set of 33 wells. This analysis indicated that wells only intersected the Upper and Lower Floridan aquifer, and the average fraction of a well's open or screened interval exposed was 71 percent for the Upper Floridan aquifer and 29 percent for the lower Floridan aquifer.

Groundwater withdrawals with the Florida portion of the NCDM domain could be largely accounted for (by volume) with the historical pumping records in the NWFWMD database. Large consumptive groundwater withdrawals typically require an Individual Water Use Permit (IWUP) and are required to submit monthly total withdrawal amounts on an annual basis. By using the pumping data directly, most of the withdrawals in Florida can be accounted for without the need to estimate them. In addition to the pumping amounts, well construction data are also kept in the NWFWMD database, and these data were used to assign withdrawals to NCDM hydrogeologic units.

Although the NWFWMD Hydrologic Database is mostly complete, there are many instances where well construction information was unavailable. In these cases, the casing and total depths of wells lacking construction information were estimated using corresponding information from nearby wells stored in the District's well construction database. For wells within the Florida portion of the NCDM domain, wells that had well construction information were used to estimate casing depth and total depth of wells with missing casing depth or

total depth (or both). Geographic Information System software was used to create a two-mile buffer around wells with missing casing or well depths. Median values of casing depth and total depth were then computed from wells with non-missing data within the two-mile buffer zone and then assigned to the well with missing data. Among the 782 DSS wells in Florida, 346 had casing depth, total depth (or both) estimated using the method previously described. Among the 24 ILG wells in Florida, 196 had casing depth or total depth (or both) estimated using the method previously described. Among the 24 livestock and aquaculture wells in Florida, 16 had casing depth or total depth (or both) estimated using the method previously described. Well construction information for all other use types was complete and did not have to be estimated.

6-1-2-2. Well Package Input File Generation

Well Package input files for each of the simulation years of interest was accomplished by distributing pumping rates associated with a given horizontal (latitude and longitude) location to model layers based on the elevation of the top and bottom of the interval of that well, model layer elevations, and the horizontal hydraulic conductivity of the NCDM at location for each layer intersected by the well's open interval. For wells with open intervals that span multiple model layers, the total pumping for a given well is distributed among each intersected layer in proportion to the product of the length of interval intersected by the layer and the horizontal hydraulic conductivity of the layer at the well's location.

6-2. Historical and Projected Condition Simulation Results

As noted previously, estimates of the impact of groundwater withdrawals from wells on groundwater flow to Jackson Blue Spring and Merritts Mill Pond during the period from January 1, 2005, until December 31, 2024, were computed from a set of five NCDM steady-state simulations, representing pumping for calendar years 2000, 2005, 2010, 2015, and 2020. Projected impacts from pumping in the year 2045 were similarly estimated with an NCDM steady-state simulation that represented projected pumping rates in 2045. The simulations in each of these years were based on the results of the model resulting from the NCDM calibration, with the only difference being that each simulation used a different MODFLOW Well Package input file with pumping rates corresponding to the year of interest. A final 'no pumping' simulation was also executed that was identical to the other six-simulations except that the simulation did not include any withdrawals from wells.

Estimated pumping impacts on groundwater flow to Jackson Blue Spring and Merritts Mill Pond were computed for each of the six years of interest (2000, 2005, 2010, 2015, 2020 and 2045) by calculating the difference between the simulated groundwater flow to the spring and pond in the 'no pumping simulation' and corresponding simulated flows associated with the pumping conditions in that year. This provided a set of six simulated 'flow change' values

for each water body (Jackson Blue Spring and Merritts Mill Pond) for each of the six years of interest, representing pumping impact estimates in each of these years. These pumping impact estimates were then assigned to the middle of their respective years (June 30th) and used to linearly interpolate daily estimates of pumping impacts of groundwater flows to Jackson Blue Spring and Merritts Mill Pond over the baseline time period from January 1, 2005, through December 31, 2024. The results from the historical conditions simulations are shown in Table 6-2. Note that the simulated pumping impacts to inflow to Merritts Mill Pond shown in Table 6-2 do not include the simulated impacts on Jackson Blue Spring. The total simulated pumping impacts on the outflow from Merritts Mill Pond are therefore equal to the sum of the Jackson Blue Spring and Merritts Mill Pond pumping impacts shown in Table 6-2.

Table 6-2. Simulated pumping impacts on groundwater discharge to Jackson Blue Spring and Merritts Mill Pond in years 2000, 2005, 2010, 2015, 2020, and 2045.

Pumping Condition	Simulated Pumping Impact, in cubic feet per second	
	Jackson Blue Spring Discharge	Merritts Mill Pond Inflow
2000	3.3	3.8
2005	3.0	3.5
2010	4.7	5.3
2015	4.5	5.2
2020	4.5	5.3
2045	5.8	6.7

7. Model Limitations

The NCDM was developed primarily as tool for simulating changes in groundwater flow to Jackson Blue Spring and nearby features, such as Merritts Mill Pond. The model can also be used for other purposes, but certain limitations should be acknowledged. For example, the model's capability for simulating flows or changes in flows for the reach of the Chipola downstream from the Altha gage is limited because a baseflow target constraint was not available for this reach during model calibration. Similar limitations apply the simulations of flows or changes in flows to the other ungaged stream or river reaches in the model, such as the upper reaches of Econfina, Holmes, or Wrights Creeks. Although stream gages do exist for the lower Chattahoochee and Apalachicola Rivers, baseflow targets weren't developed for these gages because of the difficulty in estimating groundwater discharge to these large river reaches and because the NCDM domain only includes the western parts of their respective groundwater contributing areas. Accordingly, use of the NCDM to simulate changes in flows to these river reaches from changes in pumping or other stresses in the NCDM will be subject to greater uncertainty and other tools or approaches may therefore be more suitable for estimating these changes.

Simulations of changes in groundwater levels (for example drawdown from pumping wells) should also acknowledge the limitations of using any regional or subregional model (like the NCDM) for this purpose. The NCDM grid has a horizontal resolution of 2,500 feet, which is typical of most groundwater flow models that have been developed for the Floridan aquifer system. However, groundwater-level change simulations are often used to evaluate more local impacts, such as drawdown under wetland features or nearby wells. Site-specific or more localized information, such as specific capacity or aquifer performance testing are often preferred in these situations, and site-specific numerical models or analytical methods like the Theis or Thiem equations (Stahlman, 1971) can be used to estimate a plausible range for drawdown based on more local estimates of aquifer characteristics, and without the resolution limitations of a regional model (although subject to some more restrictive assumptions).

The NCDM, as currently developed, is not intended to estimate transport of chemicals in the subsurface. Although the NCDM can be used to calculate groundwater flow paths and travel time using tools like MODPATH (Pollock, 2016), the current version of the NCDM should not be used to simulate the time of travel of chemicals within the subsurface because the NCDM was not calibrated for this purpose. Transport simulations typically depend on finer-scale variations in hydraulic conductivity and other properties, so development of models capable of simulating chemical transport would ideally include calibrating the model with historical chemical concentration data (preferably at a dense spatial resolution), historical and time-

varying chemical loading rates, and independent groundwater age estimates derived through isotopic analyses. The karstic nature of most of the NCDM model domain further complicates this process and makes simulating chemical transport and time of travel very challenging. Explicit representation of known karst features and their connections, such as cave maps, into transport modelling efforts, can help address these issues. However, data limitations associated with unmapped (or unmappable with current technologies) karst features, historical information regarding geographic variations in chemical loading rates, and lack of knowledge regarding finer-scale hydraulic conductivity variability and their impact on the uncertainty of transport predictions still need to be acknowledged.

8. Summary

A steady-state, groundwater flow model was developed to support regional water supply planning, minimum flow and minimum water levels evaluations, and water use permitting evaluations in the north-central area of the Northwest Florida Water Management District (District or NWFWMD). In particular, the model is intended primarily to support the establishment of a minimum flow for Jackson Blue Spring as a tool that can estimate changes in the flows of the spring in response to changes in groundwater withdrawals from wells. This model is referred to as the North Central District Model (NCDM) and was implemented using the U.S. Geological Survey MODFLOW-NWT (Niswonger and others, 2011) computer program for solving the three-dimensional groundwater-flow equation.

The NCDM actively simulates groundwater levels and flows within each of the major hydrogeologic units in this region: the surficial aquifer system, the upper confining unit of the Floridan aquifer system, the Upper Floridan aquifer, the middle confining unit of the Floridan aquifer system, and the Lower Floridan aquifer. The NCDM is discretized vertically into five layers that generally correspond to these hydrogeologic units, and horizontally into square grid cells that are 2500 feet on each side.

The NCDM was developed as a steady-state model, and calibrated to average conditions occurring from January 1, 2017, through December 31, 2019. Model calibration consisted of adjusting initial estimates of hydraulic conductivity, conductance of subsurface connections with river, stream, and spring features, recharge rates, and maximum rates of direct evapotranspiration from the water table to better match calibration targets defined by groundwater levels, groundwater level differences, spring flows, and stream and river baseflows during the calibration period, and to also minimize the occurrence of cells where shallow groundwater levels exceeded land surface. Summary statistics of differences between these target values and their model-simulated equivalents indicated a relatively unbiased, well-fit model, particularly for the head and spring flow targets, which were treated as higher-priority targets during the NCDM development. Calibration targets were generally most sensitive to parameters associated with the hydraulic conductivity of the Upper Floridan aquifer and groundwater recharge.

The NCDM was used to estimate the effects of historical and projected pumping from groundwater wells on groundwater discharge to Jackson Blue Spring and Merritts Mill Pond, with the latter including discharge from Jackson Blue Spring. These pumping effects were estimated by executing series of NCDM simulations, including a ‘no-pumping’ simulation and individual simulations using pumping estimates for years 2000, 2005, 2010, 2015, 2020, and 2045. Estimates of pumping impacts based on these simulations ranged from about 3.3

cubic feet per second (cfs) in 2000 to 5.8 cfs in 2045 for Jackson Blue Spring, and from 3.8 to 6.7 cfs for Merritts Mill Pond.

The NCDM was developed primarily as tool for simulating changes in groundwater flow to Jackson Blue Spring and nearby features, such as Merritts Mill Pond and Spring. The model can also be used for other purposes, but certain limitations should be acknowledged. For example, simulations of changes in groundwater levels (for example drawdown from pumping wells) with the NCDM should be carried out with caution and with an understanding of the horizontal resolution of the NCDM grid (2,500 feet) and the regional nature of the model and associated variations in hydraulic properties. Use of site-specific or more localized information, such as specific capacity or aquifer performance testing can provide more direct information than a regional model in these situations. Simple site-specific numerical models or analytical methods like the Theis or Thiem equations (Stahlman, 1971) can also be implemented to estimate an expected range for drawdown based on more local estimates of aquifer characteristics.

The NCDM only includes the western parts of groundwater contributing areas to the reaches of the Chattahoochee and Apalachicola Rivers in the NCDM, so suitable baseflow targets were not available for these river reaches that define the eastern boundary of the NCDM. Similarly, stream reaches near the western boundary (Econfina, Holmes, or Wrights Creek) and southern boundary (Chipola River downstream from the gage near Altha) did not have baseflow targets because these reaches were ungaged. Simulated changes in groundwater flow to the above reaches are therefore expected to have greater uncertainty.

The NCDM was not developed to estimate the movement and transformation of chemicals in the subsurface. Although the NCDM can be used to calculate groundwater flow paths and travel times using tools like MODPATH (Pollock, 2016), these or similar tools should not be used with the current version of the NCDM to simulate time of travel of chemicals within the subsurface because the NCDM was not calibrated for this purpose. Transport simulations typically depend on finer-scale variations in hydraulic conductivity and other properties, so development of models capable of simulating chemical transport should ideally include calibrating the model with historical chemical concentration data, historical and time-varying chemical loading rates, and independent estimates of travel time or groundwater age information. The karstic nature of most of the NCDM model domain further complicates this process and makes simulating chemical transport and time of travel very challenging.

References

Alabama Office of Water Resources, 2023. Water usage data provided to NWFWMD by personal communication, October 2023.

Albritton, C.K., 2021, Potentiometric surface of the Upper Floridan aquifer, May 2018, Florida Geological Survey Map Series 158.

Albritton, C.K., 2022, Potentiometric surface of the Upper Floridan aquifer, September 2018, Florida Geological Survey Map Series 159.

Atkins, J.B., Harper, M.J., Johnston, D.D., and Littlepage, T.M. 2017. An Assessment of The Surface Water Resources of Alabama. Alabama Office of Water Resources, a division of the Alabama Department of Economic and Community Affairs.

Balmoral Group. 2019. Florida Statewide Agricultural Irrigation Demand Estimated Agricultural Water Demand, 2017-2040. Final Technical Report. https://www.fdacs.gov/Agriculture-Industry/Water/Agricultural-Water-Supply-Planning

Balmoral Group. 2020. Florida Statewide Agricultural Irrigation Demand Estimated Agricultural Water Demand, 2018-2045. Final Technical Report. https://www.fdacs.gov/content/download/113668/file/FSAID-10-Report.pdf

Balmoral Group. 2021. Florida Statewide Agricultural Irrigation Demand Estimated Agricultural Water Demand, 2019-2045. Final Technical Report. https://www.fdacs.gov/content/download/116462/file/FSAID-11-Report.pdf

Balmoral Group, 2024, Spatial data development of groundwater use: North Central District Model area, summary of data sources and methods. Technical memo provided to the Northwest Florida Water Management District, 10 pp.

Barrios, K., Chelette, A. 2004. Chipola River Spring Inventory: Jackson and Calhoun Counties, FL. Northwest Florida Water Management District Water Resources Special Report 04-01, 54 p. https://nwfwater.com/content/download/1335/11569/wrsr0401.pdf

Clark, William and Zisa, Arnold., 1976, Physiographic Map of Georgia. Georgia Department of Natural Resources.

Crandall, C.A., Katz, B.G., and Berndt, M.P., 2013, Estimating nitrate concentrations in groundwater at selected wells and springs in the surficial aquifer system and Upper Floridan aquifer, Dougherty Plain and Marianna Lowlands, Georgia, Florida, and Alabama, 2002–50: U.S. Geological Survey Scientific Investigations Report 2013–5150, 65 pp. https://pubs.usgs.gov/sir/2013/5150/pdf/sir2013-5150.pdf

Dewitz, J., and U.S. Geological Survey, 2021, National Land Cover Database (NLCD) 2019 Products (ver. 3.0, February 2024): U.S. Geological Survey data release, https://doi.org/10.5066/P9KZCM54.

Doherty, J., 2015. Calibration and uncertainty analysis for complex environmental models. Published by Watermark Numerical Computing, Brisbane, Australia. 227 pp., ISBN: 978-0-9943786-0-6.

Doherty, John, August 2021, Groundwater Data Utilities Part A: Overview, Watermark Numerical Computing, 49 pp.

Doherty, John, May 2023, Groundwater Data Utilities Part B: Program Descriptions, Watermark Numerical Computing, 342 pp.

Doherty, John, January 2023, PEST Model-Independent Parameter Estimation User Manual Part I: PEST, SENSAN and Global Optimisers; Watermark Numerical Computing, 369 pp.

Doherty, John, April 2023, PEST Model-Independent Parameter Estimation User Manual Part II: PEST Utility Support Software, Watermark Numerical Computing, 287 pp.

Doherty, John, February 2020, PEST_HP: PEST for Highly Parallelized Computing Environments, Watermark Numerical Computing, 84 pp.

Durden, Douglas; Gordu, Fatih; Hearn, Douglas; Cera, Tim; Desmarais, Tim; Meridth, Lanie; Angel, Adam; Leahy, Christopher; Oseguera, Joanna; and Trey Grubbs, 2019, North Florida Southeast Georgia Groundwater Model (NFSEG V1.1), St. Johns River Water Management District Technical Publication SJ2019-01.

Ebersole, Sandy, Guthrie, G. M., and VanDervoort, D. S., 2019, Physiographic regions of Alabama: Alabama Geological Survey Open-File Report 1901, 20 pp., 1 plate.

Florida Department of Agriculture and Consumer Services, 2017, Florida Statewide Agricultural Irrigation Demand: Estimated Agricultural Water Demand, 2015 – 2040. (FSAID4). Florida Department of Agriculture and Consumer Services (FDACS) Office of Agricultural Water Policy. In collaboration with The Balmoral Group.

Florida Department of Agriculture and Consumer Services, 2022 Florida Statewide Agricultural Irrigation Demand: Estimated Agricultural Water Demand, 2020 – 2045. (FSAID9). Florida Department of Agriculture and Consumer Services (FDACS) Office of Agricultural Water Policy. In collaboration with The Balmoral Group.

Florida Department of Agriculture and Consumer Services, 2023 Florida Statewide Agricultural Irrigation Demand: Estimated Agricultural Water Demand, 2020 – 2045.

(FSAID10). Florida Department of Agriculture and Consumer Services (FDACS) Office of Agricultural Water Policy. In collaboration with The Balmoral Group.

Fowler, G.D., III, and Albritton, C.K., 2022a, Potentiometric surface of the Upper Floridan aquifer, May 2019, Florida Geological Survey Map Series 158.

Fowler, G.D., III, and Albritton, C.K., 2022b, Potentiometric surface of the Upper Floridan aquifer, September 2019, Florida Geological Survey Map Series 158.

Friedman, Ken, May 2022, Development of spatially distributed groundwater withdrawals for the Northwest Florida Water Management District North Central District Groundwater Flow Model, Draft Northwest Florida Water Management District Memorandum.

Grubbs, J.W.; Coates, Kathleen; Countryman, Tony; Friedman, Ken; and Sutton, James; August 2022, Development of datasets for the Eastern District Regional Groundwater Flow Model Version 1.1, Northwest Florida Water Management District Technical File Report 22-01, 91 pp.

Harbaugh, A.W., Banta, E.R., Hill, M.C., and McDonald, M.G., 2000, MODFLOW-2000, the U.S. Geological Survey modular ground-water model -- User guide to modularization concepts and the Ground-Water Flow Process: U.S. Geological Survey Open-File Report 00-92, 121 p., https://pubs.usgs.gov/publication/ofr200092

Harbaugh, A.W., 2005, MODFLOW-2005, The U.S. Geological Survey modular ground-water model—the Ground-Water Flow Process: U.S. Geological Survey Techniques and Methods 6-A16, variously p., https://pubs.usgs.gov/tm/2005/tm6A16/

Harper, M.J., Littlepage, T.M. Johnston, D.D., and Atkins, J.B., 2015. Estimated 2015 Water Use and Surface Water Availability in Alabama. Alabama Office of Water Resources, a division of the Alabama Department of Economic and Community Affairs.

Harper, M.J., and Turner, B.J. 2010. Estimated Use of Water in Alabama in 2010. Alabama Office of Water Resources, a division of the Alabama Department of Economic and Community Affairs.

Helsel, D.R., Hirsch, R.M., Ryberg, K.R., Archfield, S.A., and Gilroy, E.J., 2020, Statistical methods in water resources: U.S. Geological Survey Techniques and Methods, book 4, chap. A3, 458 pp., https://doi.org/10.3133/tm4a3. [Supersedes USGS Techniques of Water-Resources Investigations, book 4, chap. A3, version 1.1.]

Kebart, Karen, January 2020, Digital communication, District-wide LiDAR dataset based on best available data as of January 2020.

Kinnaman, S.L., Dixon, J.F., 2011, Potentiometric Surface of the Upper Floridan aquifer in Florida and in parts of Georgia, South Carolina, and Alabama, May-June 2010: U.S. Geological Survey Scientific Investigations Map 3182, 1 sheet, available online at https://pubs.usgs.gov/sim/3182/.

Mallat, S. (2009). A Wavelet Tour of Signal Processing. Academic Press, ISBN 978-0-12-374370-1, https://doi.org/10.1016/B978-0-12-374370-1.X0001-8

Marella, R.L., and Dixon, J.F., 2015. Agricultural irrigated land-use inventory for Jackson, Calhoun, and Gadsden Counties in Florida, and Houston County in Alabama, 2014: U.S. Geological Survey Open-File Report 2015–1170, 14 pp. http://dx.doi.org/10.3133/ofr20151170

McKay, L., Bondelid, T., Dewald, T., Johnston, J., Moore, R., and Rea, A., "NHDPlus Version 2: User Guide", 2012, https://www.epa.gov/system/files/documents/2023-04/NHDPlusV2_User_Guide.pdf, U.S. Environmental Protection Agency, 182 pp., revised March 13, 2019.

Mecikalski, John R.; Sumner, David M.; Jacobs, Jennifer M.; Pathak, Chandra S.; Paech, Simon J., and Douglas, Ellen M., 2018, Use of visible geostationary operational meteorological satellite imagery in mapping reference and potential evapotranspiration over Florida. https://doi.org/10.1061/(ASCE)IR.1943-4774.0001312

Miller, James A. Hydrogeologic framework of the Floridan aquifer system in Florida and in parts of Georgia, Alabama, and South Carolina; 1986; Professional Paper 1403-B. https://pubs.usgs.gov/publication/pp1403B

Niswonger, R.G., Panday, Sorab, and Ibaraki, Motomu, 2011, MODFLOW-NWT, A Newton formulation for MODFLOW-2005: U.S. Geological Survey Techniques and Methods 6-A37, 44 pp. https://doi.org/10.3133/tm6A37

Northwest Florida Water Management District. October 1996, Water Resources Special Report, 96-4, 105 pp. https://nwfwater.com/content/download/6722/48947/WRSR96-04Hydogeology_of_the_NWFWMD.compressed.pdf

Northwest Florida Water Management District, June 2011, Jackson Blue Spring Water Resources Assessment, WRA 11-01, 44 pp. https://nwfwater.com/wp-content/uploads/2022/07/WRA11-01.pdf

Northwest Florida Water Management District, December 2018, 2018 Water Supply Assessment Update, WRA 18-01, 151 pp. https://nwfwater.com/Water-Resources/Water-Supply-Planning/Water-Supply-Assessments/

Northwest Florida Water Management District, December 2023, Northwest Florida Water Management District 2023 Water Supply Assessment Update, Water Resources Assessment 23-01. Prepared by the Resource Management Division. 116 pp. https://nwfwater.com/Water-Resources/Water-Supply-Planning/Water-Supply-Assessments/

Paige, C.C. and Saunders, M.A., 1982a. LSQR: an algorithm for sparse linear equations and sparse least squares. *ACM Trans. Math. Softw.*, Vol 8: 43-71.

Paige, C.C. and Saunders, M.A. 1982b. LSQR: an algorithm for spare linear equations and sparse least squares. ACM Trans. Math. Softw., Vol 8: 192-209.

Pollock, D.W., 2016, User guide for MODPATH Version 7 -- A particle-tracking model for MODFLOW: U.S. Geological Survey Open-File Report 2016-1086, 35 pp., https://dx.doi.org/10.3133/ofr20161086.

QGIS Development Team. (2024). QGIS Geographic Information System. Open-Source Geospatial Foundation Project. https://qgis.org

Sepulveda, N., C. Tiedeman, A. M. O'Reilly, J. B. Davis, and P. Burger. 2012. Groundwater flow and water budget in the surficial and Floridan aquifer systems in east-central Florida. Scientific Investigations Report 2012–5161. Reston, VA: U.S. Geological Survey. https://pubs.usgs.gov/sir/2012/5161/

Stallman, Robert W., 1976, Aquifer-test design, observation, and data analysis: U.S. Geological Survey Techniques and Methods Book 3, Chapter B1, https://pubs.usgs.gov/twri/twri3-b1/pdf/twri_3-B1_a.pdf

Tetra Tech, May 2017, River and Spring Geodatabase Methodology Development (Final), Memorandum to the Northwest Florida Water Management District, 12 pp.

Tetra Tech, September 2024, Documentation of Tetra Tech Work on the North-Central District Model, Memorandum to the Northwest Florida Water Management District, 41 pp.

U.S. Census Bureau, 2010. TIGER/Line Shapefiles.

U.S. Department of Agriculture, 2023, National Agricultural Statistics Service (NASS). From: https://quickstats.nass.usda.gov/ Cattle Inventory by County.

Williams, L.J., and Dixon, J.F., 2015, Digital surfaces and thicknesses of selected hydrogeologic units of the Floridan aquifer system in Florida and parts of Georgia, Alabama, and South Carolina: U.S. Geological Survey Data Series 926, 24 pp. http://dx.doi.org/10.3133/ds926.

U.S. Geological Survey, 2016, National Water Information System data available on the World Wide Web (USGS Water Data for the Nation), http://waterdata.usgs.gov/nwis/

U.S. Geological Survey, 2019, Statewide reference and potential evapotranspiration datasets, https://www.usgs.gov/centers/cfwsc/science/reference-and-potential-evapotranspiration, downloaded February 3, 2022.

U.S. Geological Survey, 2022, MODFLOW and Related Programs, at https://www.usgs.gov/mission-areas/water-resources/science/modflow-and-related-programs

Vieux and Associates, Inc. 2020. Estimation of Rainfall Accumulations Using National Weather Service Weather Surveillance Radar 1988 Doppler Data. Retrieved April 13, 2021.

Vogel, C. R., 2002, Computational Methods for Inverse Problems. Society for Industrial and Applied Mathematics, ISBN 978-0-89871-550-7, 197 pp. https://doi.org/10.1137/1.9780898717570

Williams, L.J., and Dixon, J.F., 2015, Digital surfaces and thicknesses of selected hydrogeologic units of the Floridan aquifer system in Florida and parts of Georgia, Alabama, and South Carolina: U.S. Geological Survey Data Series 926, 24 pp. http://dx.doi.org/10.3133/ds926.

Williams, L.J., and Kuniansky, E.L., 2016, Revised hydrogeologic framework of the Floridan aquifer system in Florida and parts of Georgia, Alabama, and South Carolina (ver 1.1, March 2016): U.S. Geological Survey Professional Paper 1807, 140 pp., 23 pls, http://dx.doi.org/10.3133/pp1807.

Williams, C.P., Scott, T.M., and Upchurch, S.B., 2022, Florida Geomorphology Atlas: Florida Geological Survey Special Publication 59, 238 pp.